

NOAA Technical Report EDS 22



U.S. National Processing Center for GATE: B-Scale Surface Meteorological and Radiation System, Including Instrumentation, Processing, and Archived Data

Washington, D. C.
April 1977



U.S. DEPARTMENT OF COMMERCE
National Oceanic and Atmospheric Administration
Environmental Data Service

NOAA TECHNICAL REPORTS

Environmental Data Service Series

The Environmental Data Service (EDS) archives and disseminates a broad spectrum of environmental data gathered by the various components of NOAA and by the various cooperating agencies and activities throughout the world. The EDS is a "bank" of worldwide environmental data upon which the researcher may draw to study and analyze environmental phenomena and their impact upon commerce, agriculture, industry, aviation, and other activities of man. The EDS also conducts studies to put environmental phenomena and relations into proper historical and statistical perspective and to provide a basis for assessing changes in the natural environment brought about by man's activities.

The EDS series of NOAA Technical Reports is a continuation of the former series, the Environmental Science Services Administration (ESSA) Technical Report, EDS.

Reports in the series are available from the National Technical Information Service, U.S. Department of Commerce, Sills Bldg., 5285 Port Royal Road, Springfield, Va. 22151. Price: \$3.00 paper copy; \$1.45 microfiche. When available, order by accession number shown in parentheses.

ESSA Technical Reports

- EDS 1 Upper Wind Statistics of the Northern Western Hemisphere. Harold L. Crutcher and Don K. Halligan, April 1967. (PB-174-921)
- EDS 2 Direct and Inverse Tables of the Gamma Distribution. H. C. S. Thom, April 1968. (PB-178-320)
- EDS 3 Standard Deviation of Monthly Average Temperature. H. C. S. Thom, April 1968. (PB-178-309)
- EDS 4 Prediction of Movement and Intensity of Tropical Storms Over the Indian Seas During the October to December Season. P. Jagannathan and H. L. Crutcher, May 1968. (PB-178-497)
- EDS 5 An Application of the Gamma Distribution Function to Indian Rainfall. D. A. Mooley and H. L. Crutcher, August 1968. (PB-180-056)
- EDS 6 Quantiles of Monthly Precipitation for Selected Stations in the Contiguous United States. H. C. S. Thom and Ida B. Vestal, August 1968. (PB-180-057)
- EDS 7 A Comparison of Radiosonde Temperatures at the 100-, 80-, 50-, and 30-mb Levels. Harold L. Crutcher and Frank T. Quinlan, August 1968. (PB-180-058)
- EDS 8 Characteristics and Probabilities of Precipitation in China. Augustine Y. M. Yao, September 1969. (PB-188-420)
- EDS 9 Markov Chain Models for Probabilities of Hot and Cool Days Sequences and Hot Spells in Nevada. Clarence M. Sakamoto, March 1970. (PB-193-221)

NOAA Technical Reports

- EDS 10 BOMEX Temporary Archive Description of Available Data. Terry de la Moriniere, January 1972. (COM-72-50289)
- EDS 11 A Note on a Gamma Distribution Computer Program and Graph Paper. Harold L. Crutcher, Gerald L. Barger, and Grady F. McKay, April 1973. (COM-73-11401)
- EDS 12 BOMEX Permanent Archive: Description of Data. Center for Experiment Design and Data Analysis, May 1975.
- EDS 13 Precipitation Analysis for BOMEX Period III. M. D. Hudlow and W. D. Scherer, September 1975. (PB-246-870)
- EDS 14 IFYGL Rawinsonde System: Description of Archived Data. Sandra M. Hoexter, May 1976. (PB-258-057)
- EDS 15 IFYGL Physical Data Collection System: Description of Archived Data. Jack Foreman, September 1976. (PB-261-829)

(Continued on inside back cover)

NOAA Technical Report EDS 22



**U.S. National
Processing Center for GATE:
B-Scale Surface Meteorological and
Radiation System, Including
Instrumentation, Processing, and
Archived Data**

Center for Experiment Design and Data Analysis

Ward R. Seguin
Paul Sabol
Raymond Crayton
Richard S. Cram
Kenneth L. Echternacht
Monte Poindexter

Washington, D. C.
April 1977

U.S. DEPARTMENT OF COMMERCE

Juanita M. Kreps, Secretary

National Oceanic and Atmospheric Administration

Robert M. White, Administrator

Environmental Data Service

Thomas S. Austin, Director

CONTENTS

	<u>Page</u>
1. Introduction	1
1.1 Shipboard data system	6
1.2 The bow sensor acquisition module and sensors	8
1.3 The central sensor acquisition module and sensors	8
1.4 The boom platform and hardware	8
2. Sensor characteristics	11
2.1 Temperature	11
2.2 Thermistor signal conditioner	12
2.3 Wind speed	12
2.4 Wind direction	12
2.5 Atmospheric pressure	13
2.6 Radiation	13
2.7 Ship speed and heading	13
2.8 Precipitation	13
3. Pre- and post-GATE calibration	14
3.1 Temperature sensors	14
3.2 Wind sensors	16
3.3 Pressure sensors	19
3.4 Ship heading and speed sensors	19
4. Procedures for assuring quality control at sea	20
5. Data processing	23
5.1 Preprocessing	23
5.2 Central processing	23
5.3 Data review and validation	27
5.4 Peculiarities in the meteorological data	28
5.4.1 Temperature	28
5.4.2 Wind direction and speed	28
5.4.3 Ship speed and heading	30
5.4.4 Pressure	32
5.5 Final processing	33

CONTENTS (continued)

	<u>Page</u>
6. Analysis and validation of surface radiation data	37
6.1 Recording system error limitations	37
6.2 Incident and reflected solar radiation ($K\downarrow$ and $K\uparrow$)	38
6.2.1 Instrumentation and transfer equations	38
6.2.2 Data validation	38
6.3 Net radiation (Q^*)	47
6.3.1 Derivation of transfer equations	47
6.3.2 Data validation	49
6.3.3 Instrument malfunctions	55
6.3.4 Anomalous net radiation data	55
6.3.5 Radiometer sensitivity and transfer coefficients	55
6.4 Yanishevsky pyranometer data ($K\downarrow$)	57
6.5 <u>Vanguard</u> pyranometer data	58
7. Format and inventory of the archived data sets	59
7.1 Digital data on magnetic tape	60
7.2 Microfilm time-series plots	65
References	68
Appendix A. Detailed tape formats and examples	70
Appendix B. Pre-GATE intercomparison of pyranometers	82
Appendix C. Translocation of thermistor probes and bridges	86
Appendix D. Sensor and SAM transfer equations used in data processing	88

U.S. NATIONAL PROCESSING CENTER FOR GATE:
B-SCALE SURFACE METEOROLOGICAL AND RADIATION SYSTEM,
INCLUDING INSTRUMENTATION, PROCESSING, AND ARCHIVED DATA

Ward R. Seguin, Paul Sabol, and Raymond Crayton
Center for Experiment Design and Data Analysis
Environmental Data Service, NOAA
Washington, D.C.

Richard S. Cram
Air Resources Laboratories
Environmental Research Laboratories, NOAA
Boulder, Colorado

Kenneth L. Echternacht
Institute for Acoustical Research
Palisades Geophysical Institute
Miami, Florida

Monte Poindexter
Air Resources Laboratories
Environmental Research Laboratories, NOAA
Silver Spring, Maryland

ABSTRACT. This report documents the surface meteorological and radiation data collected on the four U.S. B-Scale ships Researcher, Gilliss, Dallas, and Oceanographer. The report describes the sensors and recording systems on board the ships, pre-and post-calibration procedures, and data processing and validation methods. A description and inventory of the archived products are included.

1. INTRODUCTION

The Global Atmospheric Research Program (GARP) Atlantic Tropical Experiment (GATE) was conducted during the summer of 1974 in an area centered 1000 km southwest of Dakar, Senegal. The central program of the experiment focused on the effects of smaller scale tropical weather systems on larger scale circulations. Some 70 nations supplied the needed equipment and manpower, including 39 research ships, 13 aircraft, 10 satellites, and nearly 4000 scientists and technicians, to meet the goals of GATE. The United States supplied five ships for the B-scale array: the NOAA Researcher; the University of Miami R/V Gilliss; the USCG Dallas; the NOAA Oceanographer, and the NASA Vanguard.

The acquisition of continuous, high-quality surface meteorological data was an important facet of GATE, yet making precise measurements of surface meteorological variables at sea aboard large research vessels is difficult at best. In his textbook, Physics of the Marine Atmosphere, Roll (1965) discusses many of the problems and limitations. For example, the obstacle effect of the ship distorts the wind flow, making accurate wind velocity measurements difficult. This same effect can often influence rainfall

measurements so that twice as much rainfall is measured at one place on the ship as another. The ship heating affects air temperature measurements, and the engine cooling water modifies the sea surface temperatures. To minimize these problems, four of the GATE B-scale ships (the Researcher, the Gilliss, the Dallas, and the Oceanographer) were equipped with instrumentation mounted on bow booms and the forward mast. Experience and previous research (Seguin and Garstang, 1971; Ching, 1975) have shown that instrumentation mounted on bow booms suffers the least from the above ship effects.

The Vanguard did not have a bow boom, nor the sophisticated automatic recording system carried by the other U.S. ships. However, this ship measured downward total solar radiation, $K\downarrow$, and direct solar radiation, I , and recorded these data on an analog recorder. All the U.S. ships made standard WMO surface marine meteorological observations, which were used in the validation of the automatically acquired data.

GATE was conducted from June 17 through September 23, 1974. The experiment included three formal ship Intercomparisons, each lasting 3 days, and three Phases, each lasting 20 days. Figures 1, 2, and 3 show the locations of the A/B-, B-, and C-scale ship arrays. Table 1 gives the dates of these observation periods.

Table 1.--Dates of GATE observation periods

Periods	Date
Intercomparison 1	June 17, 18, 19
Intercomparison 2	August 16, 17, 18
Intercomparison 3	September 21, 22, 23
Phase I	June 26 - July 16
Phase II	July 28 - August 16
Phase III	August 30 - September 19

This report has been prepared to familiarize the scientific community with the U.S. B-scale ship automated surface meteorological and radiation data. It describes the instrumentation used to observe and record the data, data quality assurance procedures, data processing programs and methods, and the nature and format of the data that have been placed in the archive.

The surface meteorological and radiation data were processed with computer programs at the Center for Experiment Design and Data Analysis (CEDDA). Processing included preprocessing of original acquisition tapes, central processing, and final processing. Preprocessing consisted of converting analog data to digital data and separating these multiplexed data into subsystem files. Central processing included converting new data from recording units to scientific units, automatic editing, and correcting relative wind measurements for ship heading and velocity. Final processing included re-scaling certain variables with new transfer equations, deleting certain data, and calculating low-resolution averages.

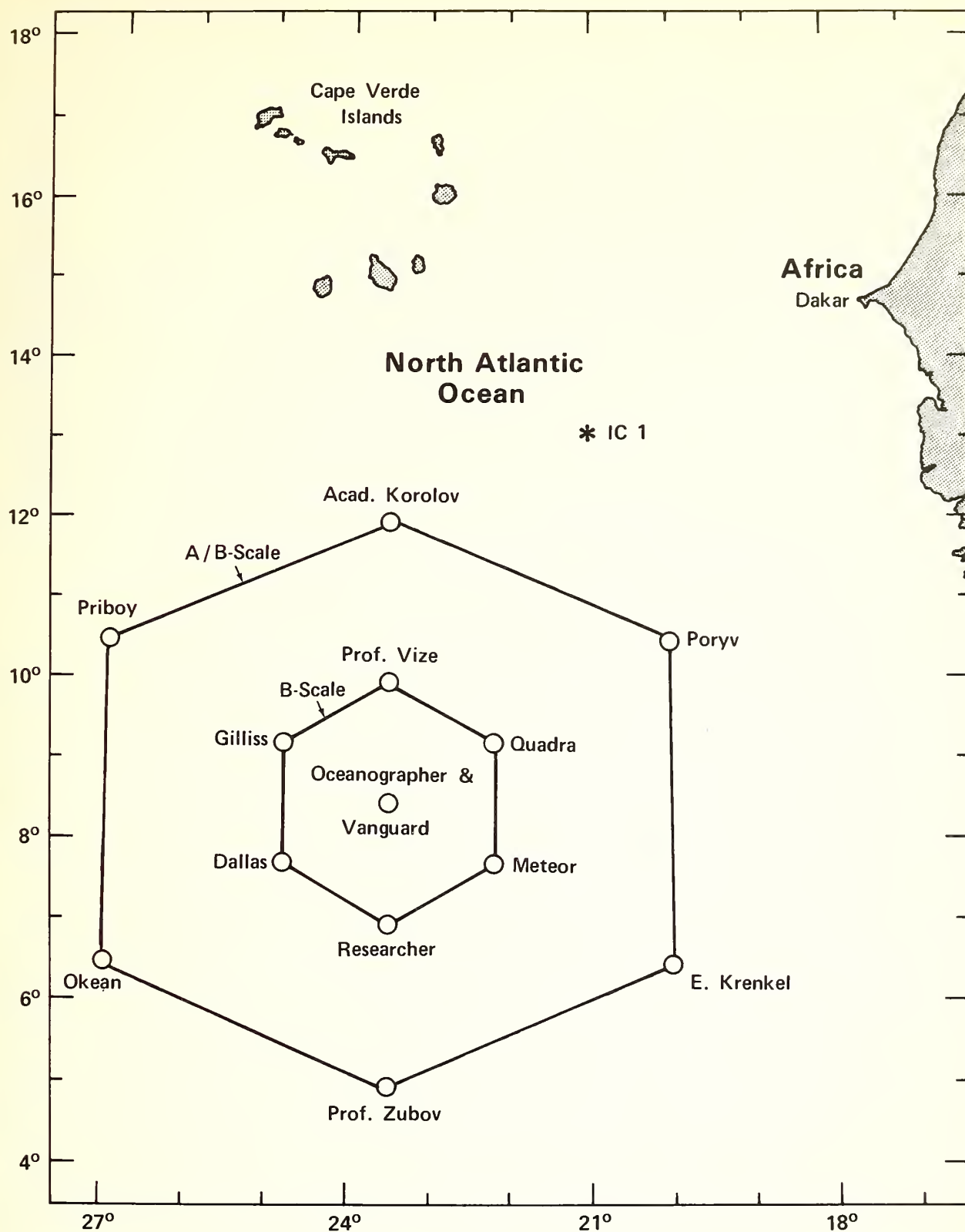


Figure 1.--Ship array during Phase I.

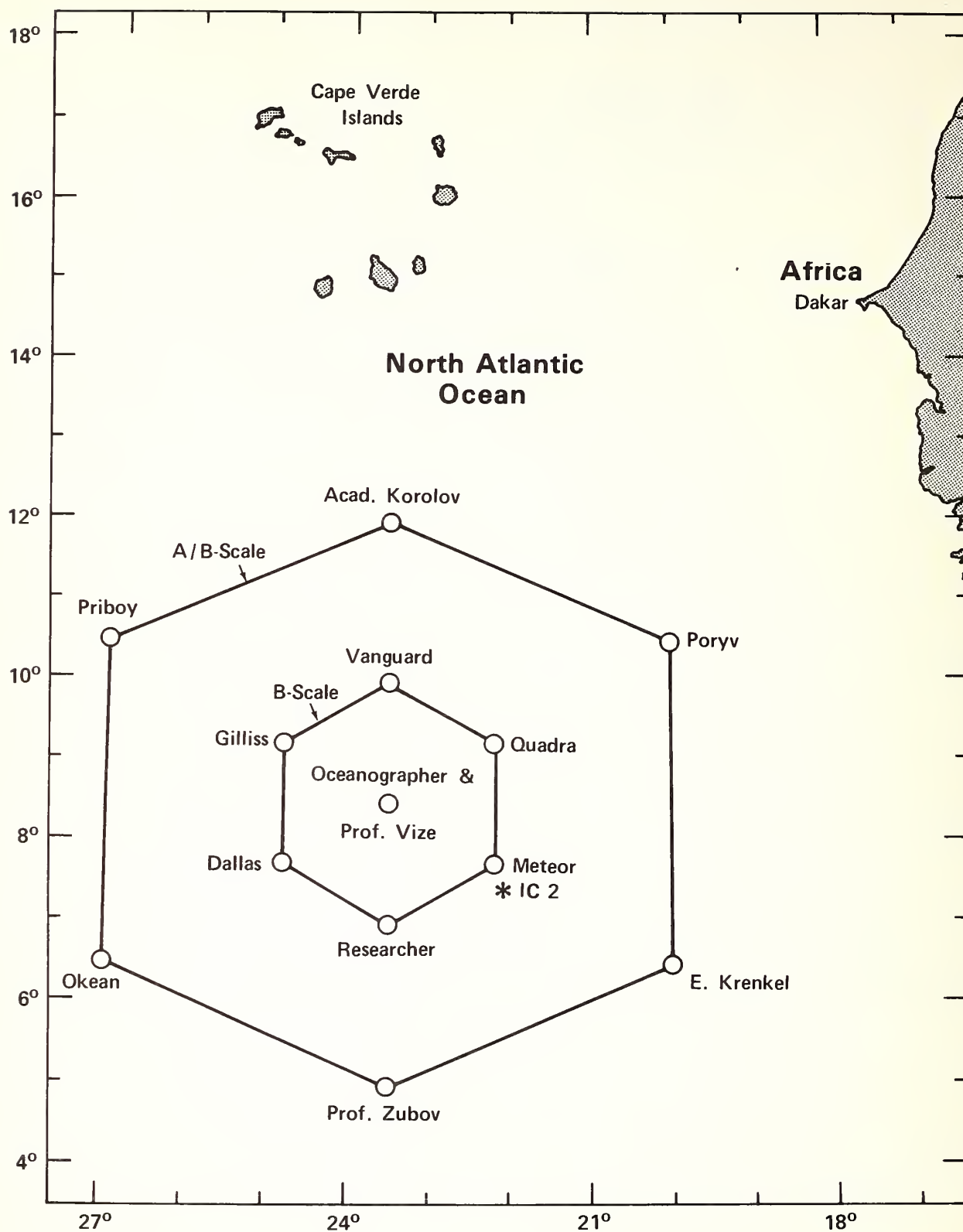


Figure 2.--Ship array during Phase II.

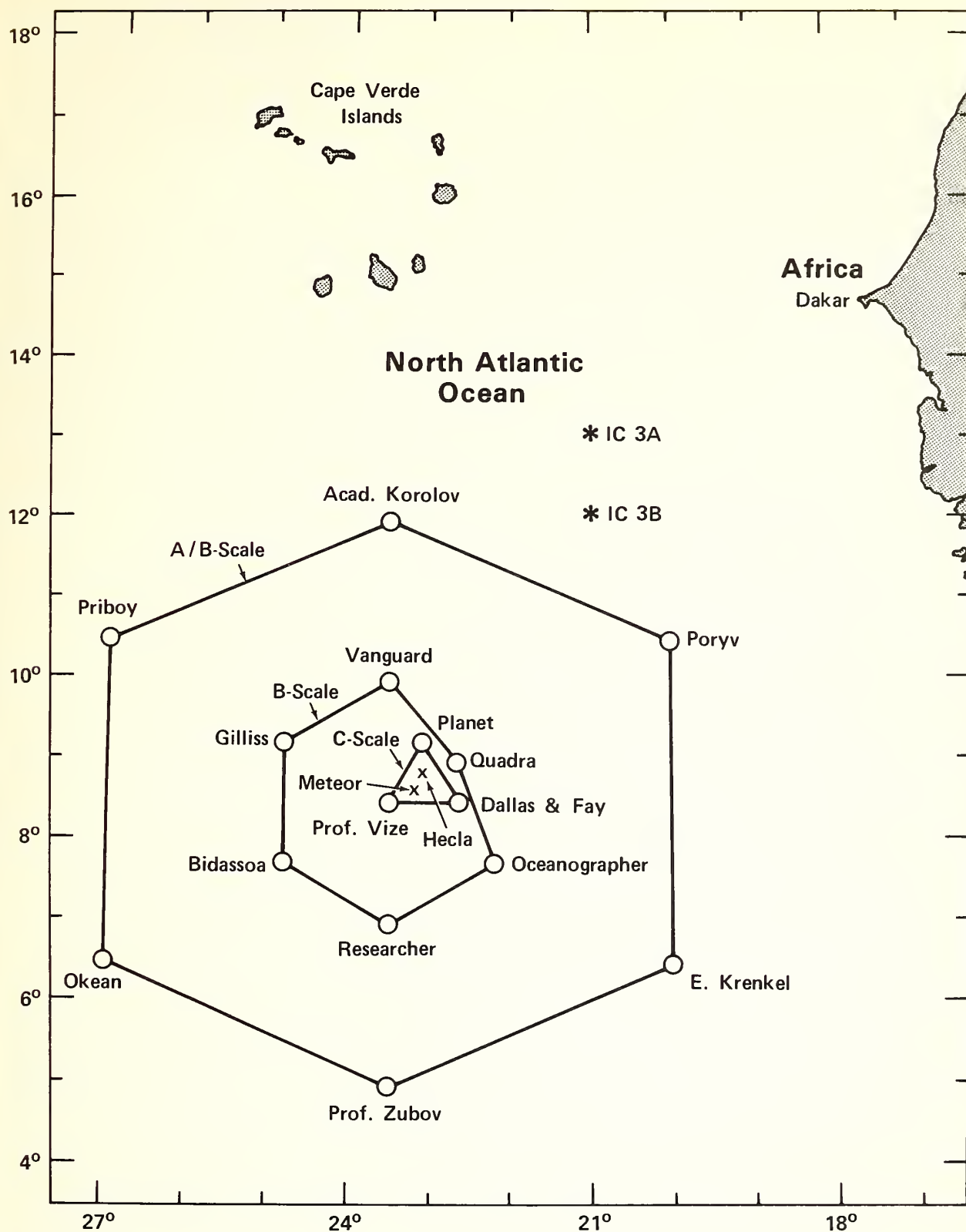


Figure 3.--Ship array during Phase III.

Between the central processing and final processing, manual data review and validation was carried out. Meteorological variables were reviewed at CEDDA, while radiation variables were reviewed at the Air Resources Laboratories in Boulder, Colorado. As a result of the review and validation, manual edit information and revised transfer equations were developed and used in the final processing.

Sections 1.1 through 1.4 present an overview of the data acquisition system, sometimes referred to as the shipboard data system (SDS). Section 2 gives, by instrument type, the sensor specifications and characteristics as defined by the manufacturer. Section 3 discusses pre- and post-GATE calibrations of meteorological and related sensors. The calibration of radiation sensors and the derivation of radiation transfer equations are discussed in section 6. Section 4 describes the procedures for assuring quality control aboard ship. Section 5 presents the details of the data processing by the U.S. National Processing center (NPC). Section 6 discusses the validation of the radiation data as carried out by the Air Resources Laboratories in Boulder. Section 7 gives an inventory of the digital data in the archives and the format of the data. Section 7.2 discusses the data available on microfilm.

Appendices in this report describe tape formats, the pre-GATE inter-comparison of pyranometers, and the translocation of thermistor probes and bridges. Transfer coefficients used in the data processing for both the meteorological sensors and the data acquisition modules are also given.

1.1 Shipboard Data System

The surface meteorological subsystem (SMSS) consisted of the pulse code modulation (PCM) tape recording system, two analog-to-digital converters used as the sensor acquisition modules (SAMs), and meteorological and radiation sensors. Figure 4 shows the total system concept in schematic form.

The GATE shipboard data system (SDS) equipment was designed to gather 8 hr of data from any or all of its subsystems onto one analog tape. The data were written in PCM form onto 1 to 7 tracks of analog tape at a real-time write speed of 1 7/8 in./s. In addition to the recording system, a 16K DEC PDP 11/20 computer was used on board all ships except the USCGC Dallas.

Each SAM (bow and central) interrogated and multiplexed a maximum of 15 sensor channels every 0.5 s. The PCM output from each SAM was then routed to the time division multiplexer. This unit combined the individual PCM signals into a single data train and converted this input into a PCM/FM output, which was then transferred to the data recording/processing patch panel for distribution to analog magnetic recorders within the data recording subsystem.

The computer, when used, converted the raw analog PCM acquisition tape to a digital "data base" tape containing all or part of the data acquired during the 8-hr acquisition period. Software also enabled some data to be reviewed by listing them in engineering units and/or plotter displays.

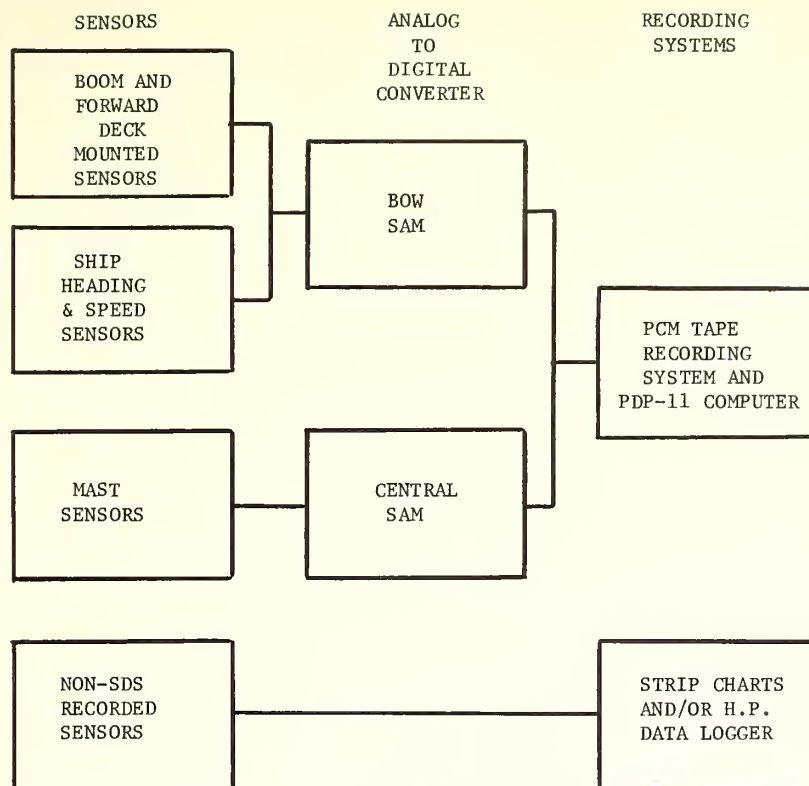


Figure 4.--Schematic of shipboard data system.

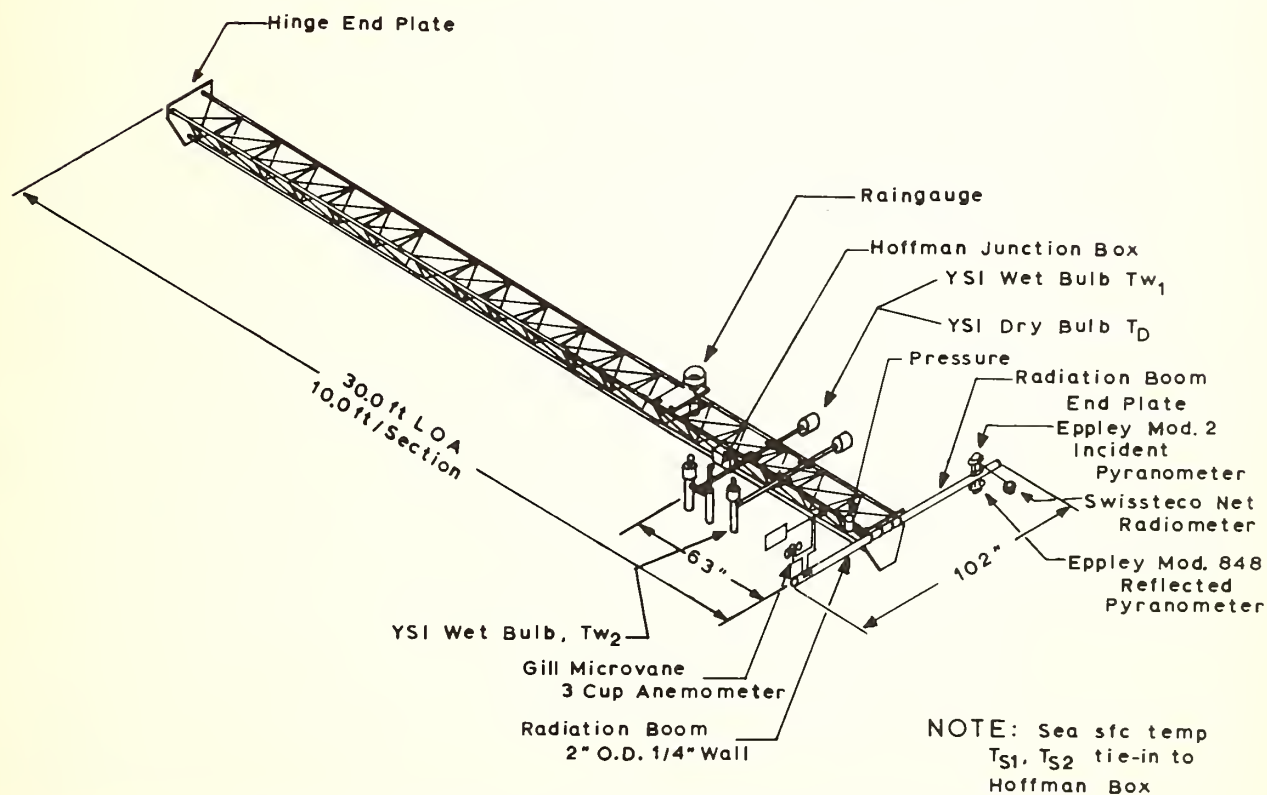


Figure 5.--Surface meteorological and radiation boom.

Simple analysis routines were available for on-board processing as well as quality control assessments.

1.2 The Bow Sensor Acquisition Module and Sensors

The bow system consisted of the 10-m bow-boom platform, SMSS sensors, and the bow SAM. The surface parameters were measured by sensors physically mounted on the boom (fig. 5) and remoted with the data signal routed to the bow SAM. Table 2 lists the sensors by SAM channel and the physical location of each. In general, the boom-mounted instruments were between 7 and 10 m above the water.

1.3 The Central Sensor Acquisition Module and Sensors

Three channels on the central SAM were devoted to SMSS sensors (table 2) and included wind speed and direction, precipitation, and atmospheric pressure. The mast instrumentation was mounted on the forward masts of the ships and ranged in height from 18 to 30 m depending on the ship.

1.4 The Boom Platform and Hardware

The bow boom system was selected as a best alternative to a meteorological instrumented buoy. The following criteria were used in the hardware design:

1. Provide the best sensor exposure with the least influence from the ship and mounting platform.
2. Minimize electronic noise from internal and external sources.
3. Sensor accessibility.
4. Incorporation of on-line and off-line standards to routinely assess sensor performance.

With the above objectives in mind, the boom (fig. 5) was constructed of lightweight tubular aluminum tower sections, with a total length of 9.1 m and a triangular cross-sectional area of 550 cm². The tubular construction provides maximum structural strength and minimizes platform cross-section. To reduce ship vibration, the boom was shock mounted at the hinge end plate, while lateral stays and uphaul and downhaul guys were used as supports to reduce horizontal and vertical flexing of the boom. The boom was attached to a moveable davit at the hinge plate so that the sensors were readily accessible for servicing. During baseline and maintenance operations, the boom was swung inboard over the ship foredeck.

During the GATE International Sea Trials (GIST) conducted in August 1973, signal problems were encountered due to radio frequency interference (RFI) and to drift of the SAM high-gain amplifiers with temperature. In an attempt to minimize RFI during GATE, all exterior cables were routed through electrical conduits to provide weather protection as well as RF shielding. The a.c. power cable to the boom was routed through a separate conduit from

Table 2.--SDS recorded sensors

Bow SAM channel	Measurement	Sensor location	Sensor height (m)			
			Researcher	Oceanographer	Gilliss	Dallas
1	Incident solar radiation	Boom	10.0	10.5	8.1	8.7
2	Reflected solar radiation	Boom	9.6	10.01	7.7	8.3
3	Net radiation	Boom	9.8	10.03	7.9	8.5
4	Spare channel	-	-	-	-	-
5	Sea temperature*	Boom	sfc	sfc	sfc	sfc
6	Excitation voltage-rain	Boom	-	-	-	-
7	Dry-bulb temperature	Boom	9.5	10.0	7.6	8.2
8	Wet-bulb temperature	Boom	"	"	"	"
9	Wet-bulb temperature	Boom	"	"	"	"
10	Spare channel					
11	Spare channel					
12	Wind direction	Boom	10.0	10.5	8.2	8.7
13	Wind speed	Boom	"	"	"	"
14	Ship heading	Midship (routed to SAM)	-	-	-	-
15	Ship speed	Midship (routed to SAM)	-	-	-	-
Central SAM channel						
6A	Wind direction-rain	Ship mast	24.1	29.6	18.3	23.8
7	Wind speed	Ship mast	"	"	"	"
8	Atmospheric pressure (Rosemount)	Ship bridge	12.6	12.3	8.2	12.5
15	Atmospheric pressure (Kollsman)	Boom	7.2	8.9	5.9	6.4

* On the Dallas, the sea surface temperature sensor was located on the bow SAM channel 10.

the signal cable. The boom-mounted Hoffman box (fig. 5) contained the thermistor signal conditioner and wind vane power supply. Remoting the signal conditioner was done to keep the thermistor leads as short as possible in an attempt to minimize RF pickup. During GATE an air-conditioned cubicle located on the foredeck aft of the boom was used to house the SAM, SAM power supply, analog recorders and test instruments, the all-sky camera, and the main cable distribution panel. This eliminated temperature-related electronic instability problems.



Figure 6.--Aspirated dry- and wet-bulb radiation shields, microvane, and cup anemometers.

2. SENSOR CHARACTERISTICS

During GIST, various types of sensors were evaluated for use in the GATE surface meteorology program. Details of the instrument evaluation are covered in earlier unpublished reports (Hanson and Poindexter, 1973; Sabol and Seguin, 1973). This section deals primarily with the SAM-recorded sensors and includes a description of the instruments and associated hardware, sensor characteristics, and, in general terms, the electronics necessary to interface the sensor output with the SAM. The SAM was set up to acquire a d.c. voltage input of 0 to + 48 mV d.c., maximum, for the radiation channels and 0 to 5 V d.c. for the meteorological channels.

2.1 Temperature

The temperatures (dry bulb, T_d ; wet bulb, T_w ; and sea surface, T_s) were measured with thermilinear thermistor probes manufactured by Yellow Springs Instruments (YSI). The nominal sensor characteristics are as follows:

1. Accuracy: $\pm 0.11^\circ\text{C}$.
2. Response time: 3.6 s (T_d), and
 ~ 9.0 s (T_w , T_s).
3. Temperature range: 15 to 45°C .
4. Range of sensor output: 0 to 50 V d.c.
5. Sensitivity: ~ 0.1660 V/ $^\circ\text{C}$.

The dry- and wet-bulb probes were housed in Gill aspirated temperature-radiation shields. The shield assembly shown in figure 6 consisted of a double wall evacuated, mirrored glass cylinder. Air was drawn up through the bottom intake and past the thermistor at a rate of approximately 4.6 m/s. The unit was oriented on the boom with the exhaust port downwind of the probe. Augstein et al. (1973) showed that radiation errors are negligible for the wet-bulb measurement if the sensor is effectively ventilated.

For the wet-bulb measurements, distilled water was fed via a wick from the water reservoir to the thermistor probe. The reservoir (fig. 6) was mounted directly above the temperature-radiation shield housing the probe. The unit was constructed of acrylic plastic, with all exterior surfaces painted with white epoxy. The "dish," convex upward, mounted above the reservoir served as a radiation shield to reduce solar heating of the reservoir water. As discussed by Hadlock, Seguin, and Garstang (1972), acrylic plastics have small values of thermal conductivity, density, and specific heat. For smooth, white surfaces, solar absorption is small.

The sea-surface temperature probe was deployed as a sea snake. A small surface float attached to the probe housing maintained the thermistor at a depth of approximately 10 cm. The sensor cable was, first, encased in an electrical shielding to minimize RF interference and this, in turn, in a

watertight plastic hosing. The thermistor was encased in a stainless steel protective housing to prevent damage to the probe. The design did, however, permit a free flow of water around the probe.

2.2 Thermistor Signal Conditioner

A signal conditioner to provide a linearized d.c. voltage output to the SAM was used for all bow-boom thermistor measurements. The units, manufactured by YSI, contained seven thermistor bridges, a 5-V d.c. power supply, and two precision calibration resistors corresponding to temperatures of 22° and 32° C. The 0- to 5.0-V d.c. bridge output corresponded to a thermistor input over the range of 15° to 45° C. During baseline operations, the calibration resistances were switched in to check each bridge output at the two calibration points. The bridge circuit excitation voltage was recorded on channel 6 (table 2) and provided a continuous monitor of the signal conditioner power supply. Since the bridge output is proportional to the excitation voltage, temperature corrections can be applied if the bridge becomes unbalanced due to changes in power supply voltage. However, the excitation voltage on all U.S. ships was extremely stable throughout GATE.

2.3 Wind Speed

The wind speed was measured with Gill three-cup anemometers manufactured by R. M. Young. The nominal sensor specifications are as follows:

1. Threshold: 0.45 to 0.54 m/s.
2. Distance constant: 2.7 m for 63 percent recovery.
3. Meteorological range: 0 to 22.4 m/s.
4. Range of sensor output: 0 to 2.4 V d.c.
5. Sensitivity: ~ 1.33 mV/0.01219 m/s.

The anemometer and wind vane were mounted on a T-shaped mounting arm on the upwind side of the boom.

2.4 Wind Direction

The sensor used to measure wind direction was the Gill microvane manufactured by R. M. Young. Its nominal specifications are:

1. Threshold: 0.45 to 0.54 m/s.
2. Delay distance: ~ 0.9 m for 50 percent recovery.
3. Meteorological range: 0° to 342° (5 percent electrical dead-band).
4. Range of sensor output: 0 to 5.0 V d.c.
5. Sensitivity: ~ 2.7 ohms/degree.

The electrical dead-band was oriented toward the stern of the ship parallel to the longitudinal axis.

2.5 Atmospheric Pressure

There were two pressure sensors on each ship: the Kollsman resonant capsule pressure transducer and the Rosemount pressure sensor. The Kollsman transducer is an aneroid capsule which is forced to vibrate at a frequency dependent upon its shape. The Rosemount sensor is a drum-like transducer with a membrane that moves inward or outward depending upon external pressure. As the membrane moves, the capacitance of the sensor changes, a quantity which is then measured and converted to pressure. The static head for the Kollsman sensor was mounted on the boom and that for the Rosemount on the mast.

2.6 Radiation

The boom-mounted radiation sensors consisted of the upfacing and down-facing pyranometers and the net radiometer. Deck-mounted units included the sunphotometer, pyrhelimeter, and pyrgeometer.

2.7 Ship Speed and Heading

Ship heading was acquired by a potentiometer mounted on a gyro repeater which was connected to the main gyro compass. Ship speed was acquired by a Sperry Doppler system on the Gilliss and by flow meters on the remaining three ships.

2.8 Precipitation

A special syphon rain gage was developed for the U.S. GATE ships. One was mounted on the bow boom and another on the foremast. These rain gages and the data derived from them is the subject of a forthcoming NOAA Technical Report ("U.S. National Processing Center for GATE: B-Scale Ship Precipitation Data," by Ward R. Seguin and Raymond Crayton).

3. PRE- AND POST-GATE CALIBRATIONS

Before, during, and after GATE, all sensors and component subsystems were calibrated or intercompared, and the results were used in the development of transfer equations. For some sensor acquisition systems, individual components were calibrated separately, and a combined transfer equation was derived to convert from raw acquisition units to scientific units. For example, temperature thermistors, thermistor bridges, and the SAMs were all calibrated separately. For other sensors, including the mast wind direction sensors and the ship heading sensor, calibrations were carried out as a single unit, from the sensor through the SAM. The transfer equations for the radiation sensors were developed as a result of the analysis and validation of the radiation data. Tables 3 and 4, and table 8 in section 6, give the transfer equations determined before and after GATE. Appendix D contains a summary of the sensor and SAM transfer equations used in the data processing.

3.1 Temperature Sensors

The thermistors for measuring air temperature, wet-bulb temperature, and sea-surface temperature were calibrated before and after GATE in May and November 1974. A third calibration of the sea-surface probes was carried out in December 1975 because of some uncertainties in the previous calibrations.

The thermistor probes were calibrated by means of a Masterline 2095 temperature water bath and circulator. Each probe was connected to the signal conditioner bridge, and the output voltage, V_o , of the signal conditioner bridge was measured as a function of temperature. The calibration was carried out in 1°C intervals over the range of 19 to 35°C as a function of, first, increasing temperature, and then decreasing temperature. The same standard, a National Bureau of Standards (NBS) traceable mercury thermometer (bomb calorimeter), was used for all probes.

Table 3 shows the transfer equation coefficients resulting from the pre- and post-GATE calibrations. The underlined values are those used in the final processing. Also shown are equivalent temperatures for 1.6- and 2.2-V output by the signal conditioners. The differences between the pre- and post- calibrations are generally less than 0.1°C . The Dallas sensor 134 and the Researcher sensor 126 failed before the last calibration.

Proper and accurate thermistor calibration required that the thermistor be calibrated while connected to the same bridge mounting used during the field operations. Most of the thermistors were calibrated in this manner. However, a few thermistors were calibrated through different bridges. For these sensors it was necessary to determine the bridge calibration. The method used to mate the bridge calibration with the sensor calibration is discussed in appendix C.

The signal conditioners contained seven separate thermistor bridges and two precision fixed resistances (calibration positions 1 and 2), which corresponded to temperatures of 22° and 32°C . The calibration of each bridge

Table 3.--Transfer equation coefficients (volts to degrees Celsius) and equivalent temperatures for pre- and post-GATE temperature probe calibrations (underlined values are those used in the processing)

Ship	Sensor and serial No.	Pre-GATE		Temperature equivalent (°C)		Post-GATE		Temperature equivalent (°C)	
		calibrations coefficients C ₁	C ₂	1.6 V	2.2 V	calibrations coefficients C ₁	C ₂	1.6 V	2.2 V
<u>Researcher</u>	T (dry bulb) - 51	5.988	15.09	24.58	28.14	5.953	15.02	24.54	28.12
	T (dry bulb #1) - 55	<u>5.996</u>	<u>15.12</u>	24.62	28.19	5.965	15.03	24.57	28.15
	T (wet bulb #2) - 56	<u>6.006</u>	<u>15.09</u>	24.59	28.16	5.951	15.03	24.55	28.12
	T (sea) - 126	<u>6.021</u>	<u>14.99</u>	24.62	28.23	unavailable			
<u>Gilliss</u>	T (dry bulb) - 53	6.009	15.09	24.70	28.31	5.994	15.03	24.62	28.22
	T (wet bulb #1) - 59	6.023	15.10	24.74	28.35	<u>6.013</u>	<u>15.02</u>	24.64	28.25
	T (wet bulb #2) - 60	5.995	15.00	24.59	28.19	<u>5.998</u>	<u>14.82</u>	24.42	28.02
	T (sea) - 127					<u>5.981</u>	<u>15.01</u>	25.77	28.17
<u>Dallas</u>	T (dry bulb) - 54	6.007	15.00	24.61	28.22	5.995	15.06	24.65	28.25
	T (wet bulb #1) - 61	5.997	15.09	24.68	28.28	<u>5.958</u>	<u>15.08</u>	24.61	28.19
	T (wet bulb #2) - 62	5.995	15.08	24.67	28.27	<u>5.988</u>	<u>15.00</u>	24.58	28.17
	T (sea) 134 (7)	6.063	15.00	24.70	28.34	unavailable			
	T (sea) 134 (4)	<u>6.054</u>	<u>14.91</u>	24.60	28.23	unavailable			
	T (sea) - unknown	unavailable				<u>5.962</u>	<u>15.15</u>	25.88	28.27
<u>Oceanographer</u>	T (dry) - 52	6.017	15.08	24.70	28.32	5.985	15.02	24.60	28.19
	T (wet bulb #1) - 57	6.010	15.03	24.65	28.25	<u>5.978</u>	<u>15.05</u>	24.62	28.20
	T (wet bulb #2) - 58	6.020	15.08	24.71	28.32	<u>5.984</u>	<u>15.14</u>	24.71	28.30
	T (sea) - 129	5.999	15.05	25.84	28.24	<u>6.005</u>	<u>14.94</u>	25.75	28.15

consisted of measuring the output voltage, V_o , as a function of resistance. A standard precision resistance decade box was used for this test. The resistance was varied over the range of 6500 to 11,999 ohms in 500-ohm intervals. Following the resistance test, the output voltage of each bridge for the two calibration positions and the output of the bridge excitation voltage, V_{oex} , were checked.

3.2 Wind Sensors

The 13 R. M. Young cup anemometers were calibrated as stand-alone sensors in the wind tunnel facility of the Department of Environmental Sciences, University of Virginia, before and after the experiment. The wind tunnel used was a large-volume, low-speed unit. The individual sensors were calibrated over the range of approximately 0.5 to 16.0 m/s.

The calibration consisted of measuring the voltage output, V_o , of the anemometer generator vs. the tunnel wind speed corrected for atmospheric pressure, temperature, and humidity. Two runs were made for each sensor: increasing wind speed from approximately 0 to 16 m/s and decreasing from 16 to 0 m/s in 21 incremental steps. Each step corresponded to an increase or decrease of 0.5 in the tunnel drive motor speed. In practice, the anemometer was allowed to settle down at each motor setting for about 5 min.

Table 4 shows the transfer equation coefficients resulting from the pre- and post-GATE calibrations of the stand-alone sensors. Pre-GATE transfer equations were used in the final processing. With the exception of the boom wind speed sensor on the Gilliss, differences between pre- and post-GATE transfer equations were generally less than 0.3 m/s.

An 1800-rpm constant-speed, synchronous drive motor was used for all baseline checks at sea. The initial calibration consisted of checking the anemometer output voltage corresponding to a rotation of 1800 rpm. All subsequent baseline values obtained at sea were referenced to the initial value.

Before GATE, the wind vanes were calibrated in position on the boom and/or mast from the sensor through the SAMs. In the case of the boom vanes, the dead-band was oriented parallel to the boom facing aft (180° relative to the boom outboard). The initial sighting in of the vane relative to the boom and the boom relative to the centerline of the ship was done with a theodolite. The vane was rotated first clockwise, then counterclockwise, taking readings of output voltage, V_o , vs. relative position in degrees rotation. The calibration positions corresponded to vane headings of 10, 60, 120, 180, 240, 300, and 357° . Second, the vane was locked in position with a pin and collar device, and V_o readings were taken at the four baseline check positions of 0, 90, 180, and 270° . The full calibration (above procedure) was carried out only for the four boom-mounted vanes. In the case of the mast vanes, the deadband was located 180° relative to the longitudinal axis of the ship. Following the experiment, the outputs of the sensors were checked for linearity but were not recalibrated.

Table 4.--Transfer equations (volts to meters per second) and equivalent wind speed for pre- and post-GATE anemometer calibrations (pre-GATE coefficients were used in the final processing)

Ship	Sensor serial No. and location	Pre-GATE calibrations coefficients		Wind speed equivalents m/s		Post-GATE calibrations coefficients		Wind speed equivalents m/s	
		C_1	C_2	0.1 V	1.0 V	C_1	C_2	0.1 V	1.0 V
<u>Researcher</u>	151-boom	<u>9.782</u>	<u>-0.05</u>	0.9	9.7	9.445	0.29	1.2	9.7
	176-mast	<u>9.721</u>	<u>0.01</u>	0.9	9.7	9.433	0.22	1.2	9.6
<u>Gilliss</u>	153-boom	<u>9.379</u>	<u>0.06</u>	1.0	9.4	8.470	2.19	3.0	10.7
	178-mast	<u>9.356</u>	<u>-0.04</u>	.9	9.3	9.275	0.23	1.2	9.5
<u>Dallas</u>	154-boom	<u>9.902</u>	<u>-0.01</u>	1.0	9.9	9.804	0.19	1.2	10.0
	182-boom	<u>9.319</u>	<u>0.03</u>	1.0	8.4	9.656	0.20	1.2	9.8
	179-mast	<u>9.917</u>	<u>-0.07</u>	1.0	9.8	9.782	0.13	1.1	9.9
<u>Oceanographer</u>	152-boom	<u>9.874</u>	<u>-0.073</u>	.91	9.8	9.565	0.48	1.1	9.7
	177-mast	<u>10.241</u>	<u>-0.057</u>	.97	10.2	10.008	-0.22	.78	9.8

C_1 = slope (m/s/V); C_2 = intercept (m/s)

Table 5.--Pre- and post-GATE pressure equivalents for
Kollsman counts derived from calibration

Ship	Sensor No.	Kollsman output counts	Pressure equivalents (mb)		Difference (mb)
			Pre-GATE	Post-GATE	
<u>Researcher</u>	101	1,019,797	1005.99	1006.13	+0.14
		1,018,302	1012.86	1013.00	+0.14
		1,016,817	1019.72	1019.88	+0.16
<u>Gilliss</u>	104	1,012,924	1006.02	1006.13	+0.11
		1,011,438	1012.96	1013.00	+0.04
		1,009,978	1019.82	1019.88	+0.06
<u>Dallas</u>	454*	901,679	1006.32	1006.13	-0.19
		900,228	1013.24	1013.00	-0.24
		898,795	1020.11	1019.88	-0.23
<u>Oceanographer</u>	102	1,023,330	1005.97	1006.13	+0.16
		1,021,794	1012.89	1013.00	+0.11
		1,020,288	1019.71	1019.88	+0.17

*The pre-GATE calibration was nearly 1 year before GATE.

3.3 Pressure Sensors

Three of the four Kollsman pressure sensors were factory calibrated immediately before GATE, and the fourth, used on the Dallas, nearly 1 year before. Following the experiment, all units were calibrated by the National Bureau of Standards (NBS). Table 5 gives the pressure equivalents for the Kollsman output (counts) derived from the pre- and post-GATE calibrations. The largest difference, a change of 0.24 mb, was shown by sensor 454, which was used on the Dallas.

3.4 Ship Heading and Speed Sensors

The ship heading sensors were precision potentiometers interfaced to one of the ship's gyro repeaters. All units were calibrated statically by manually rotating the output potentiometer in incremental steps and recording the output vs. the ship headings. The ship speed sensors were also calibrated by placing the sensor in a "simulate" mode and recording the output in incremental steps.

4. PROCEDURES FOR ASSURING QUALITY CONTROL AT SEA

The operating procedures for the surface meteorological system were designed to assure data of high quality. Systematic procedures were set up to check the SAMs and sensors individually. Five operating modes for the bow and central SAMs were defined and used operationally at sea:

1. Acquisition (bow and central SAM).
2. Simulate (bow and central SAM).
3. Baseline substitution (bow SAM only).
4. Baseline full (bow SAM - central SAM).
5. Maintenance (bow SAM - central SAM).

Figure 7 schematically illustrates the operational modes and the components they included relative to the bow-boom hardware.

The normal mode was the data acquisition mode. The boom was in an out-board position and sensors were acquiring real data.

The simulate mode was designed for checking the SAM calibration and stability. A switch on the SAM enabled the operators to take the sensors off line and input precision fixed voltages of 0, 4, 8, and 40 mV, and 2 and 4 V. The simulation was performed three times per day or once for every PCM acquisition tape. The SAM outputs corresponding to these precision input voltages were checked against strip charts, computer readouts, binary values on the voltage digitizer box and on the decommutation display units. These test data were compared with established "tolerance windows" for each SAM channel.

The baseline substitution was designed for checking the YSI thermistor bridges and the boom rain-gage electronics. To check the thermistor bridges, precision resistances corresponding to ambient temperatures of 22 and 32°C were switched in, replacing the YSI thermistors. This test together with a simultaneous reading of the bridge excitation voltage, V_{oex} , was used to assess the performance of each individual bridge, and was conducted routinely. The outputs were checked in the same way as for the simulate mode.

Table 6 gives the maximum possible temperature deviations due to the temperature bridges and the SAM instabilities based upon baseline substitutions. As seen, the hardware associated with the thermistor bridges and the SAM were extremely stable, with maximum deviations of less than 0.05°C.

The baseline full testing was used for checking the entire system (sensor through to SDS). During the test, the sensors were on-line in a controlled environment and compared against independent standards. At sea, these tests were performed on the boom temperature, precipitation, and wind sensors. The temperature sensors were placed in a stirred, water-filled

Table 6.--Maximum possible temperature deviations due to temperature bridges and SAM instabilities based on baseline substitutions

Ship	Variable	Low reference (~22°C)	High reference (~32°C)
<u>Researcher</u>	Temperature	-0.01	-0.02
	Wet-bulb temp. #1	-0.02	-0.03
	Wet-bulb temp. #2	-0.01	-0.02
	Sea surface temp.	-0.01	-0.02
<u>Gilliss</u>	Temperature	-0.01	-0.02
	Wet-bulb temp. #1	-0.00	-0.01
	Wet-bulb temp. #2	-0.01	-0.02
	Sea surface temp.	-0.01	-0.02
<u>Dallas</u>	Temperature	-0.01	-0.02
	Wet-bulb temp. #1	-0.01	-0.02
	Wet-bulb temp. #2	-0.01	-0.02
	Sea surface temp.	-0.01	-0.03
<u>Oceanographer</u>	Temperature	-0.02	-0.02
	Wet-bulb temp. #1	-0.04	-0.02
	Wet-bulb temp. #2	-0.01	-0.01
	Sea surface temp.	-0.02	-0.01

container and the readings compared with the working standard mercury thermometer. Wind speed sensors were rotated at a fixed 1800 rpm, and wind direction sensors were locked in position in the four cardinal directions relative to the boom. The rain-gage test consisted of pouring a standard volume of water, 250 ml, through the sensor at a predetermined drip rate for a period of 20 min. The outputs were checked by the same readout methods as previously described.

The maintenance mode was used whenever sensors were replaced, during periods of cleaning and preventative maintenance, and whenever the system was down for test and/or repair.

At sea, quality assurance spot checks were conducted on a nonscheduled basis. This consisted of comparing, in real time, manual instrument readings with the automatically acquired data. These "ball park" comparisons were intended as a means of identifying possible sensor and/or system malfunctions in as real time as possible. During in-port periods, baseline testing and maintenance was performed on the mast wind and precipitation sensors.

The order and frequency of the various operating modes, and the details of the procedures used have been described by Echternacht (1974a, 1974b). Field personnel deviated somewhat from the operations schedule, making it necessary for data users to go through the data logs (GATE Worksheet 42) to determine how the data quality control procedures were carried out.

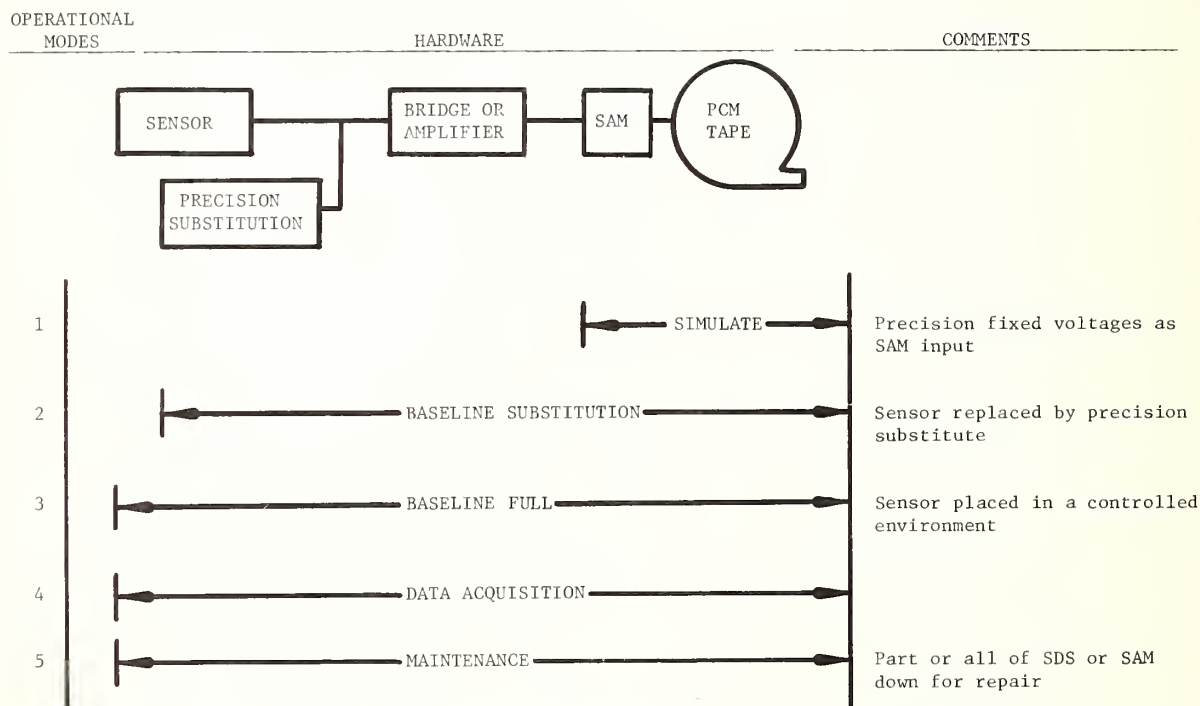


Figure 7.--The SDS components involved in the various operational modes for the bow-boom hardware.

5. DATA PROCESSING

The GATE surface meteorological data were processed in several discrete steps: preprocessing, central processing, review and validation, and final processing. The meteorological and radiation data were all passed through these processing steps at the U.S. National Processing Center, CEDDA. Review and validation of the meteorological data were also performed by CEDDA, while the Air Resources Laboratories (ARL) in Boulder reviewed and validated the radiation data. The results of ARL's analysis is the subject of section 6. Discussion of review and validation procedures in this section is limited to meteorological variables.

5.1 Preprocessing

The SDS collected data from up to six instrumentation subsystems and recorded them on one of six tracks of an analog magnetic tape in a pulse-code-modulation (PCM) form. The date and time of day was continuously recorded on the seventh track of the PCM tape. On the data tracks, information was collected as 16-bit words, forming 256-bit data frames. The frames of data from the SDS were recorded continuously onto PCM tapes. There were two PCM tape recorders with each SDS. The tapes were changed three times per day by mounting new tapes, recording in parallel on both tapes for a short time, and then dismounting the full tapes. Each tape contained approximately 8 hr of information with a short period of overlap.

The PCM tapes were decommutated and processed by the PDP-11 using the Acquisition Program. It was the function of this program to convert the data from a PCM track-per-system format to the 800-BPI NRZI format, which is readable by most modern computers. The Acquisition Program produced one 2400-ft reel of digital tape for each PCM tape, or approximately 8 hr of data.

The Acquisition Program's output tape was then run through the Clean-Up Program. This program prepared the data for the Strip Program, which followed, by manipulating and correlating data record times to ensure that incoming groups of records, called partitions, contained complete logical records.

The Strip Program stripped the data from the Clean-Up Program output file and set up continuous time-series files for each subsystem, including the surface meteorological and radiation subsystems. One of the Strip Program outputs was a digital tape (called the acquisition file) containing surface meteorological and radiation data, which were then processed by the Surface Meteorological Data Subsystem Program, discussed below.

5.2 Central Processing

The central processing program was the Surface Meteorological Data Subsystem (SMDSS) Program. This program made the first pass on the data and was designed to convert the data from recording units to scientific units, convert the relative wind velocities to true wind velocities, and

automatically edit the data. Central processing also included generation of 4-s average microfilm time-series plots for the review and validation discussed in section 5.3

The flow chart for the SMDSS Program is shown in figure 8. The program had three different and separate start procedures, and their use depended upon the following:

- o the run was on the first acquisition data tape of a series of tapes of a continuous data period;
- o the run was on an acquisition data tape following the first tape, and there were no changes in sensor transfer equations; or
- o the run was on an acquisition data tape following the first tape, and there were changes in sensor transfer equations.

In processing the initial tape of a series of tapes of a continuous set of data, the program first read a master list of constants. This list of constants defined sensor identification and serial numbers, transfer equations, and reasonable maximum and minimum values for each variable used in editing. The constants were then saved on an output file of the SMDSS Program at the termination of processing of the initial acquisition tape. This output file was called the partially processed file (PPF).

With the start of processing of the second, and subsequent, acquisition tapes, the SMDSS Program read the PPF that contained the constants of the master list and partial sums of averages of data spanning the first and second tapes (or adjacent tapes). On restarts it was occasionally necessary to modify some of the transfer equations for certain data. When this was required, the PPF and then an updated master list were read.

On the initial run, the SMDSS Program was required to set up tables and a directory in order to keep track of sensor identification numbers, serial numbers, and transfer equations; to determine which sensors collected the data; and to compute the number of sensors measuring each variable. This was particularly important to ensure that each incoming data value was processed with the proper constants. These tables and the directory were saved from one tape to the next through the PPF.

The program was also required to properly position the acquisition file of the next tape to that of a previously terminated run if termination occurred before the end of the data had been reached.

Once the SMDSS Program had completed all preliminary steps mentioned above, it read records of meteorological and navigation data and began processing with subroutine CLOUD. This subroutine converted the raw data from recording units (counts) to scientific units, compared the data with reasonable maximum and minimum values, compared data on the same variable but measured by different sensors, and converted the relative wind velocities to true wind velocities using ship heading and velocity. Only the Kollsman

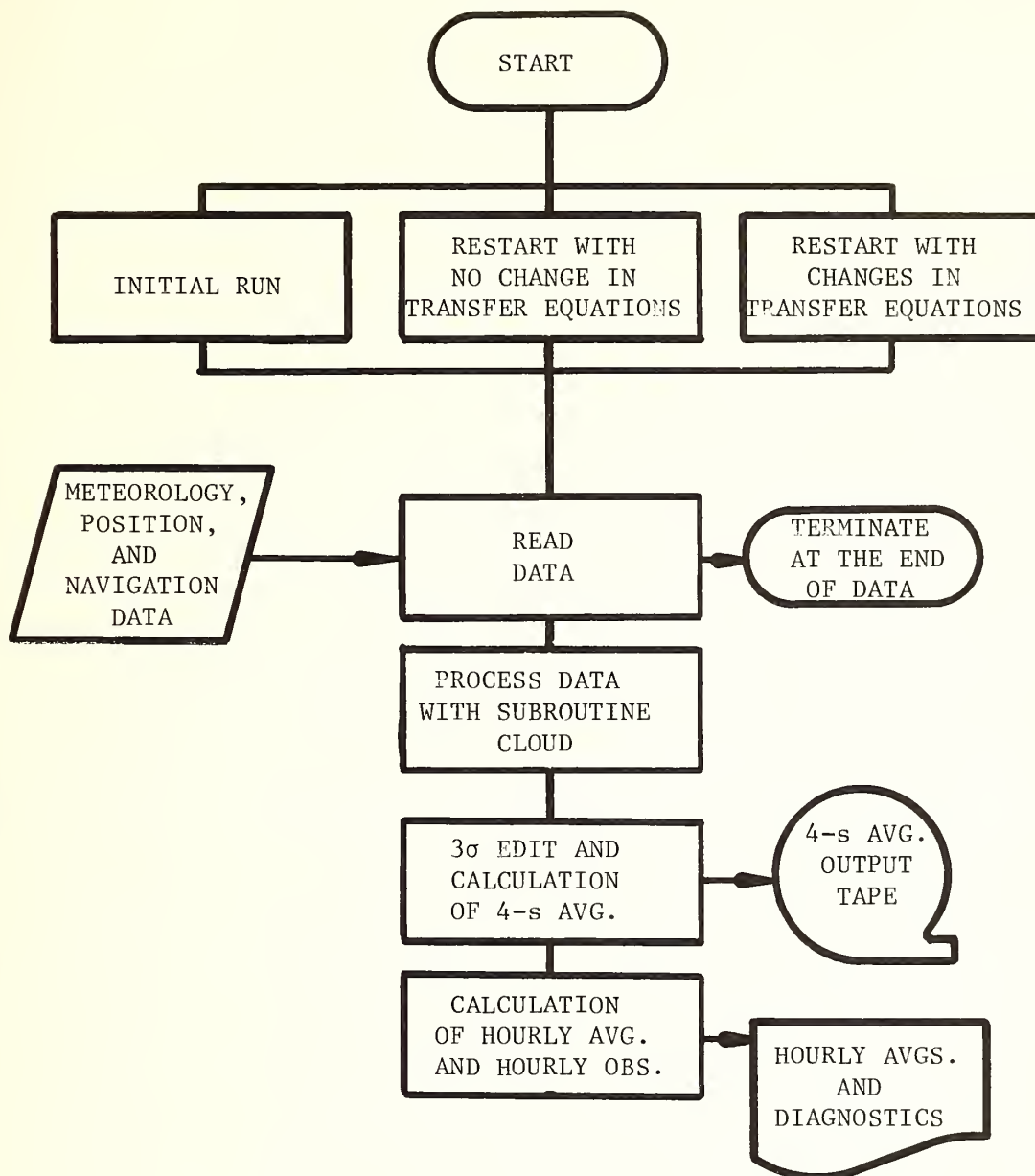


Figure 8.--The SMDSS Program.

pressure data required nonlinear transfer equations (sec. 3). All pressure transfer equations were adjusted so that the pressures were true at sea level. The program also kept track of how long a particular sensor or variable was bad and printed this information out for later diagnostic review.

Each half-second value of relative wind direction was corrected as follows for ship velocity and heading:

First the direction corrected for ship heading was calculated,

$$dd_c = dd_r + H,$$

where

dd_r = relative or raw wind direction in degrees, and

H = ship heading in degrees.

If dd_c was less than zero, 360° were added to it. Using the relative wind speed ff_r , the u_r - and v_r - components of the relative wind were calculated,

$$u_r = ff_r * \sin \left[(dd_c - 180) / \pi \right],$$

$$v_r = ff_r * \cos \left[(dd_c - 180) / \pi \right].$$

The u - and v -components of the ship's velocity (u_s , v_s , respectively) were added to u_r and v_r to produce the components of the absolute velocity of wind (u_a , v_a , respectively).

$$u_a = u_r + u_s \text{ and } v_a = v_r + v_s,$$

and the magnitude and direction of the winds were calculated using

$$ff_a = \left(u_a^2 + v_a^2 \right)^{1/2}$$

and

$$dd_a = \text{ARCTAN2}(u_a, v_a) * \pi + 180^\circ \cdot \frac{2}{\pi}$$

*The ARCTAN2 is a special IBM 360/65 computer function that returns angles between -180 and $+180$, and angles increase in a positive sense.

Once the u - and v -components of the wind had been calculated, all the scalar variables^a (including the u - and v -components of the wind) were edited with a 3-standard deviation rejection scheme. Three minutes of data from each variable (360 values for the 0.5-s data) were used to calculate a 3-min average and standard deviation. Any values exceeding plus or minus 3 standard deviations of the mean were flagged as erroneous data.

The program then calculated a 4-s average from the unflagged data and placed these on an output file. At the same time, the program accumulated these 4-s averages to calculate hourly averages and hourly observations. The hourly averages were calculated by summing data from 00.0 to 59.9 min of each hour. The hourly observations were calculated by summing and averaging each variable except pressure from 50.0 to 59.9 min of each hour. Pressure was summed and averaged from 55.0 to 04.9 min of each hour.

If any of the components used to calculate the true wind speed were missing, such as the ship's heading or the ship's velocity, the true wind velocity and its components were not computed. Average wind directions were calculated from corrected average wind components,

$$\overline{dd}_a = \text{ARCTAN2}(\overline{u}_a, \overline{v}_a) * \pi + 180,$$

where the averaging interval (shown by the bar) varied from 4 s to 1-hr average.

The average wind speeds were not computed from the wind velocity components. The corrected half-second wind speeds were used to calculate 4-s average scalar wind speeds, and from these, the hourly averages and observations were calculated.

The program generated an output file of digital 4-s averages, which were used in generating microfilm time-series plots. The time-series plots, in turn, were used in data validation and review, discussed below.

The SMDSS Program terminated when it reached the end of the input data files. It then saved the PPF, which contained the master list of constants, the partial sums of averages, and the directory of incoming data.

5.3 Data Review and Validation

The data were reviewed and validated in several ways. First, the time-series plots of 4-s average data were reviewed for bad data that the automatic editing schemes of the SMDSS Program had failed to catch. For example, radio transmissions often interfered with the temperature data and occasionally the wet-bulb wicks dried out. The hourly observations were compared with the standard WMO marine observations made on every ship. This was accomplished by computer. In addition, the observations from the formal Intercomparisons were available for most of the ships that participated in them, and these were also used for validation purposes. The results of the analysis of the international data are available in a Convection Subprogram Data Center report (Godshall et al., 1976).

The times of the erroneous data were noted for deletion in the final processing discussed in section 5.5. In instances where serious biases were noted and could be explained, new transfer equations were derived and applied to the data in final processing.

5.4 Peculiarities in the Meteorological data

Each of the sensors used had its own particular difficulty, and the behavior of some sensors varied from ship to ship. The variables and the sensing systems used to measure them are discussed in detail below.

5.4.1 Temperature

All the temperature data, including the dry- and wet-bulb temperatures and the sea-surface temperatures, were degraded by RF noise caused by the ships' radios. Figure 9 shows an example of this problem in the temperature data, collected by the Oceanographer, which operated its radios intermittently throughout the day. The Dallas generally restricted its transmissions to the periods 0800 to 0900 and 2100 to 2200 GMT.

In the wet-bulb temperature sensors, the wet-bulb wick occasionally dried out. This problem was most serious during Intercomparison 1 (IC 1). Subsequently, the design of the wet-bulb wick wetting system was changed, and the problem was almost completely resolved. On the Gilliss however, the problem remained an intermittent one.

The sea-surface temperatures contained two additional sources of error in addition to the RF noise mentioned above. First, whenever the sensor was pitched out of the water because of ship motion, or when the sensor was lifted out of the water, the wet-bulb cooling effect could be seen in the data as erroneously cool temperatures. The second source of error was caused by pools of engine cooling water (warm water), which stagnated around the ship. This problem was particularly acute during IC 3. Figure 10 shows an example of the warm engine cooling and its influence on the sea-surface temperatures around the Gilliss. The Oceanographer had a similar problem, but its effects were not as evident as on the Gilliss and therefore were more difficult to isolate and remove.

In general, all these effects on the temperature data were removed from the final archived data. There were periods during IC 3 for the Oceanographer when removing the warm water effects of the engine would have meant deleting a large percentage of the data.

5.4.2 Wind Direction and Speed

The quality of the processed and archived wind data depends not only upon the quality of the relative wind speeds and directions measured on ships but also upon the ships' heading and velocity data. The ship heading data were derived from the main gyros on each ship. Ship velocities were derived from the navigation data, which have been archived at the National Climatic Center, Asheville, North Carolina. The processing of these data is discussed in a report now in preparation (Seguin and Crayton, 1977).

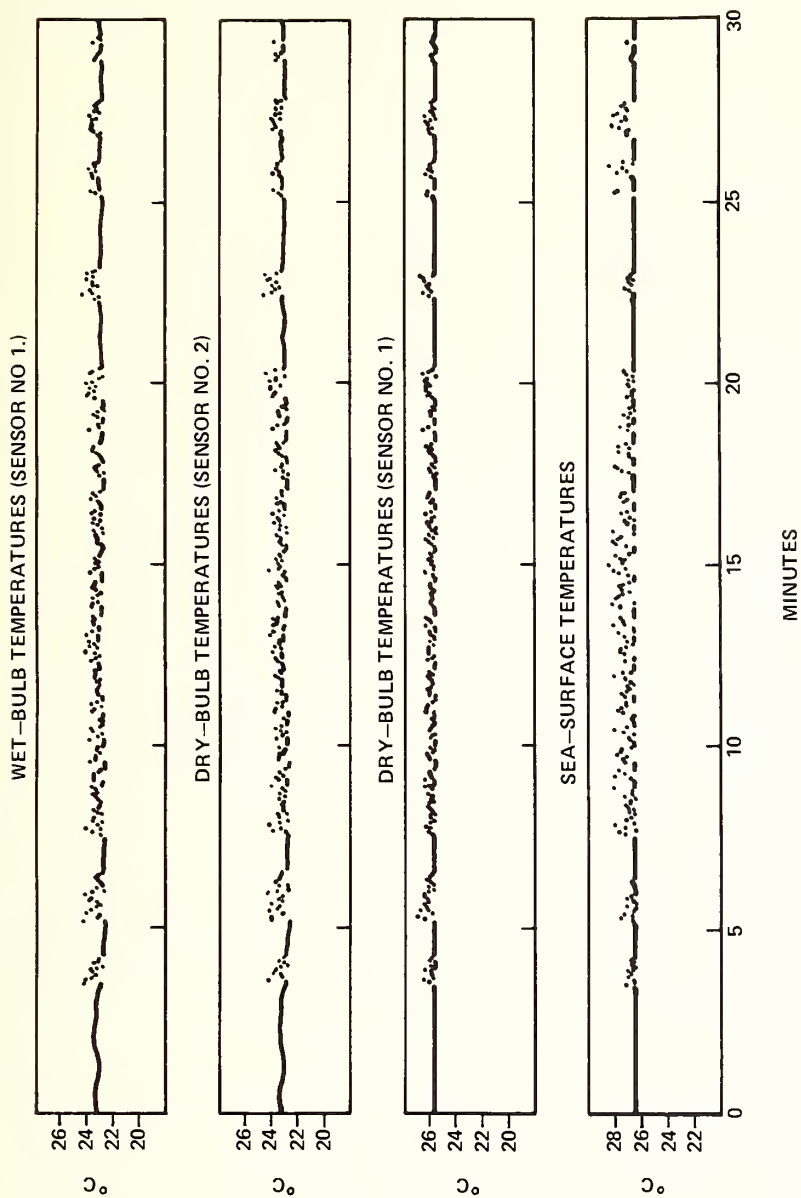


Figure 9.--Example of RF noise in the temperature data.

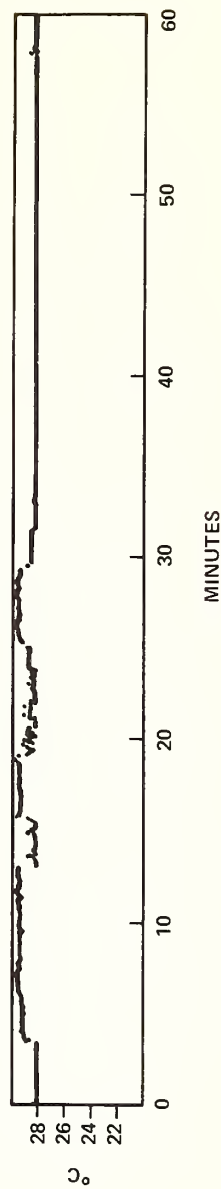


Figure 10.--Example of ship engine cooling water influence on sea-surface temperature data.

The wind speed and direction sensors yielded very good data. The exterior shell of the Researcher's mast wind direction sensor rotated 47° before the start of IC 1. The sensor was readjusted after IC 1, and no problems were encountered during the remainder of GATE. The data for IC 1 were corrected based upon the result of a comparative analysis of the data from the Researcher and other international ships.

The Dallas' boom wind speed data, which have been archived, are questionably low for the time periods of Phase III shown in table 7. The problem is believed to be linked to a faulty sensor.

Table 7.-- Questionable Dallas bow-boom wind speed data

From		To	
Date	Time (GMT)	Date	Time (GMT)
Sept. 8	0600	Sept. 8	2200
Sept. 9	0900	Sept. 10	0700
Sept. 11	2200	Sept. 12	0000
Sept. 12	1300	Sept. 15	0600
Sept. 16	1400	Sept. 18	0100

The Dallas ship heading data required special processing because of sensor abnormalities discussed in the next section.

The Gilliss data exhibited two other peculiarities. First, the ship would steam occasionally with the wind and sometimes at approximately the same speed as the mean wind speed. In such instances, the boom anemometer cups would stop. Yet the indicated wind speed was greater than zero. The velocity of the ship was not zero, however, and it is this velocity that caused the non-zero wind speed.

Second, the rocking motion of the Gilliss frequently shows up in the wind speeds and directions as measured by both mast and boom sensors. This feature is most noticeable during periods of light wind speed. Figure 11 shows this effect in some 0.5-s data. Note that amplitude of the oscillations in the mast wind directions exceeds that of the boom.

5.4.3 Ship Speed and Heading

The ship speeds as measured by underwater sensors are of poor-to-useless quality for all the U.S. ships. Relative changes in the speeds are discernible for the Oceanographer and Dallas, but the magnitudes are not correct. The Gilliss sensor apparently failed after Phase I and the Researcher's sensor was not recorded after Intercomparison 2. None of these ships' speeds were used as part of the ship velocity corrections to the wind speeds.

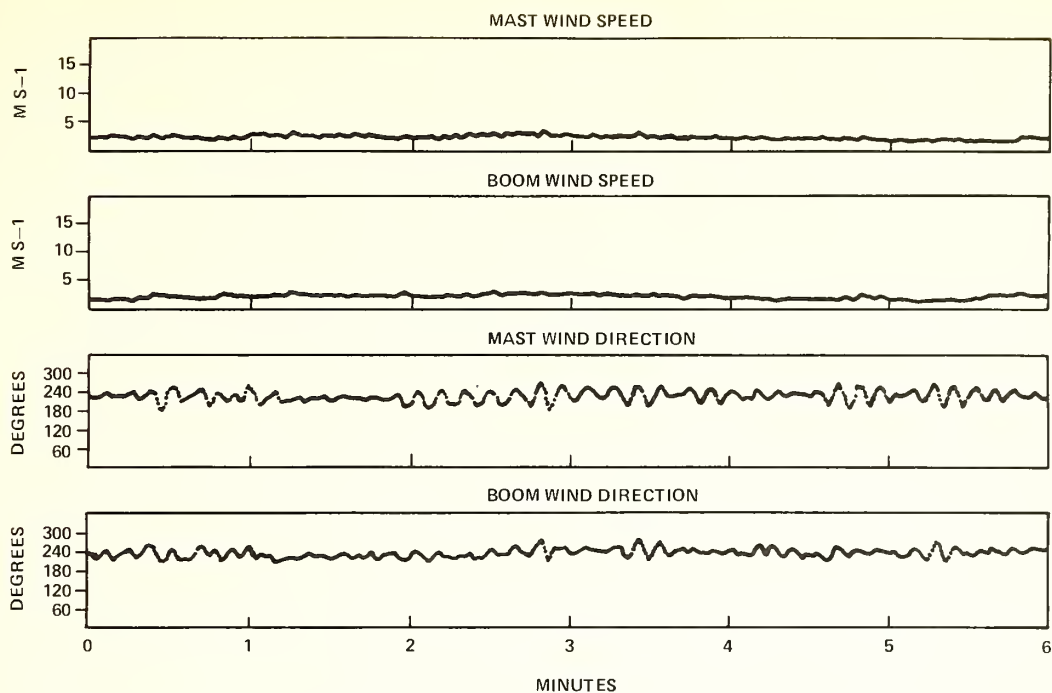


Figure 11.--Example of oscillations in Gilliss 0.5-s wind speed data caused by ship's roll.

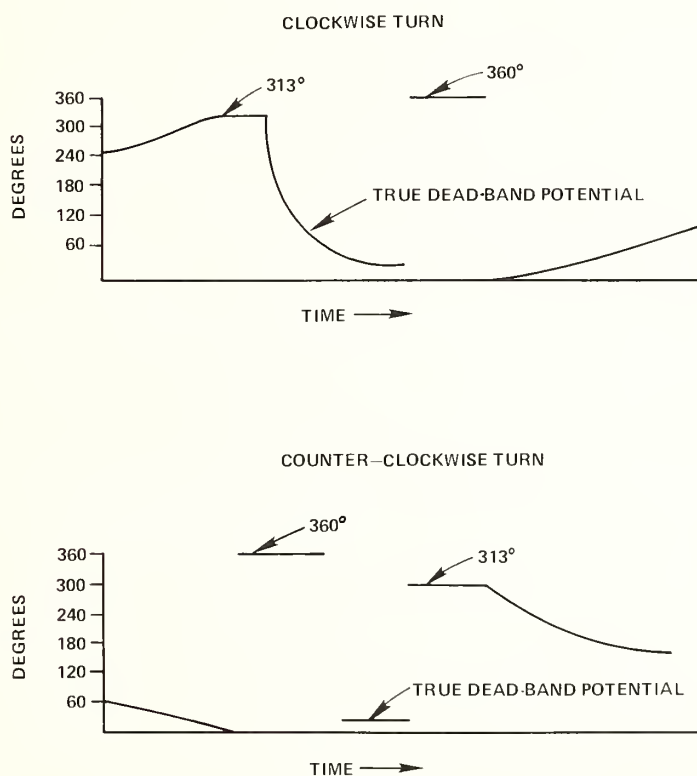


Figure 12.--Dallas indicated ship headings for clockwise and counterclockwise turns.

The Dallas was the only ship that had problems with its ship heading sensing system. The principal problem originated with the potentiometer, which was mounted on a repeater of the main gyro compass and had abnormally large contact strips at each end. The net result was a loss of continuous direction information between 313° and 360° , since the voltage put out by the potentiometer was constant for the directional width of the strip. Figure 12 shows a time-series plot of the ship heading for a clockwise and for a counterclockwise turn. For a clockwise turn, the indicated ship headings in passing from 313° to 360° would stall for a while on 313° and then exhibit an exponential decay and finally jump to 360° , remaining there until the ship heading had reached 01° . This exponential decay was due to the falloff in the electrical potential through the potentiometer as ship headings passed through the true dead-band of the potentiometer.

To determine the width of the contact strips in terms of ship heading in degrees, an analysis was made of the Dallas heading data for periods when the ship made a continuous and uniform turn through 313° to 360° . Only cases where the rate of turn was held constant were used. It was found that while the ship heading was indicated as 313° , the direction could be any value between and including 313° and 334° . For an indicated direction of 360° , the ship heading could have been 338° to 360° . The true dead-band of the potentiometer was 335° to 337° . In an attempt to recover what amounted to lost ship heading data and hence wind velocity data, a value of 324° was assigned to the ship heading whenever the output indicated 313° , a value of 349° was assigned whenever the output indicated 360° , and a value of 336° was assigned whenever the ship reading was in the dead-band of the potentiometer. This assured that the maximum error in ship heading would be 11° .

A computer program was designed to automatically assign the above ship headings whenever the indicated ship heading fell between 313° and 360° . The time periods when the ship headings were in the dead-band were determined by examining microfilm time-series plots. This information was entered into the program that corrected the ship headings.

The ship heading data for the remaining three ships presented few if any problems. In general, the few problem areas that did exist were removed from the archived data.

5.4.4 Pressure

There were two pressure sensing systems on each of the U.S. ships, the Kollsman and Rosemount. Generally speaking, the Kollsman is more accurate and more stable. The Rosemount pressure sensor drifted by 0.5 to 1.0 mb in both the long and short term (Godshall et al., 1976). The Oceanographer's Kollsman sensor functioned erratically during the experiment and much of these data are missing for Phase II. In addition, the Oceanographer's Kollsman data contain high-frequency fluctuations that are not contained in the Researcher, Gilliss, or Dallas Kollsman data. Late in Phase II, the Dallas Kollsman sensor drifted almost 1 mb.

5.5 Final Processing

The objectives of the final processing programs were to rescale some of the data using revised transfer equations, to delete bad data, and to calculate averages for the 3-, 10-, 30-, and 60-min averages, and the hourly observations. The input to these programs were the 4-s average data processed by the SMDSS Program. Three computer programs were used in the reprocessing: DALSH, OCESH, and RADREPRO. The first two were special processing programs that were used on the Dallas and Oceanographer ship heading data, respectively. DALSH was used to recover the ship heading data between 313° and 360° as discussed in section 5.4.3. OCESH was used to rescale the Oceanographer's ship heading data.

Because ship heading data were used to calculate absolute wind velocity from relative velocity, reprocessing meant correcting the wind velocities as well as the ship headings. This was accomplished by reversing the steps used to calculate the absolute wind velocity (sec. 5.2). The Oceanographer's original ship headings were then rescaled, and fixed headings of 324° , 336° , and 349° were assigned to the Dallas ship heading data as discussed in section 5.4.3. With the adjusted ship headings, the absolute wind velocities were then recalculated using the scheme described in section 5.2.

Program RADREPRO was used to rescale some of the temperature data and all of the radiation data, to delete bad data that were not removed in the automatic editing of the central processing steps, and to compute the average data sets. The processing flow is shown in figure 13.

The program first read the processing constants and control features into the computer. For the first run of a series of tapes containing continuous data, the program set up a directory to keep track of incoming data. On continuation runs, the program read in a partially processed file that provided the necessary information for a restart.

Next, the program read a record of data and loaded it into the processing array. Some of the temperature and radiation variables were rescaled using revised linear transfer equations, and the program then deleted the bad data in the record.

The ship heading data of each record were divided into north-south (SH_{NS}) and east-west (SH_{EW}) components in order to compute the average ship headings. Assuming the speed was unity,

$$SH_{NS} = 1 * \sin (\theta),$$

and

$$SH_{EW} = 1 * \cos (\theta),$$

where θ is the ship heading in degrees. These components were then averaged, and were used to compute the average ship headings.

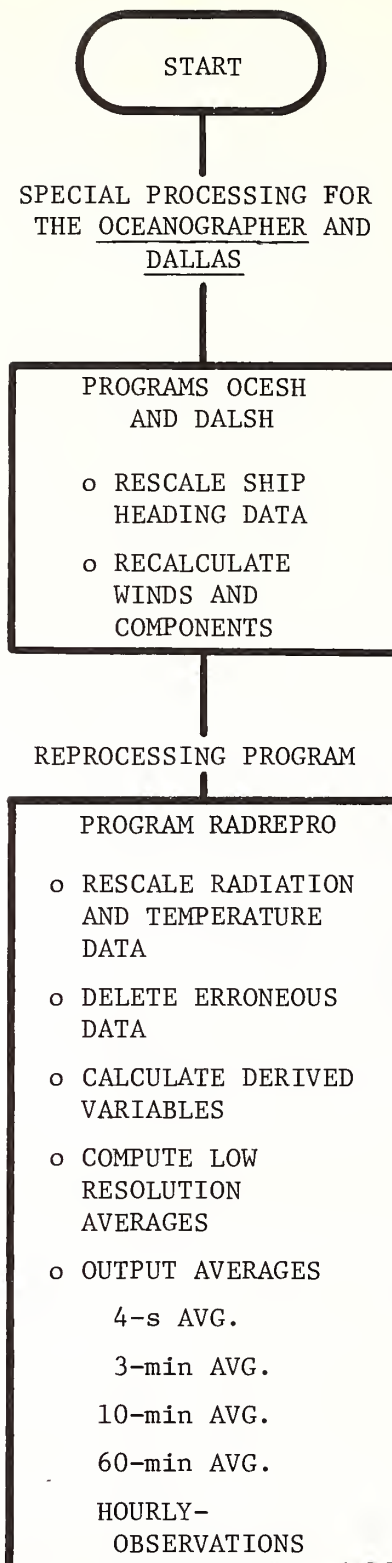


Figure 13.--RADREPRO program processing flow.

The program also computed the dew-point and specific-humidity values for each wet-bulb temperature. The specific humidity (q) was computed from

$$q = \frac{0.622 * e}{(p - 0.378 e)} ; p = 1013.246 \text{ mb},$$

where e is the ambient vapor pressure, and p is the atmospheric pressure, both in millibars. The vapor pressure was computed from

$$e = e_{wb} - A \cdot p \cdot (T_{dry} - T_{wet}),$$

where

$$A = 0.00066 (1 + 0.00115 T_{wet}),$$

T_{dry} = the dry-bulb temperature,

T_{wet} = the wet-bulb temperature, and

e_{wb} = the saturation vapor pressure at the wet-bulb temperature.

The saturation vapor pressure at the wet-bulb temperature was computed by using the Goff-Gratch formulation (Smithsonian Meteorological Tables, 1951),

$$e_{wb} = 10^{(B+C+D)},$$

where

$$B = -7.90298 (373.16/T_{wet} - 1)$$

$$+ 5.02808 \text{ ALOG}_{10} (373.16/T_{wet}),$$

$$C = (-1.3816 \times 10^{-7}) \cdot (10^F - 1.0),$$

$$D = 0.0081328 \cdot (10^G - 1.0) + 3.0057,$$

and

T_{wet} = wet-bulb temperature in absolute degrees,

$$F = 11.334 \cdot (1.0 - T_{wet}/373.16),$$

$$G = -3.49149 \cdot (373.16/T_{wet} - 1.0).$$

The dew-point temperature was calculated using Tetten's equation in the following form:

$$T_{DP} = \frac{237.3 \cdot \text{ALOG}_{10} \frac{e}{6.11}}{7.5 - \text{ALOG}_{10} \frac{e}{6.11}},$$

where e is the ambient vapor pressure.

As each record of data was processed, each record containing a 4-s average of each variable, it was placed on an output file. At the same time, the 4-s average samples were added to accumulations for the low-resolution averages. Sums and averages were calculated for the following time intervals (in minutes) of each hour:

3-min average: 58.5 to 01.49, 01.5 to 04.40, etc.

10-min average: 55.0 to 4.99, 05.0 to 14.99, etc.

30-min average: 45.0 to 14.99 and 15.0 to 44.99.

60-min average: 00.0 to 59.9.

Hourly observations: 50.0 to 59.9 for all variables except pressure;
55.0 to 04.9 for pressure.

Note that the hourly observations of pressure were 10-min averages centered on the hour.

The average wind directions were calculated from absolute average wind components (\bar{u} , \bar{v}). The 4-s average wind speeds were used in calculating the above scalar wind speeds, i.e., the average wind speeds were not computed from the wind velocity components.

The average ship headings were calculated from the ship heading components (SH_{NS} , SH_{EW}) with the unit speed as discussed above. All other average scalar values, including the derived variables of specific humidity, dew point, and the u - and v -components of the absolute wind velocity were calculated by normal summing and averaging.

As the individual averages (3 min, 10 min, etc.) were generated, these were placed on output files, which were subsequently copied on to the archive tapes. At the same time, these data were used to generate microfilm time-series plots that correspond to the digital data. In addition to the average values given in each data set, the number of 4-s averages used to generate this average is given.

6. ANALYSIS AND VALIDATION OF SURFACE RADIATION DATA

The incident solar radiation data, the reflected solar radiation, and the net radiation data were all subjected to careful intercomparison and validation. As a result of these analyses, transfer equations for the net radiation data were developed for the first time, and revised transfer equations were derived for the incident and reflected solar radiation data. The following sections describe how the data were validated, and the transfer equations used.

6.1 Recording System Error Limitations

The SAM, as described in section 1.1, had a voltage range of 0 to 5 V, which was divided into 65,535 counts. The millivolt input signal from each radiometer was fed through an amplifier with a gain of 1000 to accommodate the range of the recording system. The amplifiers showed small variations with time and were sensitive to temperature changes. To check the stability of the recording system, a set of known voltages was put through the system. For the high-gain radiation channels, these voltages were 0 mV, 4 mV, 8 mV, and 40 mV. This procedure, called simulate, was completed three times each day as discussed in section 4. The simulate records for the radiation channels were analyzed to determine the magnitude of the error produced by variations in the amplifiers.

All radiation data were recorded as counts. To determine the transfer equations between the recorded counts and the equivalent radiation in W/m^{-2} , the counts-to-millivolt relationship for the SAM had to be developed. The millivolt-per-count ratio defined the slope of the transfer equation, and the instrument zero offset determined the intercept. Variations in the amplifier caused a change in the ratio of millivolts to counts (the slope of the transfer equation), while variations in the 0-mV count value changed to intercept. An analysis of the simulate records showed that the change in slope was not related to the change in the 0-mV count.

The linearity of the slope was checked by comparing the millivolt-count calculated for each simulate voltage interval (4-0 mV, 8-0 mV, and 40-0 mV). The results showed that each channel was linear over the range of the recording system.

Because the sensors and recording system had different impedances, the instrument zero was not the same as the recording system zero. The mean of the nighttime values measured by the pyranometers throughout GATE was taken to be the instrument zero offset, and the intercept of the transfer equation was adjusted accordingly. Variations in the sensor zero offset can be attributed, in part, to changes in the amplifiers of the recording system, and the effect of other factors can be determined by calculating the variation in the mean offset and removing the known effect of the amplifiers.

Errors due to the change in the ratio of millivolts to counts are less than 0.2 percent. Variations in the 0-mV count value and the instrument zero offset caused an error of 1 to 3 W/m^{-2} , or 0.8 percent of the mean net radiation integrated over daylight hours. The total error attributed to the

recording system and the instrument zero is less than 1 percent of the daily integrated net radiation.

6.2 Incident and Reflected Solar Radiation

6.2.1 Instrumentation and Transfer Equations

The pyranometers mounted on the U.S. ships during GATE were the Eppley models 2 and 8-48. The model 2 was used to measure the global solar radiation on the four U.S. B-scale ships and the reflected solar radiation on the Oceanographer only. The reflected solar radiation was measured by the model 8-48 on the Gilliss, Researcher, and Dallas.

The sensitivity (calibration factor) of the pyranometers, as given in table 8, was determined during the Miami intercomparison in April 1974 (see appendix B). Transfer equations were determined from the instrument sensitivities and the simulate records. The intercept of the transfer equation was adjusted in accordance with the mean instrument zero offset discussed in the previous section. The 0-mV count value for both Dallas pyranometers was not offset. Since the recording system did not record negative voltages, the sensor zeros were suppressed. Intercomparison data show that the Dallas data are in agreement with data from the other ships within the limits of error. This indicates that the zero suppression of the Dallas instruments was small, and the recording system zero was therefore taken as the intercept of the transfer equation.

The simulate records of the Gilliss show that the zero of the model 2 pyranometer measuring solar radiation was suppressed until July 4 (Julian day 185) when the simulate zero was adjusted to a positive count value. Intercomparison 1 data show the Gilliss solar radiation to be approximately 15 W/m^{-2} lower than the other ships. This is due to the instrument zero suppression during Intercomparison 1. Because of the change in the 0-mV count value, two transfer equations were developed for the Gilliss upfacing pyranometer. As with the Dallas, the intercept was taken to be zero until July 5, and approximately -15 W/m^{-2} after that time. This adjustment brings the Gilliss Intercomparison data into agreement with the other ships.

6.2.2 Data Validation

Figures 14 to 18 show the hourly integrated solar radiation data ($K\downarrow$, $K\uparrow$) for the U.S. ships and the Canadian Ship Quadra during the Intercomparison periods. The Canadian data were used as an independent check for both solar and net radiation to further verify the quality of the data. The Gilliss did not participate in Intercomparison 2, and the Dallas was absent from Intercomparison 3. Also, the Oceanographer and Quadra took part in Intercomparison 3A while the Researcher and Gilliss took part in Intercomparison 3B (fig. 3, sec. 1).

The solar radiation data from all these ships agree to well within the 5 to 6 percent recommended accuracy. Differences between ships in the hourly integrated radiation is due primarily to variations in cloud cover over each ship during a particular hour. The curves for Intercomparison 2

Table 8.--Sensitivity and transfer coefficients for U.S. GATE radiometers

		Intercomparisons			Field phases		
		K↓	K↑	Q*	K↓	K↑	Q*
<u>Gilliss</u>							
Serial No.		12562	12472	6988	12562	12472	6988
Sensitivity ₂ (mV/cal/cm min ⁻¹)		7.00	5.18	18.31	7.00	5.18	18.85
Transfer equation slope (W/m ⁻² /count)		0.07618	0.04086	0.11869	0.07618	0.04086	0.11532
Intercept (W/m ⁻²)		-15.24*	-2.39	-115.485	-14.52*	-2.48	-113.821
<u>Oceanographer</u>							
Serial No.		11548	12560	6964	11538	12560	6964
Sensitivity ₂ (mV/cal/cm min ⁻¹)		7.26	6.77	21.15	7.26	6.77	**
Slope ₂ (W/m ⁻² /count)		0.07370	0.03168	0.10182	0.07370	0.03168	**
Intercept (W/m ⁻²)		-15.42	-9.27	-100.089	-13.49	-8.75	

Table 8.--Sensitivity and transfer coefficients for U.S. GATE radiometers (continued)

	Intercomparison			Field phases		
	K↓	K↑	Q*	K↓	K↑	Q*
Serial No.	12159	11079	6921	12159	11079	6921
Sensitivity (mV/cal/cm ⁻² /min ⁻¹)	6.91	7.13	32.25	6.91	7.13	29.33
Slope ₂ (W/m ⁻² /count)	0.07722	0.02971	0.06595	0.07722	0.02971	0.07252
Intercept (W/m ⁻²)	-3.08	-3.35	-65.818	-2.69	-4.33	-74.406
<u>Dallas</u>						
Serial No.	12502	12316	7025	12502	12316	7025
Sensitivity (mV/cal/cm ⁻² min ⁻¹)	6.64	7.49	15.83	6.64	7.49	15.45
Slope ₂ (W/m ⁻² /count)	0.08108	0.02904	0.13563	0.08108	0.02904	0.13890
Intercept (W/m ⁻²)	0.71	0.00	-135.409	0.00	0.00	-140.567

Table 8.--Sensitivity and transfer coefficients for U.S. GATE radiometers (continued)

Date (1974)	Julian day	Slope	Intercept	Sensitivity
		<u>Net radiometer (6969)</u>		
June 28-Aug. 2	179-214	0.10634	-105.170	20.34
Aug. 3-Aug. 28	215-240	0.10049	- 99.385	21.11
Aug. 29-Sept. 19	241-262	0.10640	-105.230	20.24
		<u>Yanischevsky pyranometer**</u>		
June 17-June 19	168-170	0.08480	- 6.6984	10.13
June 28-July 11	179-192	0.08726	- 6.6984	9.84
July 12-Aug. 18	193-230	0.10071	- 6.6984	8.52
Aug. 19-Sept. 19	231-262	0.10713	- 6.6984	8.01

* The Gilliss K4 intercept is 0.0 W/m^{-2} for June 17 to July 5 (Julian days 168 to 186).

** The net radiometer and Yanischevsky pyranometer on the Oceanographer showed variations in sensitivity during GATE.

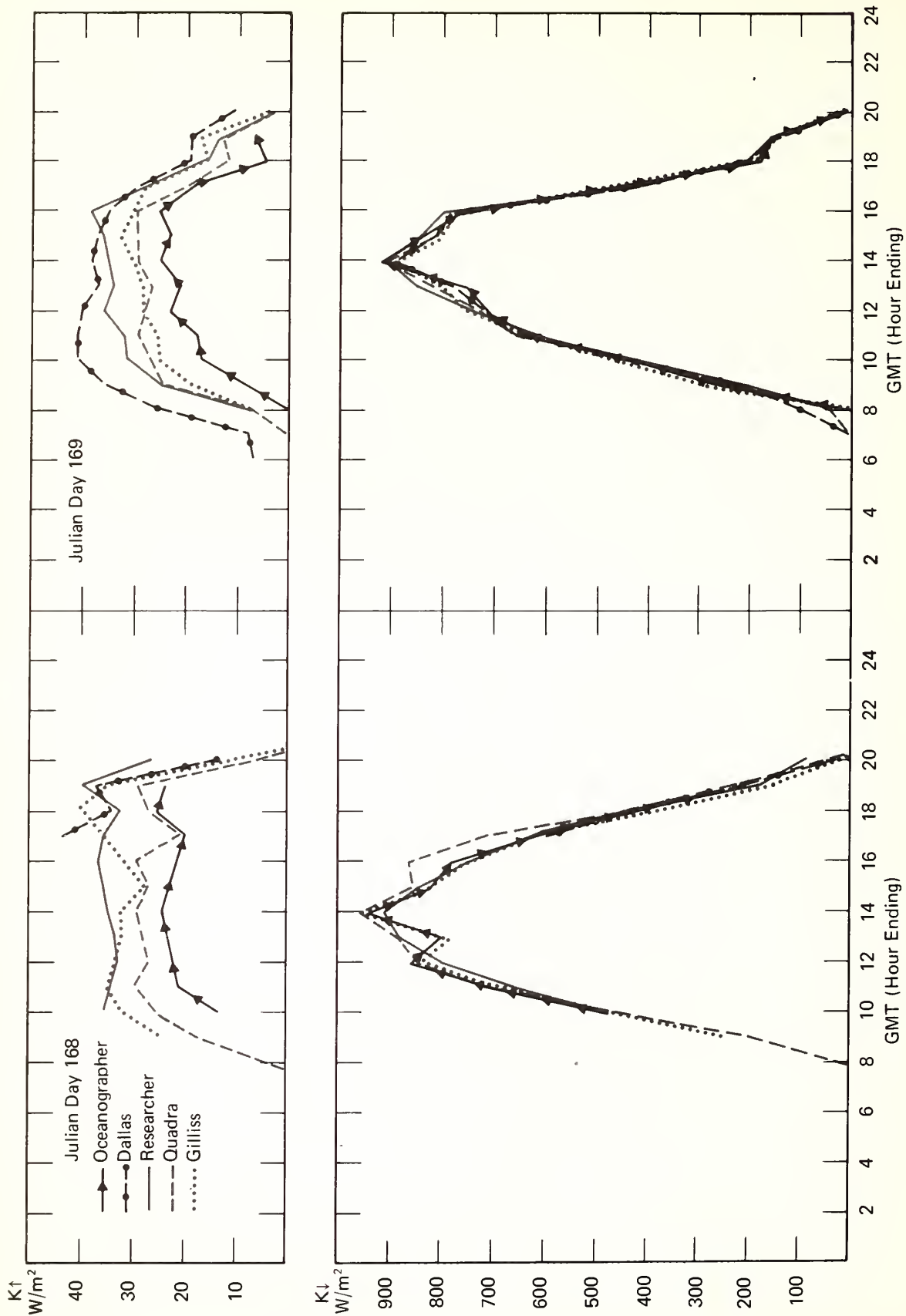


Figure 14.--Hourly integrated solar radiation data, U.S. and Canadian ships, June 17 and 18 (Julian days 168 and 169).

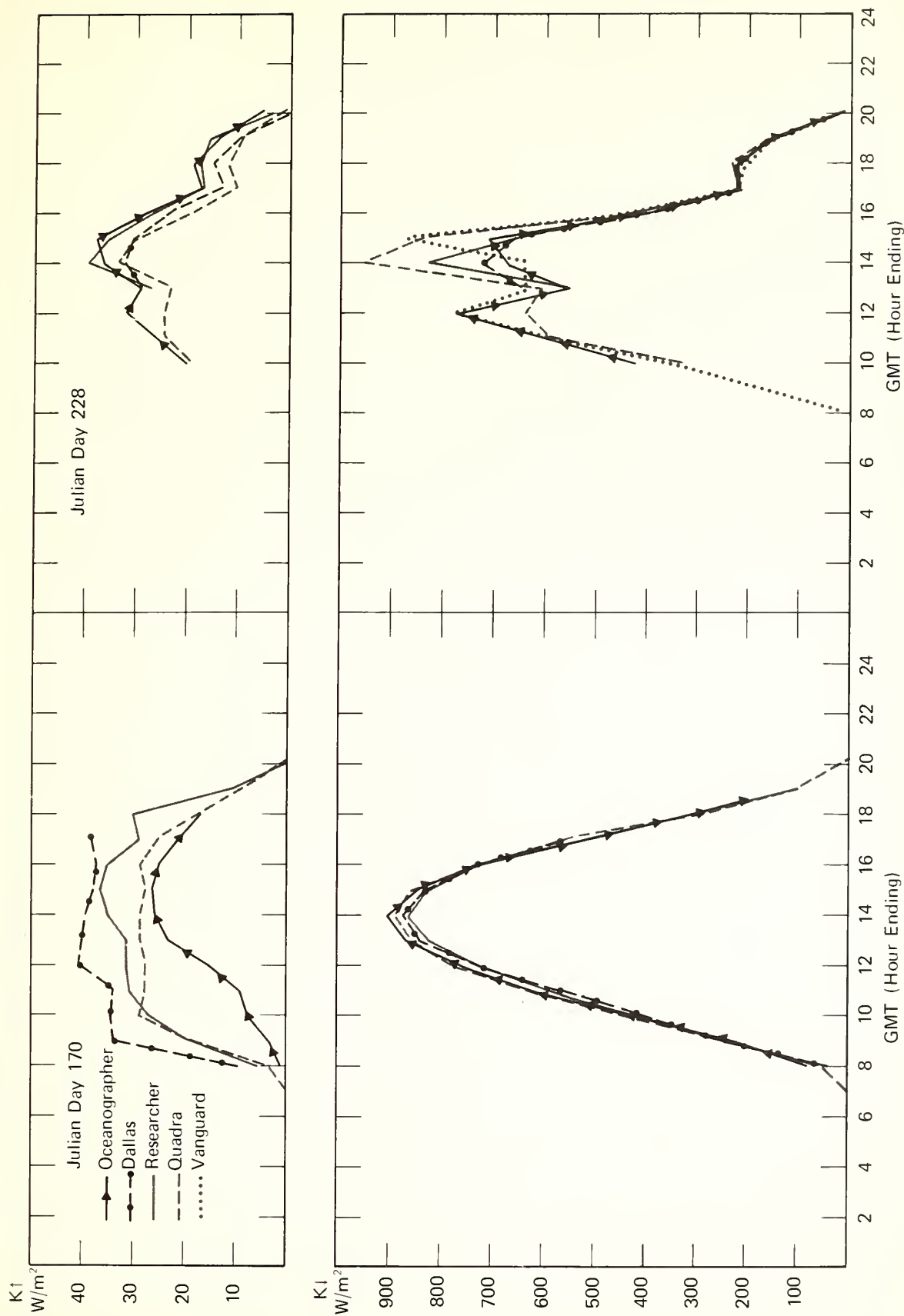


Figure 15.--Hourly integrated solar radiation data, U.S. and Canadian ships, June 19 and August 16 (Julian days 170 and 228).

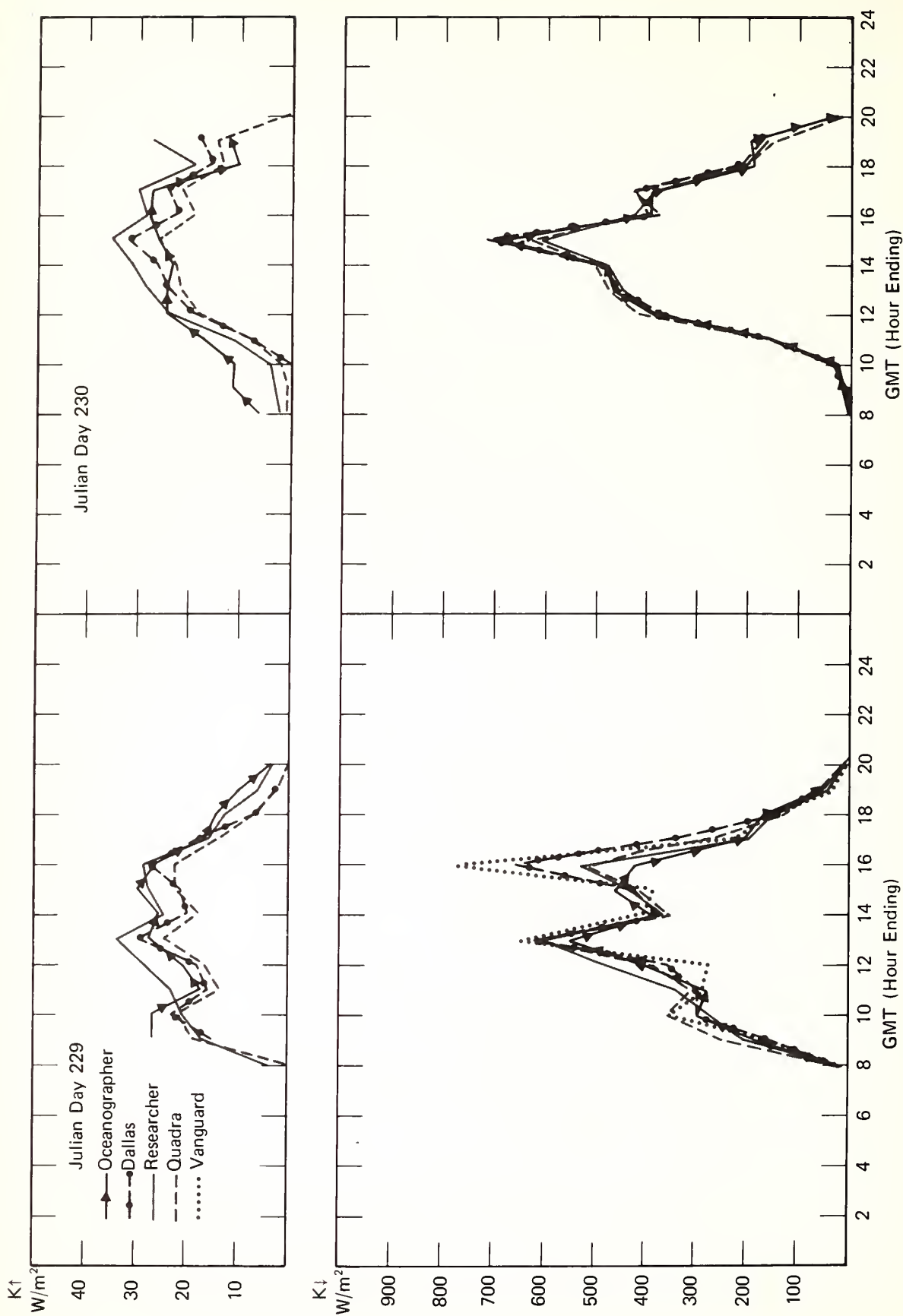


Figure 16.--Hourly integrated solar radiation data, U.S. and Canadian ships, August 17 and 18 (Julian days 229 and 230).

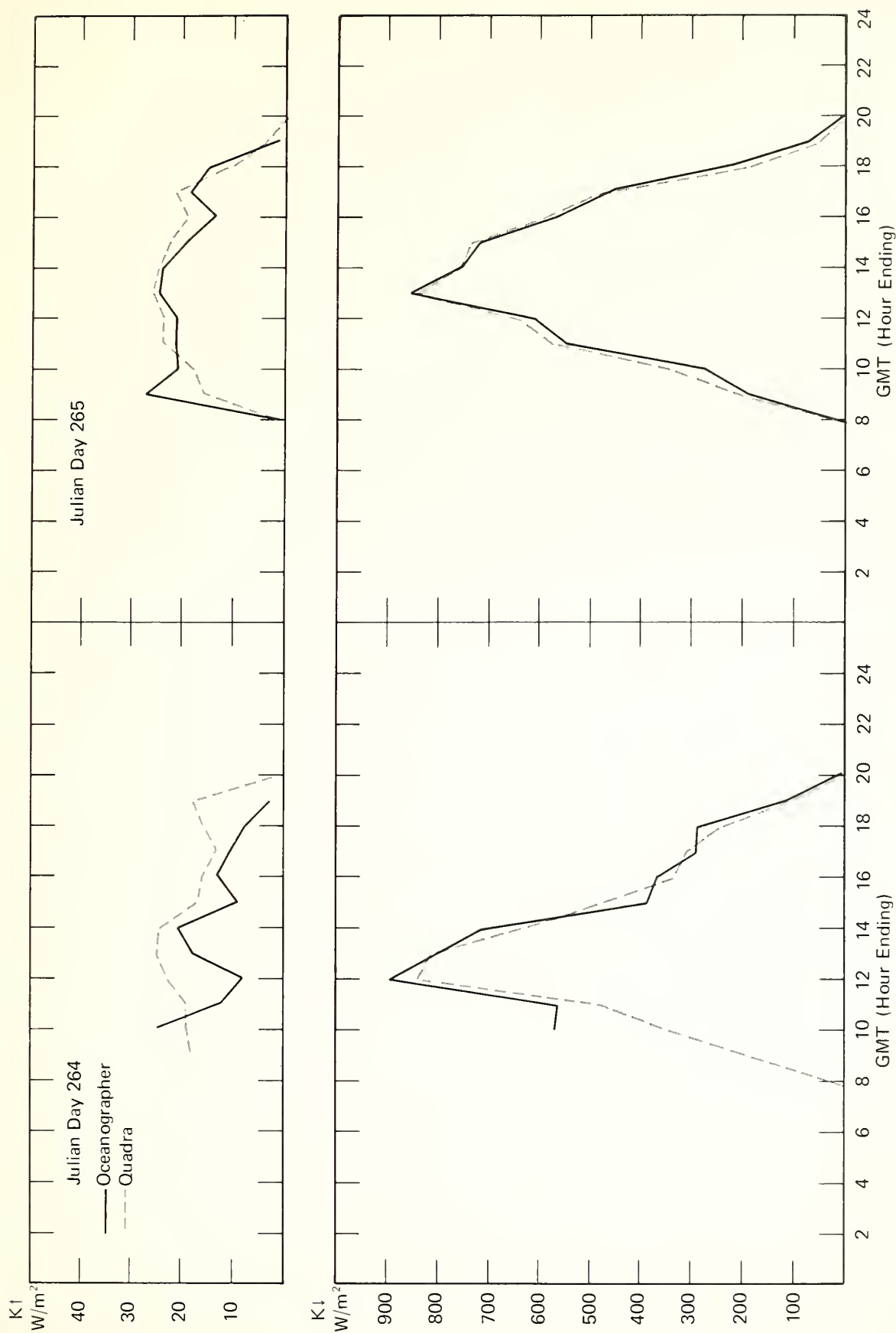


Figure 17.---Hourly integrated solar radiation data, Oceanographer and Quadra, September 21 and 22 (Julian days 264 and 265).

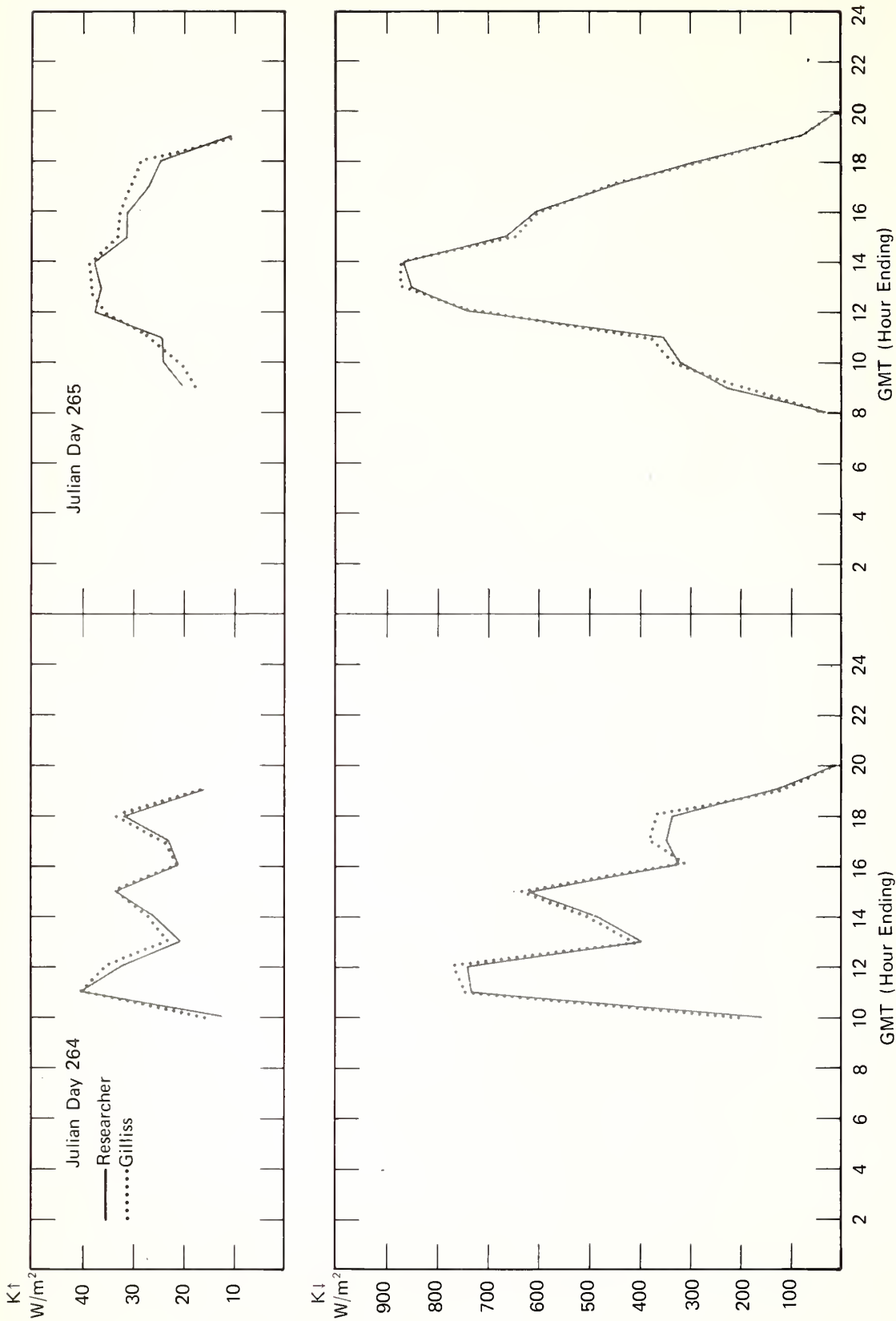


Figure 18.--Hourly integrated solar radiation data, Researcher and Gilliss, September 21 and 22 (Julian days 264 and 265).

(figs. 15 and 16), an excessively cloudy period, show much larger anomalies in the hourly values than are seen in the other figures. Data collected during clear periods agree to within 2 percent.

Table 9 shows the ratio of the simultaneous radiation measurements on each ship to the measurements on the Oceanographer. Ratios are given for each day of the Intercomparison periods when simultaneous hourly values were available. For Intercomparison 3B, the ratios of the Gilliss data to the Researcher data are shown. The large ratios of $K\downarrow$ for individual days are primarily due to the hourly variation in cloudiness over each ship.

The very large difference in reflected radiation can be attributed to the location of the downfacing pyranometer as well as to instrument characteristics. The pyranometers were mounted on booms extending beyond the bow of the ships. They were at different heights above the ocean surface and the bow of each ship was within the instrument's field of view. At low solar elevation angles, the shadow of the ship may have fallen below the sensor. The response of a pyranometer is highly variable when receiving energy from low angles and the model 2 pyranometer has a different cosine response than the model 8-48 (see appendix B).

Comparison of the simultaneous values of reflected radiation obtained from the model 8-48 pyranometer and averaged over all three Intercomparison periods for the Dallas, Gilliss, and Researcher shows that these data are in agreement within 3 percent. The model 2 pyranometer on the Oceanographer indicated much lower reflected energy, except during Intercomparison 2 cloudy periods. This does not imply that the model 8-48 produces a more accurate value, but only that pyranometers of the same type have similar characteristics. The GATE Intercomparison data show that the relative accuracy of the reflected solar radiation data collected from shipboard is marginal and can be estimated only to approximately $\pm 10 \text{ W/m}^{-2}$.

6.3 Net Radiation (Q^*)

6.3.1 Derivation of Transfer Equations

The net radiometers mounted aboard the U.S. ships were not calibrated prior to GATE. The sensitivity (calibration factor) of the instruments was determined from an analysis of the data collected during the experiment. The net radiation is defined as the difference between the incoming and outgoing radiation, given by the following equation:

$$Q^* = (K\downarrow + L\downarrow) - (K\uparrow + L\uparrow)$$

where

Q^* = net flux of total radiation,

$K\downarrow$ = downward direct and reflected solar radiation,

$K\uparrow$ = upward solar radiation,

Table 9.--Ratio of simultaneous shipboard $K\downarrow$, $K\uparrow$, and Q^* data to the
Oceanographer data during GATE Intercomparison periods

Date (1974)	Intercomparison 1			Intercomparison 2			Intercomparison 3			Composite averages	
Julian day	June 17	June 18	June 19	Aug. 16	Aug. 17	Aug. 18	Sept. 21	Sept. 22	Sept. 23	IC 1,2,&3A	IC3B
	168	169	170	228	229	230	264	265	266		
$K\downarrow$											
<u>Gilliss</u>	0.968	1.002	-	-	-	-	1.041	1.002	0.988	0.983	1.012
<u>Researcher</u>	1.000	1.011	1.076	1.025	1.060	0.990	-	-	-	1.028	
<u>Dallas</u>	-	1.010	0.970	1.013	1.084	1.022	-	-	-	1.010	
<u>Quadra</u>	1.074	1.019	1.011	1.151	1.094	1.029	0.965	1.040	-	1.044	
<u>Vanguard</u>	-	-	-	1.022	1.090	-	-	-	-	1.047	
<u>Oceo. (Yan.)</u>	1.005	1.009	0.977	1.068	1.013	1.000	1.041	1.001	-	1.012	
$K\uparrow$											
<u>Gilliss</u>	1.551	1.419	-	-	-	-	1.053	1.017	1.026	1.490	1.032
<u>Researcher</u>	1.623	1.626	1.763	0.997	0.988	1.245	-	-	-	1.355	
<u>Dallas</u>	-	1.880	2.127	0.844	0.802	0.963	-	-	-	1.262	
<u>Quadra</u>	1.259	1.337	1.553	0.810	0.744	0.872	1.590	1.055	-	1.109	
Q^*											
<u>Gilliss</u>	-	-	-	-	-	-	1.136	0.931	1.054	-	1.042
<u>Researcher</u>	0.909	0.950	1.088	-	0.945	-	-	-	-	0.979	
<u>Dallas</u>	-	-	1.058	0.918	1.027	0.984	-	-	-	1.000	
<u>Quadra</u>	0.988	0.930	1.023	0.945	1.058	0.926	0.926	0.992	-	0.971	

The larger ratios of $K\downarrow$ shown for individual days are primarily due to the hourly variation in cloudiness over individual ships.

$L\downarrow$ = downward atmospheric radiation, and

$L\uparrow$ = upward terrestrial surface and atmospheric radiation.

The incoming solar radiation ($K\downarrow$) is measured accurately by the upfacing pyranometer, and the upward terrestrial radiation ($L\uparrow$) is calculated from the sea-surface temperature. An estimate of the reflected solar radiation ($K\uparrow$) is known from the downfacing pyranometer. Since the reflected radiation is more than an order of magnitude smaller than the other radiation terms, it is unnecessary to know its precise value. The error in the determination of the net radiometer sensitivity will be insignificant as long as $K\downarrow$ and $L\uparrow$ are accurately determined.

The equation defining the net radiation can be solved for the downward atmospheric radiation term ($L\downarrow$), which for daylight hours is given by

$$L\downarrow = Q^* - K\downarrow + K\uparrow + L\uparrow, \quad (2)$$

and at night, when the solar terms are zero, becomes

$$L\downarrow = Q^* + L\uparrow. \quad (3)$$

Variations in the downward atmospheric radiation are primarily due to changes in the water vapor content of the atmosphere and the amount of cloudiness. The tropical atmosphere over ocean areas and away from the continental land masses has the unique characteristics of a high and relatively constant moisture content and little or no diurnal variation in moisture or cloudiness. We may therefore assume that, over the many days of GATE, the mean atmospheric radiation is the same during daylight and nighttime hours, and we can set eqs. (2) and (3) equal to each other,

$$(Q^* + L\uparrow)_{\text{night}} = (Q^* - K\downarrow + K\uparrow + L\uparrow)_{\text{day}}. \quad (4)$$

By adjusting the sensitivity of the net radiometer until equality in eq. (4) is reached, the correct sensitivity is derived.

6.3.2 Data Validation

To determine their accuracy, the hourly integrated net radiation data were compared in the same manner as the solar radiation data. Figures 19 to 23 show the hourly net radiation data for each day during the Intercomparison periods, and table 9 (sec. 6.2) shows the ratio with respect to the Oceanographer. The Canadian Quadra data are also included as an independent check and to verify the method used in determining the net radiometer sensitivities. The Canadians verified their net radiation data by an entirely different approach. They took simultaneous measurements with similar instruments and also measured the four radiation components directly. They found good agreement between the measured and calculated quantities.

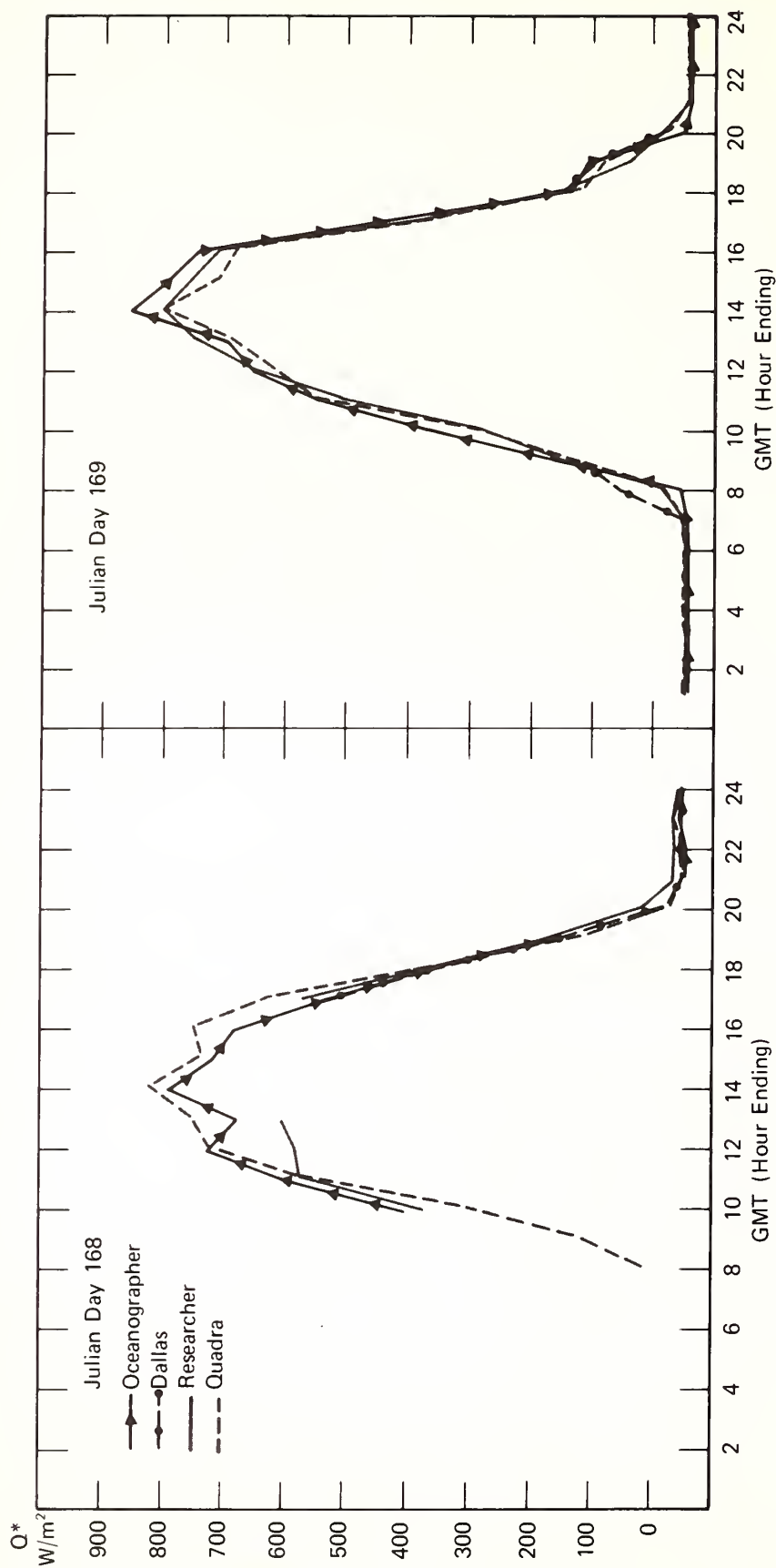


Figure 19.---Hourly integrated net radiation data, U.S. and Canadian ships, June 17 and 18 (Julian days 168 and 169).

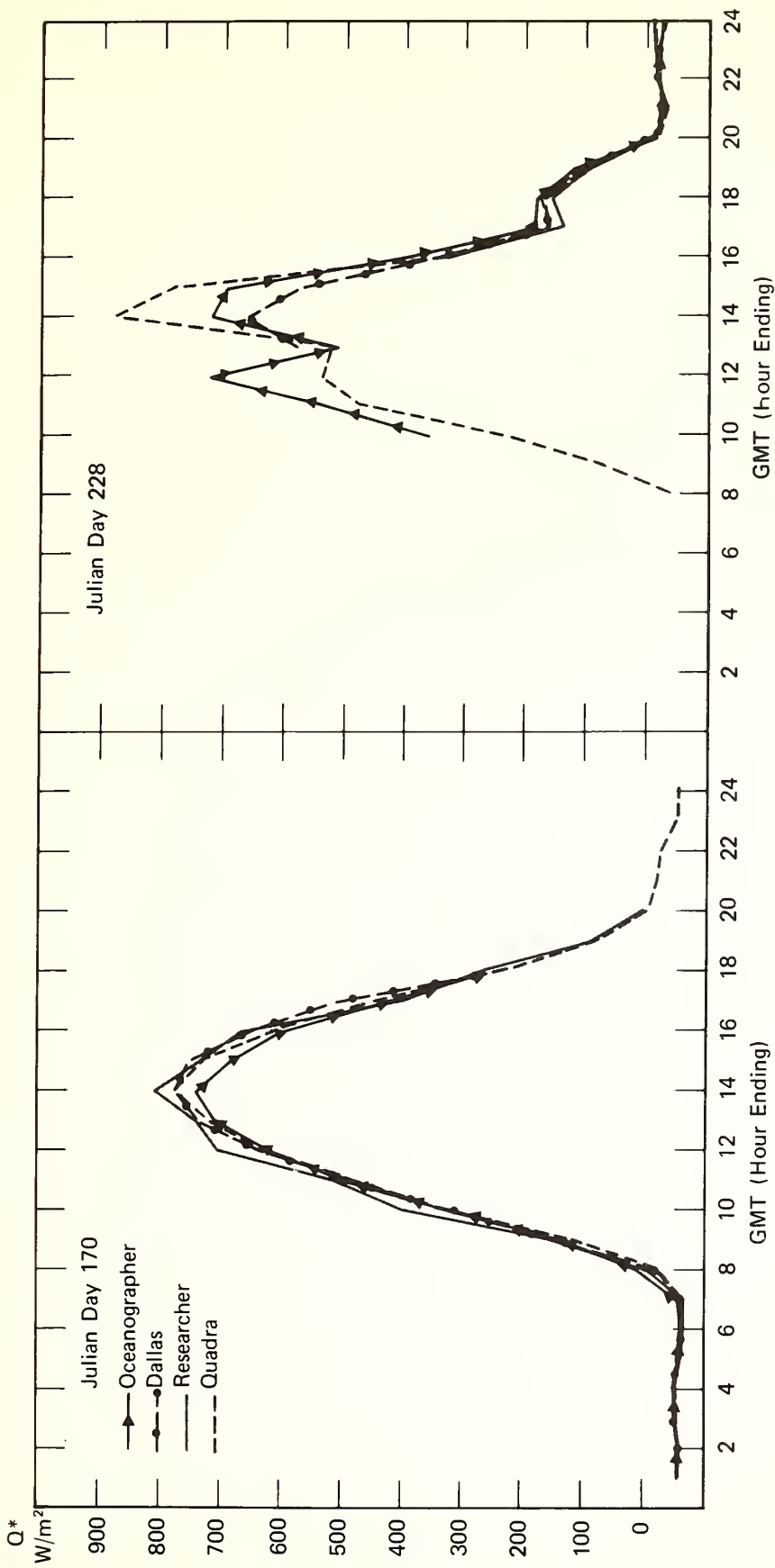


Figure 20. --Hourly integrated net radiation data, U.S. and Canadian ships, June 19 and August 16 (Julian days 170 and 228).

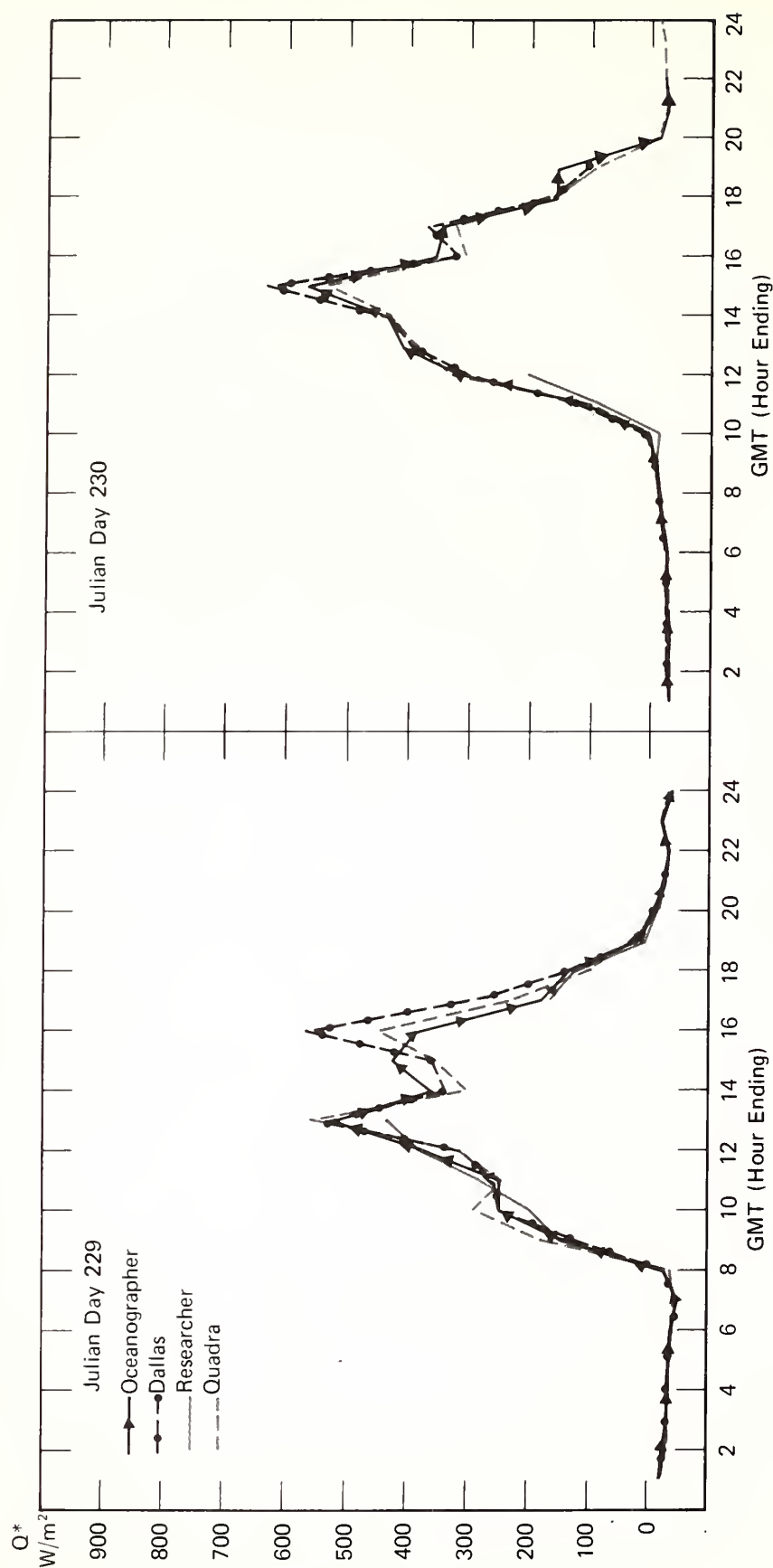


Figure 21.---Hourly integrated net radiation data, U.S. and Canadian ships, August 17 and 18 (Julian days 229 and 230).

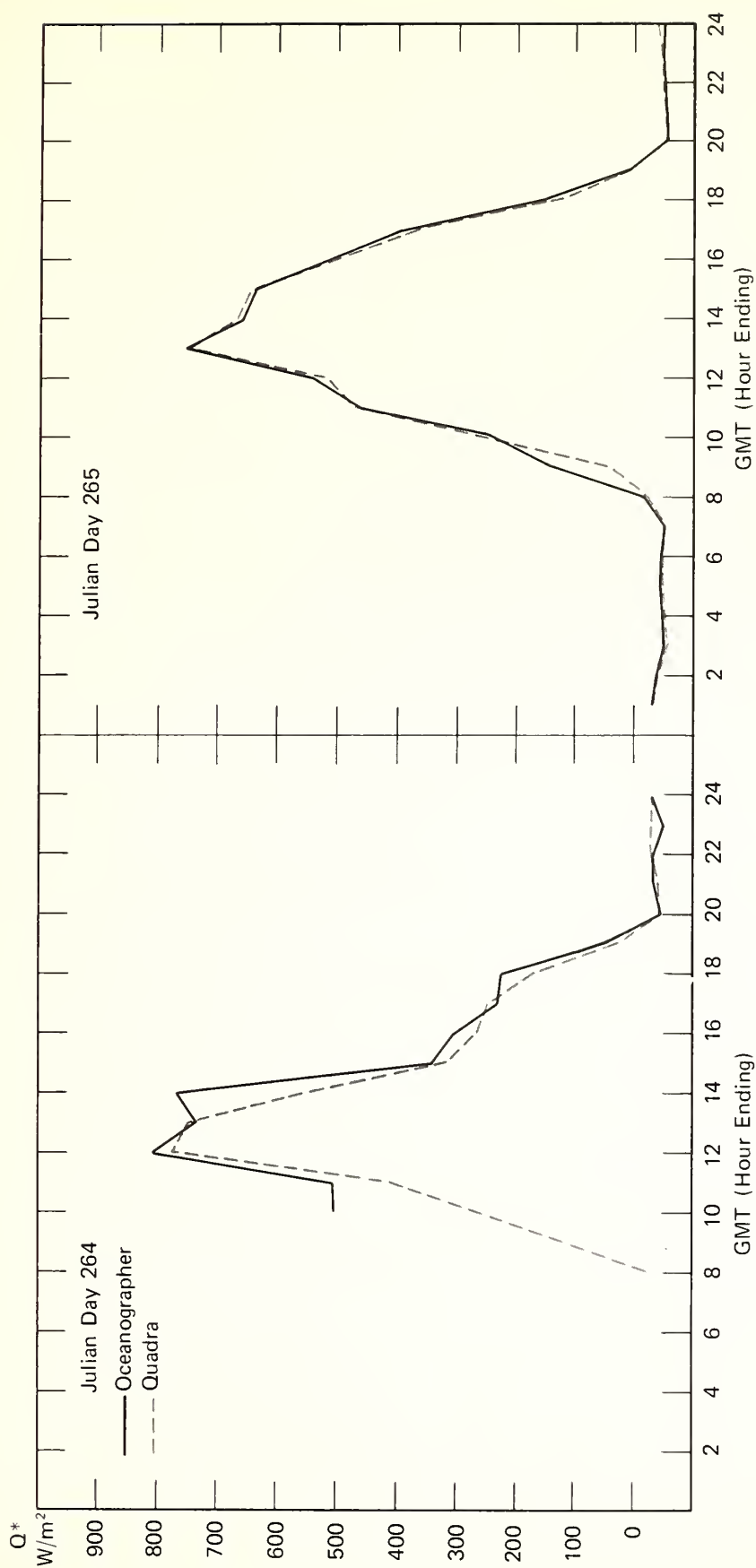


Figure 22.--Hourly integrated net radiation data, Oceanographer and Quadra, September 21 and 22 (Julian days 264 and 265).

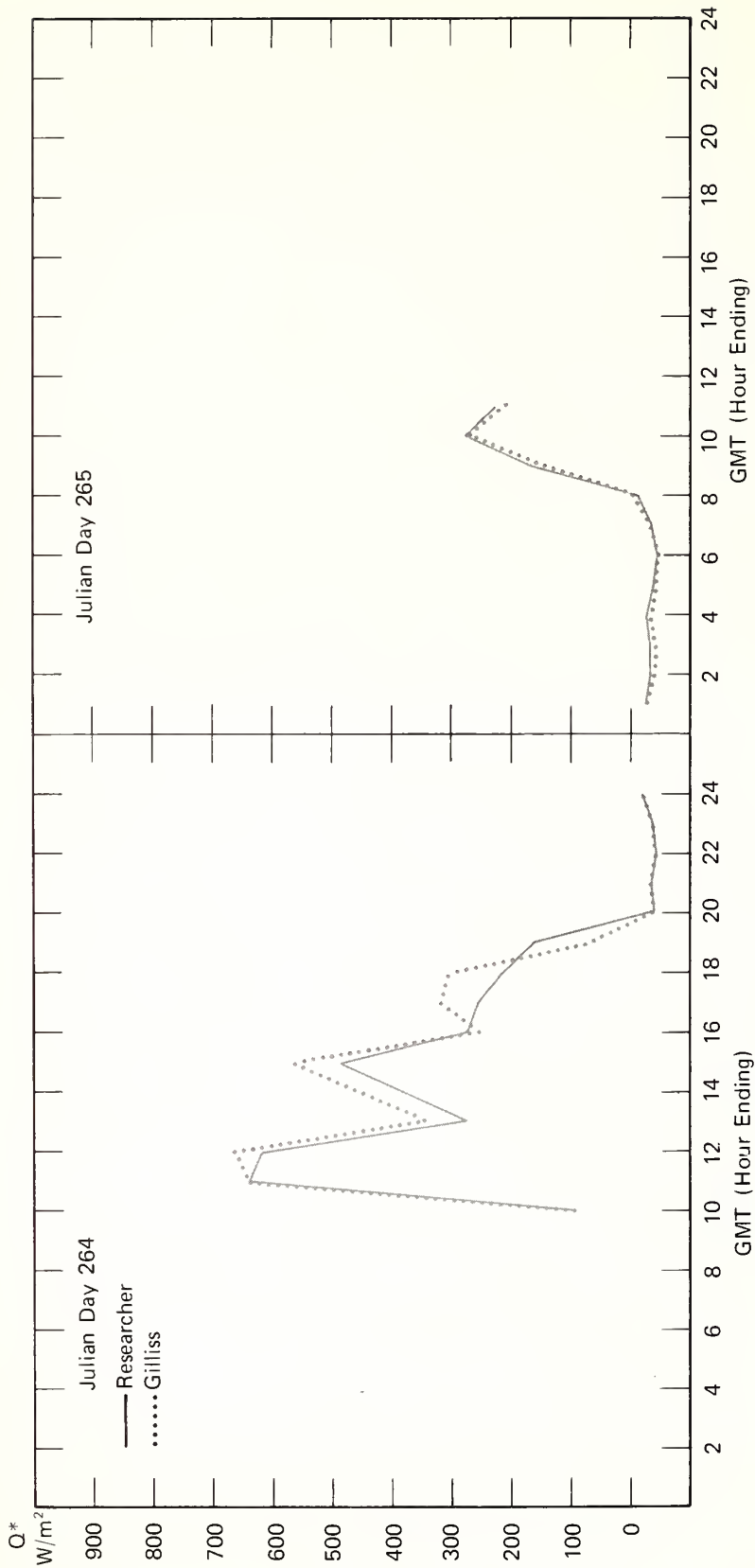


Figure 23.--Hourly integrated net radiation data, Researcher and Gilliss, September 21 and 22 (Julian days 264 and 265).

The net radiation traces in figures 19 to 23 show that the hourly values are in agreement. Variations in cloud conditions over individual ships cause the largest differences in the hourly values, as is the case with the incoming solar radiation. Intercomparison 2, the period of heaviest cloudiness, shows the largest fluctuations in the hourly integrated net radiation. The mean of the hourly averages over all three Intercomparison periods is well within the recommended 6-percent accuracy.

6.3.3 Instrument Malfunctions

During Intercomparison 1, the Gilliss net radiometer was found to have a ripped polyethylene dome. It was removed on June 18 (Julian day 169) at 2109 GMT, and the open channel of the recording system affected the other high-gain radiation channels. The Gilliss net radiation data for the 3 days of Intercomparison 1 were deleted because of the instrument damage. The solar radiation data ($K\downarrow$ and $K\uparrow$) for June 19 (Julian day 170) were also deleted because of excessive noise caused by the open net radiometer channel. These problems were corrected before the start of Phase I of GATE.

The Researcher net radiometer was removed on July 10 (Julian day 191) because of malfunction, and remained off line until the end of Phase I. Figure 24 shows three curves of the 4-s average radiation data for the Researcher, which indicate random drops of from 100 to 450 W/m^{-2} in the energy received by the ship's sensor. Two such anomalies can be seen in the net radiation trace in figure 24. Note that a similar drop does not occur in the incoming solar trace. These net radiometer anomalies occur randomly throughout GATE, and are most likely due to a malfunction of the recording system. However, no evidence of this can be found in the simulate records. Net radiation for the Researcher has been eliminated from the archived data set for these periods.

6.3.4 Anomalous Net Radiation Data

An analysis of the downward atmospheric radiation calculated from the Canadian GATE data shows fluctuations of less than ± 10 percent of the mean value. Since $L\downarrow$ is derived from eq. (2) for the U.S. shipboard data, any large fluctuations in $L\downarrow$ can be attributed to a malfunction of the net radiometer. The terms $K\downarrow$, $K\uparrow$, and $L\uparrow$ are well known within reasonable limits, so that anomalies in $L\downarrow$ must be the result of anomalies in the net radiation measurement, Q^* . Hourly downward atmospheric radiation data were calculated for the four U.S. ships, and net radiation data were deleted for periods when the downward atmospheric radiation exceeded the ± 10 percent criterion determined from the Canadian data. In most cases these anomalies are caused by the suspected malfunction of the Researcher's recording system. However, a few bad net radiation data were determined for the other ships, and these data were not included in the final data set.

6.3.5 Radiometer Sensitivity and Transfer Coefficients

The requirements for data validation and international data exchange are defined in GATE Report 13 (de la Moriniere, 1974), which specified that surface data from ship platforms for the Intercomparison periods were to be

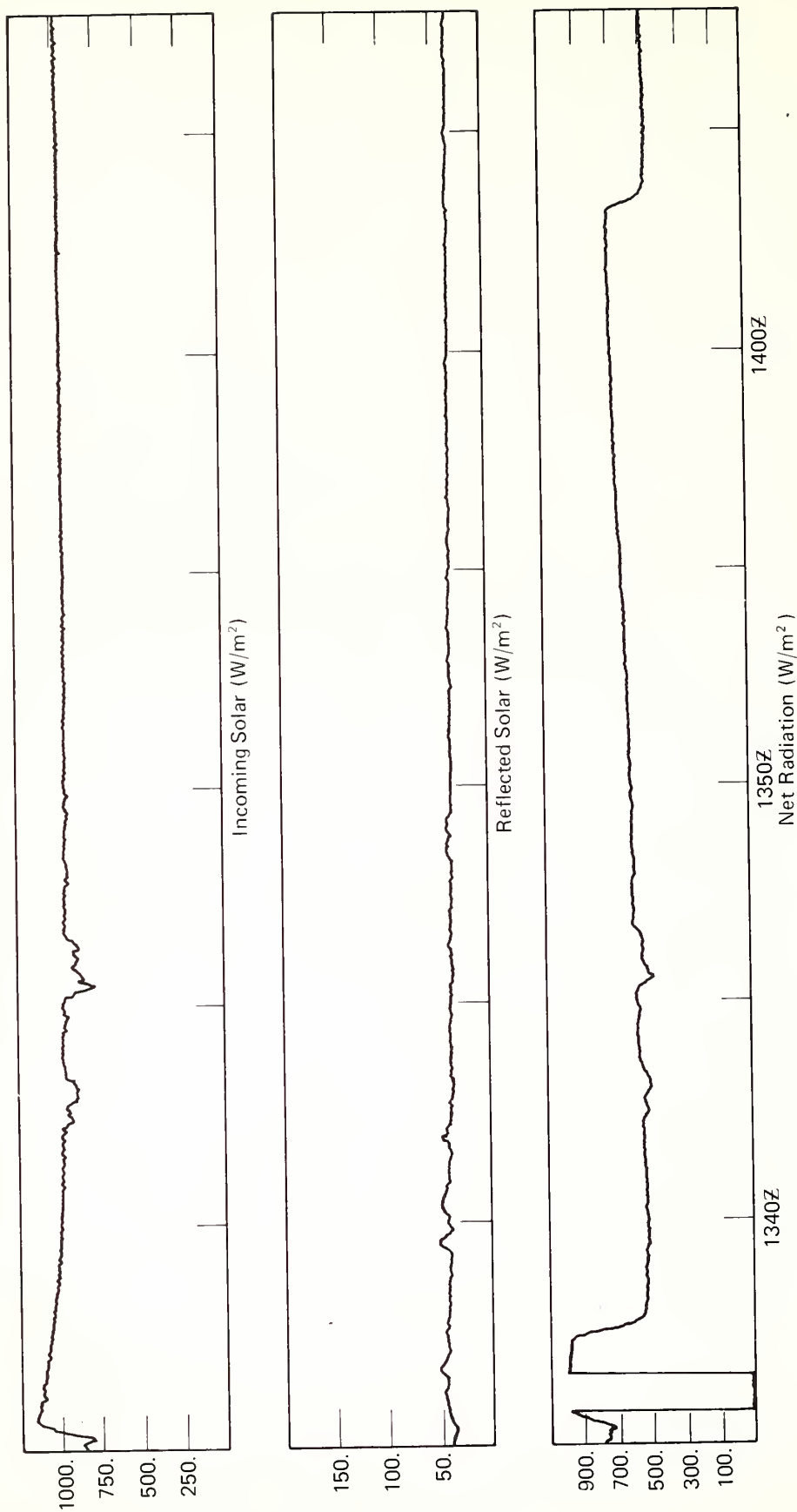


Figure 24.--Four-second averages of solar, reflected solar, and net radiation; Researcher data, Phase II.

validated and delivered to the World Data Centers (WDCs) within 6 months after the end of GATE, and that the validated data for the three field phases were due at the WDCs within 18 months. Because of these regulations, the surface radiation data for the Intercomparison periods were processed first. Consequently, two sets of transfer coefficients were derived for the U.S. GATE radiometers. These are given in table 8 (sec. 6.2).

The sensitivities of the pyranometers that measured incoming and reflected solar radiation were determined prior to GATE and did not change (except the Yanishevsky pyranometer discussed in the next section). Therefore, the slope of the transfer equations for the Intercomparison and field Phases data is identical. The intercept of the transfer equations varies slightly because of the adjustment made for the mean instrument zero offset discussed in section 6.1. The change in the intercept value between the Intercomparison and field Phase data sets is less than 1 W/m^{-2} in all cases, except for the Oceanographer sensor, No. 11538, which has a variation of less than 2 W/m^{-2} .

As seen in table 8, the slope of the transfer equations varies between the two data sets by less than 5 percent, with the exception of the Researcher, which shows a 10-percent variation. This larger variation is due to the smaller magnitude of the slope for the Researcher net radiometer and the apparent recorder malfunction (sec. 6.3.3), which caused a limited amount of usable data to be obtained from the ship during the Intercomparisons. The intercept of the net radiometer transfer equations is calculated from the mean 0-mV simulate values, which were nearly constant throughout GATE,

The net radiometer aboard the Oceanographer showed an abrupt change in sensitivity on August 3 (Julian day 215), which was apparently caused by the replacement of the polyethylene domes on the net radiometer. On August 29 (Julian day 241) another abrupt change in the instrument sensitivity occurred. The reason is not known. Because these changes occurred abruptly and degradation of the sensor with time was not evident, three separate sensitivities and transfer equations were derived for the Oceanographer net radiometer for the time intervals given in table 8 (sec. 6.2).

6.4 Yanishevsky Pyranometer Data (K†)

The USSR and the United States exchanged pyranometers during GATE so that direct comparison could be made. The USSR instrument loaned to the United States, a Yanishevsky pyranometer, was mounted on the bow of the Oceanographer. During Phase I, condensation frequently occurred inside the dome of the sensor, and repeated attempts to dry the instrument were unsuccessful. On July 12 (Julian day 193) an abrupt decrease in sensitivity occurred, most likely due to inadvertent damage to the sensing surface of the instrument while the condensation from the dome was removed. The black and white coating may have been brushed during maintenance. The sensor remained mounted until the conclusion of GATE; further maintenance was not performed. Between Phases II and III another abrupt decrease in the sensitivity was observed. Inspection of the sensor did not indicate that it had been damaged during the in-port period, and no probable explanation for this second decrease has been determined.

New sensitivities were derived for the Yanishevsky pyranometer and used to produce the final data set. Separate sensitivities were derived for the periods indicated in table 8. The ratio of the simultaneous solar radiation data from this pyranometer to the Oceanographer Eppley pyranometer data is given in table 9 (sec. 6.2). The mean radiation of the two sensors totaled over the three Intercomparison periods is in agreement within 1.2 percent.

6.5 Vanguard Pyranometer Data

The NASA ship Vanguard joined GATE shortly before the start of Phase I. The ship was equipped with a model 2 Eppley pyranometer and an Eppley normal incidence pyrliometer during the in-port period between Phases I and II. Data were recorded on an analog chart recorder, and the charts were analyzed by hand. Hourly integrated averages of solar radiation ($K\downarrow$) were calculated for July 27 to September 18 (Julian days 208-261). A table of the Vanguard hourly integrated averages of $K\downarrow$ is available from world data centers WDC-A (Asheville, North Carolina, USA) and WDC-B (Moscow, USSR). The pyrliometer data can be found in the documentation for the U.S. shipboard NIP (normal incident pyrliometer) and Sun Photometer GATE data, archived at the World Data Centers. The Vanguard participated for 2 days during Intercomparison 2. The ratios of the Vanguard pyranometer data to the Oceanographer data listed in table 9 show agreement within 5 percent for the 2-day period.

7. FORMAT AND INVENTORY OF THE ARCHIVED DATA SETS

The U.S. B-scale ship surface meteorological data are available in the form of hourly averages, hourly observations, 30-min averages, 10-min averages, 3-min averages, and 4-s averages. Surface radiation data are available at the same time-averaged resolutions except 4-s averages. Data sets that include both surface meteorological and radiation data are listed under U.S.A. Ship, General (Boom), in the WDC-A GATE Data Catalog, issued by the National Climatic Center, Asheville, North Carolina. The 4-s averaged data set is listed under U.S.A. Ships, Surface Meteorological (Boom). The meteorological and radiation variables in the combined data sets include pressure, dry-bulb temperature, wet-bulb temperature, sea-surface temperature, wind speed and direction from both bow-boom and mast sensors, incident solar radiation, reflected solar radiation, net solar radiation, and ship speed.

The data have been placed in the archive on digital magnetic tape and in the form of time-series plots on 35-mm microfilm. The magnetic tapes also include the derived parameters of specific humidity and dew point for each wet-bulb temperature, and the u- and v-components of the total absolute wind velocity. Also included on digital tapes are the longitude (negative for west longitude) and latitude positions for each observation. The number of 4-s averages used to construct the other low-resolution averages are given.

The ship speed and heading data contained on the digital data tapes and on the microfilm time-series plots are not representative of the true ship velocity during the GATE ship Intercomparisons and the Phases. For true ship direction of motion and speed information, the U.S. B-Scale Ship Navigation Data should be used.

7.1 Digital Data on Magnetic Tape

The following tapes contain the U.S. B-scale ships' boom meteorological and radiation 3-min averages, hourly averages, and hourly observations:

<u>Tape No.</u>	GATE tape identifier (bytes 7-24 of tape header record; not to be used for ordering)	<u>Ship</u>	<u>Period</u>
1	020410bbbbbbB79264	<u>Researcher</u> <u>Gilliss</u> <u>Dallas</u> <u>Oceanographer</u>	IC 1, 2, 3 IC 1, 3 IC 1, 2 IC 1, 2, 3
2	020410bbbbbbB79290	<u>Researcher</u> <u>Gilliss</u> <u>Dallas</u> <u>Oceanographer</u>	Phase III Phase III Phase III Phase III
3	020410bbbbbbB79288	<u>Researcher</u> <u>Gilliss</u> <u>Dallas</u> <u>Oceanographer</u>	Phase II Phase II Phase II Phase II
4	020410bbbbbbB79289	<u>Researcher</u> <u>Gilliss</u> <u>Dallas</u> <u>Oceanographer</u>	Phase I Phase I Phase I Phase I

b = blank

The following tape contains the U.S. B-scale ships' boom meteorological and radiation hourly averages, 30-min averages, and 10-min averages:

<u>Tape No.</u>	GATE tape identifier (bytes 7-24 of tape header record; not to be used for ordering)	<u>Ship</u>	<u>Period</u>
1	020410bbbbbbB79157	<u>Researcher</u> <u>Gilliss</u> <u>Dallas</u> <u>Oceanographer</u>	Phase I, II, III Phase I, II, III Phase I, II, III Phase I, II, III

b = blank

The following tapes contain the U.S. B-scale ships' boom automated high-resolution meteorological data (4-s averages):

Tape No.	GATE tape identifier (bytes 7-24 of tape header record; not to be used for ordering)	Time period (GMT)	
		Beginning (mo/day/hr:min)	Ending (mo/day/hr:min)

Researcher - Phase III

1	020410bbbbbbB79129	8/29/23:53	9/01/23:59
2	020410bbbbbbB79130	9/02/00:00	9/04/23:59
3	020410bbbbbbB79131	9/05/00:00	9/07/23:59
4	020410bbbbbbB79132	9/08/00:00	9/10/23:59
5	020410bbbbbbB79133	9/11/00:00	9/13/23:59
6	020410bbbbbbB79134	9/14/00:00	9/16/23:59
7	020410bbbbbbB79135	9/17/00:00	9/19/15:00

Gilliss - Phase III

8	020410bbbbbbB79136	8/30/01:23	9/01/23:59
9	020410bbbbbbB79137	9/02/00:00	9/04/23:59
10	020410bbbbbbB79138	9/05/00:00	9/07/23:59
11	020410bbbbbbB79139	9/08/00:00	9/10/23:59
12	020410bbbbbbB79140	9/11/00:00	9/13/23:59
13	020410bbbbbbB79141	9/14/00:00	9/16/23:59
14	020410bbbbbbB79142	9/17/00:00	9/19/17:18

Dallas - Phase III

15	020410bbbbbbB79143	8/30/08:39	9/01/23:59
16	020410bbbbbbB79144	9/02/00:00	9/04/23:59
17	020410bbbbbbB79145	9/05/00:00	9/07/23:59
18	020410bbbbbbB79146	9/08/00:00	9/10/23:59
19	020410bbbbbbB79147	9/11/00:00	9/13/23:59
20	020410bbbbbbB79148	9/14/00:00	9/16/23:59
21	020410bbbbbbB79149	9/17/00:00	9/18/23:45

Oceanographer - Phase III

22	020410bbbbbbB79150	8/30/01:45	9/01/23:59
23	020410bbbbbbB79151	9/02/00:00	9/04/23:59
24	020410bbbbbbB79152	9/05/00:00	9/07/23:59
25	020410bbbbbbB79153	9/08/00:00	9/10/23:59
26	020410bbbbbbB79154	9/11/00:00	9/13/23:59
27	020410bbbbbbB79155	9/14/00:00	9/16/23:59
28	020410bbbbbbB79156	9/17/00:00	9/19/12:21

Researcher

29	020410bbbbbbB79293	IC 1
30	020410bbbbbbB79294	IC 2
31	020410bbbbbbB79295	IC 3B

b = blank

Tape No.	GATE tape identifier (bytes 7-24 of tape header record; not to be used for ordering)	Time period (GMT)	
		Beginning (mo/day/hr:min)	Ending (mo/day/hr:min)
<u>Gilliss</u>			
32	020410bbbbbbB79296		IC 1
33	020410bbbbbbB79297		IC 3B
<u>Dallas</u>			
34	020410bbbbbbB79298		IC 1
35	020410bbbbbbB79299		IC 2
<u>Oceanographer</u>			
36	020410bbbbbbB79100		IC 1
37	020410bbbbbbB79101		IC 2
38	020410bbbbbbB79102		IC 3A
<u>Researcher - Phase II</u>			
39	020410bbbbbbB79265	7/28/00:00	7/30/23:59
40	020410bbbbbbB79266	7/31/00:00	8/02/23:59
41	020410bbbbbbB79267	8/03/00:00	8/05/23:59
42	020410bbbbbbB79268	8/06/00:00	8/07/22:40
43	020410bbbbbbB79269	8/10/11:15	8/12/23:59
44	020410bbbbbbB79270	8/13/00:00	8/16/06:00
<u>Gilliss - Phase II</u>			
45	020410bbbbbbB79271	8/06/20:45	8/09/23:59
46	020410bbbbbbB79272	8/10/00:00	8/12/23:59
47	020410bbbbbbB79273	8/13/00:00	8/15/23:59
48	020410bbbbbbB79274	8/16/00:00	8/18/00:00
<u>Dallas - Phase II</u>			
49	020410bbbbbbB79275	7/28/05:00	7/30/23:59
50	020410bbbbbbB79276	7/31/00:00	8/02/23:59
51	020410bbbbbbB79277	8/03/00:00	8/05/23:59
52	020410bbbbbbB79278	8/06/00:00	8/08/23:59
53	020410bbbbbbB79279	8/09/00:00	8/11/23:59
54	020410bbbbbbB79280	8/12/00:00	8/14/23:59
55	020410bbbbbbB79281	8/15/00:00	8/15/19:10
<u>Oceanographer - Phase II</u>			
56	020410bbbbbbB79282	7/28/00:00	7/30/18:00
57	020410bbbbbbB79283	8/02/21:30	8/04/23:59

b = blank

Tape No.	GATE tape identifier (bytes 7-24 of tape header record; not to be used for ordering)	Time period (GMT)	
		Beginning (mo/day/hr:min)	Ending (mo/day/hr:min)

Oceanographer - Phase II continued

58	020410bbbbbbB79284	8/05/00:00	8/07/23:59
59	020410bbbbbbB79285	8/08/00:00	8/10/23:59
60	020410bbbbbbB79286	8/11/00:00	8/13/23:59
61	020410bbbbbbB79287	8/14/00:00	8/15/23:46

Researcher - Phase I

62	020410bbbbbbB79103	6/27/20:15	6/30/23:59
63	020410bbbbbbB79104	7/01/00:00	7/03/23:59
64	020410bbbbbbB79105	7/04/00:00	7/06/23:59
65	020410bbbbbbB79106	7/07/00:00	7/09/23:59
66	020410bbbbbbB79107	7/10/00:00	7/12/23:59
67	020410bbbbbbB79108	7/13/00:00	7/15/23:59
68	020410bbbbbbB79109	7/16/00:00	7/16/22:59

Gilliss - Phase I

69	020410bbbbbbB79110	6/27/23:30	6/30/23:59
70	020410bbbbbbB79111	7/01/00:00	7/03/23:59
71	020410bbbbbbB79112	7/04/00:00	7/06/23:59
72	020410bbbbbbB79113	7/07/00:00	7/09/23:59
73	020410bbbbbbB79114	7/10/00:00	7/12/23:59
74	020410bbbbbbB79115	7/13/00:00	7/15/23:59
75	020410bbbbbbB79116	7/16/00:00	7/13/23:59

Dallas - Phase I

76	020410bbbbbbB79117	6/28/00:00	6/30/23:59
77	020410bbbbbbB79118	7/01/00:00	7/03/23:59
78	020410bbbbbbB79119	7/04/00:00	7/06/23:59
79	020410bbbbbbB79120	7/07/00:00	7/09/23:59
80	020410bbbbbbB79121	7/10/00:00	7/12/23:59
81	020410bbbbbbB79122	7/13/00:00	7/16/21:30

Oceanographer - Phase I

82	020410bbbbbbB79123	6/27/21:38	6/30/23:59
83	020410bbbbbbB79124	7/01/00:00	7/03/23:59
84	020410bbbbbbB79125	7/04/00:00	7/06/23:59
85	020410bbbbbbB79126	7/07/00:00	7/09/23:59
86	020410bbbbbbB79127	7/10/00:00	7/12/23:59
87	020410bbbbbbB79128	7/13/00:00	7/16/22:30

b = blank

When ordering data from WDC-A (National Climatic Center, Asheville, North Carolina 28801), include the following identifications and descriptive information on the request form for each tape: .

<u>Identification</u>				<u>Description</u>
S.	TT.	CC.	DDD.	
<u>3</u>	<u>30</u>	<u>02</u>	<u>102</u>	Magnetic Tape No./N

N is the appropriate tape number taken from the inventory in the GATE Data Catalog. In addition, provide an indication of desired magnetic tape recording characteristics (options for the number of tracks, recording density, and recording code).

7.2 Microfilm Time-Series Plots

There are four microfilm groups, one for each of the ships. Each group of low-resolution averages (3-min averages, 10-min averages, etc.) contains four microfilm frame types. The contents of each frame and the units of each variable are as follows:

Frame Type 1:

1. Ship speed (m/s).
2. Ship heading ($^{\circ}$)
3. Pressure, Rosemount (mb).
4. Pressure, Kollsman (mb).

Frame Type 2:

1. Wind speed, bow boom (m/s).
2. Wind speed, mast (m/s).
3. Wind direction, bow boom ($^{\circ}$).
4. Wind direction, mast ($^{\circ}$).

Frame Type 3:

1. Sea temperature ($^{\circ}\text{C}$).
2. Dry-bulb temperature ($^{\circ}\text{C}$).
3. Wet-bulb temperature #1 ($^{\circ}\text{C}$). Note: On August 8, 1974, at 1900 GMT, during Phase II, the Oceanographer converted one of its wet bulbs to a dry bulb; wet-bulb #2 became dry bulb #2.
4. Wet-bulb temperature #2 ($^{\circ}\text{C}$).

Frame Type 4:

1. Incident solar radiation (Eppley, W/m^2).
2. Incident solar radiation (Yanishevsky, W/m^2), mounted on the Oceanographer only.
3. Reflected solar radiation (W/m^2).
4. Net radiation (W/m^2).

The high-resolution data set (4-s averages) does not have Frame Type 4.

The following microfilm reels contain the U.S. B-scale ship boom surface meteorological and radiation data. Each microfilm frame of the hourly averages, hourly observations, 30-min averages, and 10-min averages represents 72 hr of information. The tick marks on the abscissa indicate time. The times along the abscissa are in Greenwich Mean Time (GMT) and the Julian day is indicated at the beginning of the frame.

Hourly Averages, Hourly Observations,
and 3-Minute Averages

<u>Reel No.</u>	<u>Data</u>	<u>Ship</u>	<u>Time Period</u>
1	Hourly averages and hourly observations	<u>Researcher, Gilliss</u> <u>Dallas, Oceanographer</u>	IC 1, 2, 3
2	Time series of 3-min averages	<u>Researcher, Gilliss</u> <u>Dallas, Oceanographer</u>	IC 1, 2, 3
3	Time series of 3-min averages	<u>Researcher, Gilliss</u> <u>Dallas, Oceanographer</u>	Phase II
4	Time series of 3-min averages	<u>Researcher, Gilliss</u> <u>Dallas, Oceanographer</u>	Phase I
5	Time series of 3-min averages	<u>Researcher, Gilliss</u> <u>Dallas, Oceanographer</u>	Phase III
6	Hourly averages and hourly observations	<u>Researcher, Gilliss</u> <u>Dallas, Oceanographer</u>	Phases I, II, III

10- and 30-Minute Averages

<u>Reel No.</u>	<u>Data</u>	<u>Ship</u>	<u>Time Period</u>
1	Time series plots of 30-min and 10-min averages	<u>Researcher</u> <u>Gilliss</u> <u>Dallas</u> <u>Oceanographer</u>	Phase I, II, III Phase I, II, III Phase I, II, III Phase I, II, III

Each microfilm frame of 4-s averages represents a 1-hr time period, with the exception of the Gilliss Phase III data. Each tick-mark on the abscissa is labeled in Julian seconds since the beginning of the year, and the tick-marks are spaced every 10 min with the exception of the Gilliss Phase II data. The first time of each frame is also given in terms of the Julian day and the Greenwich Mean Time (GMT) hour and minute. Each frame of the Gilliss Phase III data represents 30 min of time and the tick-marks are spaced every 5 min.

4-Second Averages

<u>Reel No.</u>	<u>Data</u>	<u>Ship</u>	<u>Time Period</u>
1	Time series of the 4-s averages	<u>Researcher, Gilliss</u> <u>Dallas, Oceanographer</u>	IC 1, 2, 3
2	Time series of the 4-s averages	<u>Researcher</u>	Phase I
3	Time series of the 4-s averages	<u>Gilliss</u>	Phase I

4-Second Averages (continued)

<u>Reel No.</u>	<u>Data</u>	<u>Ship</u>	<u>Time Period</u>
4	Time series of the 4-s averages	<u>Dallas</u>	Phase I
5	Time series of the 4-s averages	<u>Oceanographer</u>	Phase I
6	Time series of the 4-s averages	<u>Researcher</u>	Phase II
7	Time series of the 4-s averages	<u>Gilliss</u>	Phase II
8	Time series of the 4-s averages	<u>Dallas</u>	Phase II
9	Time series of the 4-s averages	<u>Oceanographer</u>	Phase II
10	Time series of the 4-s averages	<u>Researcher</u>	Phase III
11	Time series of the 4-s averages	<u>Gilliss</u>	Phase III, Part 1
12	Time series of the 4-s averages	<u>Gilliss</u>	Phase III, Part 2
13	Time series of the 4-s averages	<u>Dallas</u>	Phase III
14	Time series of the 4-s averages	<u>Oceanographer</u>	Phase III

When ordering these data from WDC-A, include the following identification and descriptive information on the request form for each microfilm:

<u>Identification</u>	<u>Description</u>
S. TT. CC. DDD.	
<u>3</u> <u>30</u> <u>02</u> <u>103</u>	Microfilm Reel No. 35/N

N is the appropriate reel number taken from the inventory given above.

REFERENCES

- Augstein, E., H. Hoerber, and L. Krugermeyer, 1974: Fehler bei Temperatur-Feuchte- und Windmessungen auf Schiffen in tropischen Breiten (Errors of temperature, humidity, and wind measurements from ships in tropical latitudes). Meteorologische Forschung-Ergebnisse, B9, pp. 1-10.
- Ching, J. K. S., 1976: Ship's Influence on Wind Measurements Determined from BOMEX Mast and Boom Data. Journal of Applied Meteorology, 15, pp. 102-106.
- de la Moriniere, T. C., 1974: The International Data Management Plan for the GARP Atlantic Tropical Experiment, Part 1, GATE Report No. 13, World Meteorological Organization, Geneva, Switzerland, 224 pp.
- Echternacht, K. L., 1974a: Section VII - Surface Meteorological Subsystem (SMSS). Included in GATE Shipboard Data Systems (SDS) Operations Manual, NOAA Data Buoy Office, Bay St. Louis, Mississippi. 21 pp. (Written for use during GATE.)
- Echternacht, K. L., 1974b: Section 1.2 - The Automatic Boom and Standard Surface Meteorological and Radiation and Related Hardware. Included in Operation Plan, Annex Q, Scientific Observations. U.S. GATE Project 1-74, NOAA Data Buoy Office, Bay St. Louis, Mississippi. 50 pp. (Written for use during GATE.)
- Echternacht, K. L., 1975: The Surface Meteorological Subsystem (SMSS): Pre-GATE Calibrations and Operations Manual. ONR Final Report, Report No. IAR 75001, Office of Naval Research, Washington, D.C., 76 pp.
- Hadlock, R., W. R. Seguin, and M. Garstang, 1972: A Radiation Shield for Thermistor Deployment in the Atmospheric Boundary Layer. Journal of Applied Meteorology, 11, pp. 393-399.
- Hanson, K. J., and M. Poindexter, 1973: Report of the Radiation and Surface Meteorology (Boom) Program on the Researcher during GIST. Unpublished report, Atlantic Oceanographic and Meteorological Laboratories, NOAA, Miami, Florida, 10 pp.
- Hanson, K. J., and J. R. Latimer, 1974: Preliminary Report of the GATE Pyranometer Comparison, Miami, Florida, April 15-30, 1974. Unpublished report, Atlantic Oceanographic and Meteorological Laboratories, NOAA, Miami, Florida.
- Roll, H. U., 1965: Physics of the Marine Atmosphere. Academic Press, New York, N. Y., 426 pp.
- Seguin, W. R., and P. Sabol, 1973: A Preliminary Evaluation of the Automated Surface Meteorological Instrumentation Used During the GATE International Sea Trials (GIST). Unpublished report, Center for Experiment Design and Data Analysis, Environmental Data Service, NOAA, Washington, D.C., 8 pp.

Seguin, W. R., and M. Garstang, 1971: A Comparison of Meteorological Sensors Used on the USCGSS Discoverer During the 1968 Barbados Experiment. Bulletin of the American Meteorological Society, 52, pp. 1071-1076.

World Meteorological Organization, 1974: The Third International Pyrheliometer Comparison (IPC-III), Davos and Locarno, 1970. Final Report, WMO-No. 362 (1974), Geneva, Switzerland, 7 pp.

APPENDIX A

Detailed Tape Formats and Examples

The tapes containing the U.S. GATE B-scale ship data have been written according to the specifications put forth in GATE Report No. 13, Part 1, Appendix E (World Meteorological Organization, Geneva, Switzerland). Each data set has been written on a 9-track, 800 BPI, odd-parity tape in EBCDIC, with the data blocked into fixed length physical records of 1920 characters. Each tape consists of six types of physical records separated by inter-record gaps and blocked into files (separated by end-of-file marks, EOFs, also called tape marks) in the following sequence:

Test file		
EOF		
Tape header record		
EOF		
Type 1 file header record	}	Meteorological and radiation data file No. 1.
Type 2 file header record		
Data		
EOF		
Type 1 file header record	}	Meteorological and radiation data file No. 2.
Type 2 file header record		
Data		
EOF		
.		
.		
.		
.		
(Additional meteorological and radiation data files)		
EOF		
End-of-tape record		
EOF		
EOF.		

The test file consists of 300 test records, each containing 1920 test characters. A test character is defined as all 1s, octal "77" in BCD, hexadecimal "FF" in EBCDIC, and binary "11111111" in Minsk-32 code (i.e., $11111111_2 \equiv FF_{16}$).

The tape header record contains the tape identification, name of the country and institution writing the tape, the creation date, the type of computer used, and the GATE translation table (character code), which defines the characters used by the computer writing the tape.

The files containing the meteorological and radiation data begin with one Type 1 file header record and two or more Type 2 file header records. Figures A.1 and A.2 show Type 1 and Type 2 file header records for the 4-s average and 3-min average data sets, respectively. Selected characters in Type 1 and Type 2 file headers are as follows:

Byte character numbers	Description
2-6	The word GATE
13-24	File number (for example - S4I3SFC4S001) S4 \equiv ship 4 where (1 \equiv <u>Researcher</u> 2 \equiv <u>Gilliss</u> 3 \equiv <u>Dallas</u> 4 \equiv <u>Oceanographer</u>) I3 \equiv Intercomparison 3 (I \equiv Intercomparison P \equiv Phase) SFC \equiv surface 4S \equiv 4-s data set (3M \equiv 3-min average 10 \equiv 10-min average 30 \equiv 30-min average HR \equiv hourly average HO \equiv hourly observation) 001 \equiv tape number
30-35	Date this file was created (YYMMDD) YY \equiv Year, MM \equiv Month, DD \equiv Day
42-59	Country - United States
60-77	Institution generating tape - CEDDA
84-87	Platform type - Ship
96-119	Platform name
130-153	Chief scientist
242-258	Date and time of first observation (CCYYMMDDHHMMSSMMM)
259-265	Latitude of the ship at the first observation (\pm DDMMHH)
266-273	Longitude of the ship at the first observation (\pm DDMMHH)
322-338	Date and time of the last observation (CCYYMMDDHHMMSSMMM)
339-345	Latitude of the ship for the last observation (\pm DDMMHH)
346-353	Longitude of the ship for the last observation (\pm DDMMHH)

[illegible]

Figure A.1.--Header file records, 4-s averages.

20100DATE	012YYMMDD	1.0	0.0	0.0009999999	001
29999999	800 DIGITAL CLOCK				002
20000TIME	022HHMMSST	1.0	0.0	0.0009999999	003
29999999	800 DIGITAL CLOCK				004
21200LATITUDE	125DEGREES	1.0	0.0	0.0009999999	005
29999999	803 POSITION DERIVED FROM NAVIGATION DATA SET				006
21300LONGITUDE	125DEGREES	1.0	0.0	0.0009999999	007
29999999	803 POSITION DERIVED FROM NAVIGATION DATA SET				008
22990SHIP SPEED	210METERS/SEC.	1.0	0.0	0.0429999999	009
29999999	SN 415 801 SPERRY DOPPLER SPEED LOG				010
21410SHIP HEADING	140DEGREES	1.0	0.0	0.0009999999	011
29999999	SN 414 800 SPERRY GYROCOMPASS				012
24000KOLLS.PRESSURE	400MILLIBARS	1.0	0.0	0.0429999999	013
29999999	SN 102 801 KOLLSMAN PRESSURE SENSOR				014
24000ROSE.PRESSURE	400MILLIBARS	1.0	0.0	0.0009999999	015
29999999	SN 137 801 ROSEMOUNT PRESSURE SENSOR				016
25030SEA SURF.TEMP.	500DEG.CELCIUS	1.0	0.0	0.0009999999	017
29999999	SN 129 802 YELLOW SPRING INST. THERMISTOR				018
25010DRY BULB TEMP.	1500DEG.CELCIUS	1.0	0.0	0.0009999999	019
29999999	SN 52 802 YELLOW SPRING INST. THERMISTOR				020
25010DRY BULB TEMP.	2500DEG.CELCIUS	1.0	0.0	0.0009999999	021
29999999	SN 58 802 YELLOW SPRING INST. THERMISTOR				022
25020WET BULB TEMP.	1500DEG.CELCIUS	1.0	0.0	0.0009999999	023
29999999	SN 57 802 YELLOW SPRING INST. THERMISTOR				024

Figure A.1.--Header file records, 4-s averages (continued).

25020WET BULB TEMP.	2500DEG.CELCIUS	1.0	0.0	0.0999999999	025
29999999	SN 58 802 YELLOW SPRING INST. THERMISTOR				026
25400SPEC.HUMIDITY	1520GRAMS/KG.	1.0	0.0	0.0009999999	027
29999999	802 DERIVED FROM DRY BULB 1 AND WET BULB 1				028
25400SPEC.HUMIDITY	2520GRAMS/KG.	1.0	0.0	0.0999999999	029
29999999	802 DERIVED FROM DRY BULB 1 AND WET BULB 2				030
25040DEW PT.TEMP.	1 500DEG.CELCIUS	1.0	0.0	0.0009999999	031
29999999	802 DERIVED FROM DRY BULB 1 AND WET BULB 1				032
25040DEW PT.TEMP.	2 500DEG.CELCIUS	1.0	0.0	0.0999999999	033
29999999	802 DERIVED FROM DRY BULB 1 AND WET BULB 2				034
22590WIND SPEED-BOOM	210METERS/SEC.	1.0	0.0	0.0009999999	035
29999999	SN 152 801 R.M.YOUNG GILL 3-CUP ANEMOMETER				036
22590WIND SPEED-MAST	210METERS/SEC.	1.0	0.0	0.0009999999	037
29999999	SN 177 801 R.M.YOUNG GILL 3-CUP ANEMOMETER				038
22010WIND DIR.-BOOM	200DEGREES	1.0	0.0	0.0009999999	039
29999999	SN 202 800 R.M.YOUNG GILL MICROVANE				040
22010WIND DIR.-MAST	200DEGREES	1.0	0.0	0.0009999999	041
29999999	SN 227 800 R.M.YOUNG GILL MICROVANE				042
22460WIND, U-COM, BOOM	230METERS/SEC.	1.0	0.0	0.0009999999	043
29999999	801 DERIVED FROM BOOM WIND SPEED AND DIRECTION				044
22470WIND, V-COM, BOOM	230METERS/SEC.	1.0	0.0	0.0009999999	045
29999999	801 DERIVED FROM BOOM WIND SPEED AND DIRECTION				046
22460WIND, U-COM, MAST	230METERS/SEC.	1.0	0.0	0.0009999999	047
29999999	801 DERIVED FROM MAST WIND SPEED AND DIRECTION				048

Figure A.1.--Header file records, 4-s averages (continued).

22470WIND, V-COM, MAST230METERS/SEC.	1.0	0.0	0.0009999999	049
299999999	801 DERIVED FROM	MAST	WIND SPEED AND DIRECTION	050
2				051
2				052
2				053
2				054
2				055
2				056
2				057
2				058
2				059
2				060
2				061
2				062
2				063
2				064
2				065
2				066
2				067
2				068
2				069
2				070
2				071
2				072

Figure A.1.--Header file records, 4-s averages (continued).

[illegible]

Figure A.2.--Header file records, hourly averages.

20100DATE	012YYMMDD	1.0	0.0	0.0009999999	001
29999999	800 DIGITAL CLOCK				002
20000TIME	022HHMMSS	1.0	0.0	0.0009999999	003
29999999	800 DIGITAL CLOCK				004
21200LATITUDE	125DEGREES	1.0	0.0	0.0009999999	005
29999999	803 POSITION DERIVED FROM NAVIGATION DATA SET				006
21300LONGITUDE	125DEGREES	1.0	0.0	0.0009999999	007
29999999	803 POSITION DERIVED FROM NAVIGATION DATA SET				008
22990SHIP SPEED	210METERS/SEC.	1.0	0.0	0.0429999999	009
29999999	SN 415 801 SPERRY DOPPLER SPEED LOG				010
29900CNTS,SHIP SPEED	910INTEGER	1.0	0.0	0.0009999999	011
29999999	800 NO. OF 4-SEC. RECORDS USED TO COMPUTE AVG.				012
21410SHIP HEADING	140DEGREES	1.0	0.0	0.0009999999	013
29999999	SN 414 800 SPERRY GYROCOMPASS				014
29900CNTS,SHIP HEAD.	910INTEGER	1.0	0.0	0.0009999999	015
29999999	800 NO. OF 4-SEC. RECORDS USED TO COMPUTE AVG.				016
26320INC.SOL.RAD. 1	610WATTS/SQ.M.	1.0	0.0	0.0009999999	017
29999999	SN 11538 801 EPPELY MODEL 2 PYRANOMETER				018
29900CNTS,INC.SOL.1	910INTEGER	1.0	0.0	0.0009999999	019
29999999	800 NO. OF 4-SEC. RECORDS USED TO COMPUTE AVG.				020
26320INC.SOL.RAD. 2	610WATTS/SQ.M.	1.0	0.0	0.0009999999	021
29999999	SN 02 801 YANISHEVSKI MODEL M-80				022
29900CNTS,INC.SOL.2	910INTEGER	1.0	0.0	0.0009999999	023
29999999	800 NO. OF 4-SEC. RECORDS USED TO COMPUTE AVG.				024

Figure A.2.--Header file records, hourly averages (continued).

26330REFL.SOL.RAD.	610WATTS/SQ.M.	1.0	0.0	0.0009999999	025
29999999	SN 12560 801 EPPELY MODEL	8-48	PYRANOMETER		026
29900CNTS,REFL.SOLAR910INTEGER	1.0	0.0	0.0009999999		027
29999999	800 NO. OF 4-SEC. RECORDS USED TO COMPUTE AVG.				028
26370NET RADIATION	610WATTS/SQ.M.	1.0	0.0	0.0009999999	029
29999999	SN 6964 801 SWISSTECTO MODEL	51			030
29900CNTS,NET RAD.	910INTEGER	1.0	0.0	0.0009999999	031
29999999	800 NO. OF 4-SEC. RECORDS USED TO COMPUTE AVG.				032
24000KOLLS.PRESSURE	400MILLIBARS	1.0	0.0	0.0429999999	033
29999999	SN 102 801 KOLLSMAN PRESSURE SENSOR				034
29900CNTS,KOLLS.PRES910INTEGER	1.0	0.0	0.0009999999		035
29999999	800 NO. OF 4-SEC. RECORDS USED TO COMPUTE AVG.				036
24000ROSE.PRESSURE	400MILLIBARS	1.0	0.0	0.0009999999	037
29999999	SN 137 801 ROSEMOUNT PRESSURE SENSOR				038
29900CNTS,ROSE.PRES.910INTEGER	1.0	0.0	0.0009999999		039
29999999	800 NO. OF 4-SEC. RECORDS USED TO COMPUTE AVG.				040
25030SEA SURF.TEMP.	500DEG.CELCIUS	1.0	0.0	0.0009999999	041
29999999	SN 129 802 YELLOW SPRING INST. THERMISTOR				042
29900CNTS,SURF.TEMP.910INTEGER	1.0	0.0	0.0009999999		043
29999999	800 NO. OF 4-SEC. RECORDS USED TO COMPUTE AVG.				044
25010DRY BULB TEMP.	1500DEG.CELCIUS	1.0	0.0	0.0009999999	045
29999999	SN 52 802 YELLOW SPRING INST. THERMISTOR				046
29900CNTS,DRY BULB	1910INTEGER	1.0	0.0	0.0009999999	047
29999999	800 NO. OF 4-SEC. RECORDS USED TO COMPUTE AVG.				048

Figure A.2.--Header file records, hourly averages (continued).

```

25010 DRY BULB TEMP. 2500 DEG. CELCIUS      1.0  0.0  0.0009999999 049
29999999 SN 58      802 YELLOW SPRING INST. THERMISTOR          050
29900 CNTS, DRY BULB 2910 INTEGER          1.0  0.0  0.0009999999 051
29999999      800 NO. OF 4-SEC. RECORDS USED TO COMPUTE AVG. 052
25020 WET BULB TEMP. 1500 DEG. CELCIUS      1.0  0.0  0.0009999999 053
29999999 SN 57      802 YELLOW SPRING INST. THERMISTOR          054
29900 CNTS, WET BULB 1910 INTEGER          1.0  0.0  0.0009999999 055
29999999      800 NO. OF 4-SEC. RECORDS USED TO COMPUTE AVG. 056
25020 WET BULB TEMP. 2500 DEG. CELCIUS      1.0  0.0  0.0999999999 057
29999999 SN 58      802 YELLOW SPRING INST. THERMISTOR          058
29900 CNTS, WET BULB 2910 INTEGER          1.0  0.0  0.0999999999 059
29999999      800 NO. OF 4-SEC. RECORDS USED TO COMPUTE AVG. 060
25400 SPEC. HUMIDITY 1520 GRAMS/KG.          1.0  0.0  0.0009999999 061
29999999      802 DERIVED FROM DRY BULB 1 AND WET BULB 1 062
25400 SPEC. HUMIDITY 2520 GRAMS, KG.          1.0  0.0  0.0999999999 063
29999999      802 DERIVED FROM DRY BULB 1 AND WET BULB 2 064
25040 DEW PT. TEMP. 1 500 DEG. CELCIUS      1.0  0.0  0.0009999999 065
29999999      802 DERIVED FROM DRY BULB 1 AND WET BULB 1 066
25040 DEW PT. TEMP. 2 500 DEG. CELCIUS      1.0  0.0  0.0999999999 067
29999999      802 DERIVED FROM DRY BULB 1 AND WET BULB 2 068
22590 WIND SPEED-800 M210 METERS/SEC.        1.0  0.0  0.0009999999 069
29999999 SN 152      801 R.M. YOUNG GILL 3-CUP ANEMOMETER          070
29900 CNTS, W.S.-800 M 910 INTEGER          1.0  0.0  0.0009999999 071
29999999      800 NO. OF 4-SEC. RECORDS USED TO COMPUTE AVG. 072

```

Figure A.2.--Header file records, hourly averages (continued).

```

22590WIND SPEED-MAST210METERS/SEC.      1.0      0.0      0.0009999999      073
29999999      SN 177      801 R.M.YOUNG GILL 3-CUP ANEMOMETER      074
29900CNTS,W.S.-MAST 910INTEGER      1.0      0.0      0.0009999999      075
29999999      800 NO. OF 4-SEC. RECORDS USED TO COMPUTE AVG.      076
22010WIND DIR.-BOOM 200DEGREES      1.0      0.0      0.0009999999      077
29999999      SN 202      800 R.M.YOUNG GILL MICROVANE      078
29900CNTS,W.D.-BOOM 910INTEGER      1.0      0.0      0.0009999999      079
29999999      800 NO. OF 4-SEC. RECORDS USED TO COMPUTE AVG.      080
22010WIND DIR.-MAST 200DEGREES      1.0      0.0      0.0009999999      081
29999999      SN 227      800 R.M.YOUNG GILL MICROVANE      082
29900CNTS,W.D.-MAST 910INTEGER      1.0      0.0      0.0009999999      083
29999999      800 NO. OF 4-SEC. RECORDS USED TO COMPUTE AVG.      084
22460WIND,U-COM,BOOM230METERS/SEC.      1.0      0.0      0.0009999999      085
29999999      801 DERIVED FROM BOOM WIND SPEED AND DIRECTION      086
22470WIND,V-COM,BOOM230METERS/SEC.      1.0      0.0      0.0009999999      087
29999999      801 DERIVED FROM BOOM WIND SPEED AND DIRECTION      088
22460WIND,U-COM,MAST230METERS/SEC.      1.0      0.0      0.0009999999      089
29999999      801 DERIVED FROM MAST WIND SPEED AND DIRECTION      090
22470WIND,V-COM,MAST230METERS/SEC.      1.0      0.0      0.0009999999      091
29999999      801 DERIVED FROM MAST WIND SPEED AND DIRECTION      092
2          2          093
2          2          094
2          2          095
2          2          096

```

Figure A.2.--Header file records, hourly averages (continued).

Starting with character 652, the format for the data records on the tape are given. The first 30 characters (or bytes) of each data record contain mandatory information, which is defined in GATE Report No. 13. The remaining characters as defined by the format statement are the values of the meteorological and radiation variables listed in the Type 2 file header records. Following the format specification is a paragraph describing the data set.

The Type 2 file header records describe the meteorological and radiation variables contained in the file. The order in which they are listed corresponds to the data format given in the Type 1 record. For the low-resolution data sets (the 3-min averages, the 10-min averages, etc.), the Type 2 data file headers constitute four physical records. For the high-resolution data sets (the 4-s averages), they constitute two physical records.

The meteorological and radiation data follow the Type 1 and Type 2 headers in each data file. They are given in order of time sequence, with each logical record corresponding to an observation time, and the data in each logical record are written according to the format given in the Type 1 file header records.

There are as many data files as data sets placed on the tape. Each is followed by an EOF. At the end of the data is an End-of-Tape Record containing the name and address of the Director, CEDDA. This is followed by two EOFs, indicating the end of information on the tape.

Users should dump the tape and several data records upon receipt, and check the data against the format to verify that the tape can be read.

APPENDIX B

Pre-GATE Intercomparison of Pyranometers

Intercomparisons of the pyranometers to be used on the U.S. ships during GATE were made at NOAA's Atlantic Oceanographic and Meteorological Laboratories, in Miami, Florida, from April 5 to 30, 1974. Measurements were based on the International Pyrheliometric Scale (IPS) of 1956 (World Meteorological Organization, 1974). All test pyranometers were compared against a Canadian reference standard Eppley No. 10036 pyranometer whose calibration was traceable to the IPS via the Canadian standard, PACRAD, Eppley-Kendall No. 11399 pyrheliometer.

The instruments were compared for periods of at least 3 days, and new sensitivities were derived for the GATE pyranometers (table 8, sec. 6.2) based on the integrated daily total radiation. The 67 pyranometers tested in Miami agreed to within 4 percent for the daily totals over the entire period, and two-thirds of the instruments agreed within 1 percent.

Curves of the ratio of the test instrument to the standard were plotted against true solar time. Examples of the response, shown in figures B.1, B.2, and B.3, clearly indicate that, as groups, the Eppley 2 and 8-48, and the Yanishevsky pyranometers behave in much the same way. Energy differences of as much as 3 percent or more may occur for solar zenith angles of less than 70° , depending on instrument type. For solar zenith angles larger than 70° , the variation in response between instrument types is much greater. The variation in response between the Eppley model 2 pyranometers, as seen in figure B-1, implies that instruments of the same type show large variations in output for energy received at low angles of incidence. This may explain the large differences in the measurements of reflected solar radiation during the GATE Intercomparison periods. Not only were different types of instruments used, but the energy received by the sensors was of low intensity and was scattered from the ocean surface, which means that most of the energy was received at low angles of incidence.

The results of the tests in Miami indicated that the stated accuracy requirements (5 to 6 percent) for shipboard measurements during GATE could be achieved.

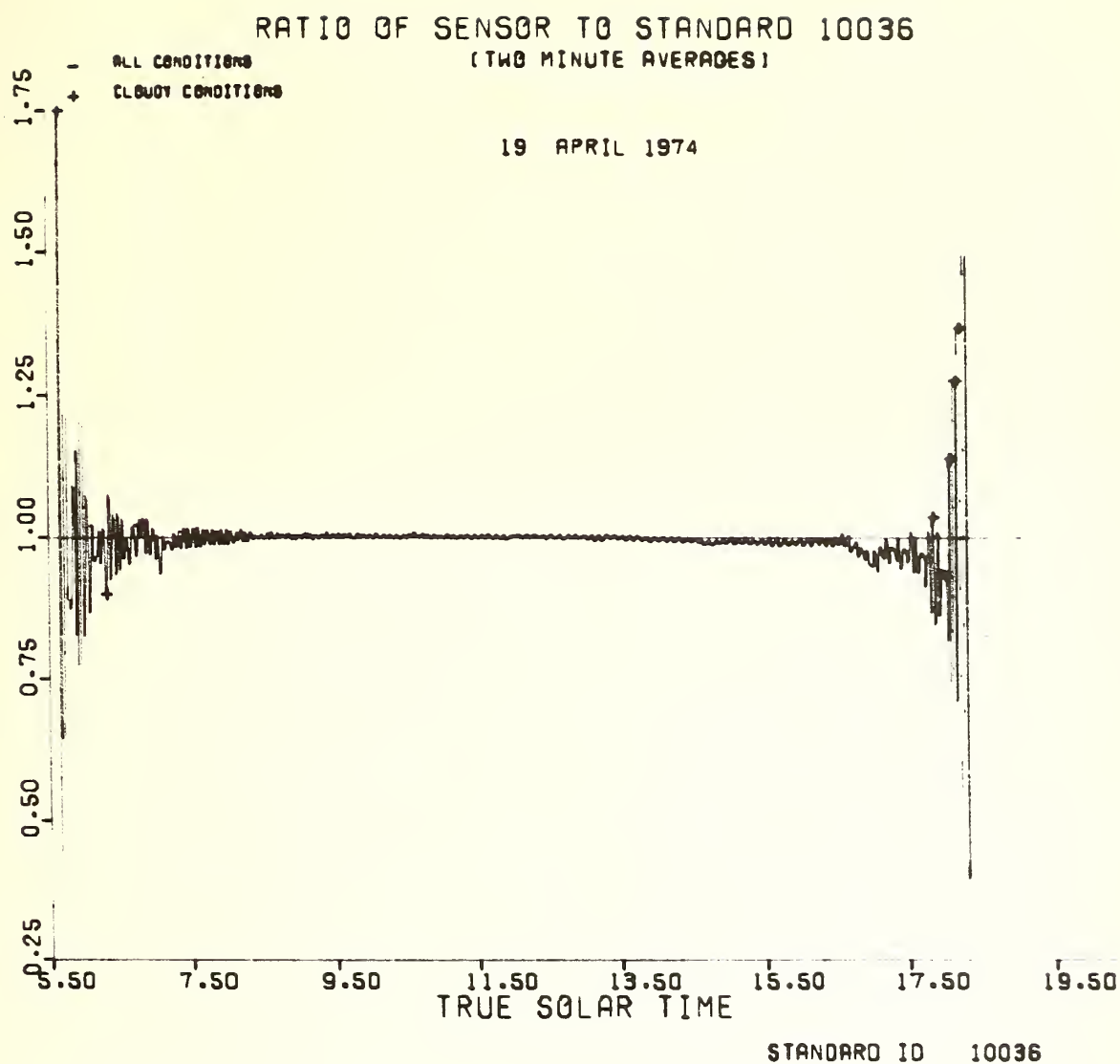


Figure B.1.--Response of an Eppley 2 pyranometer.

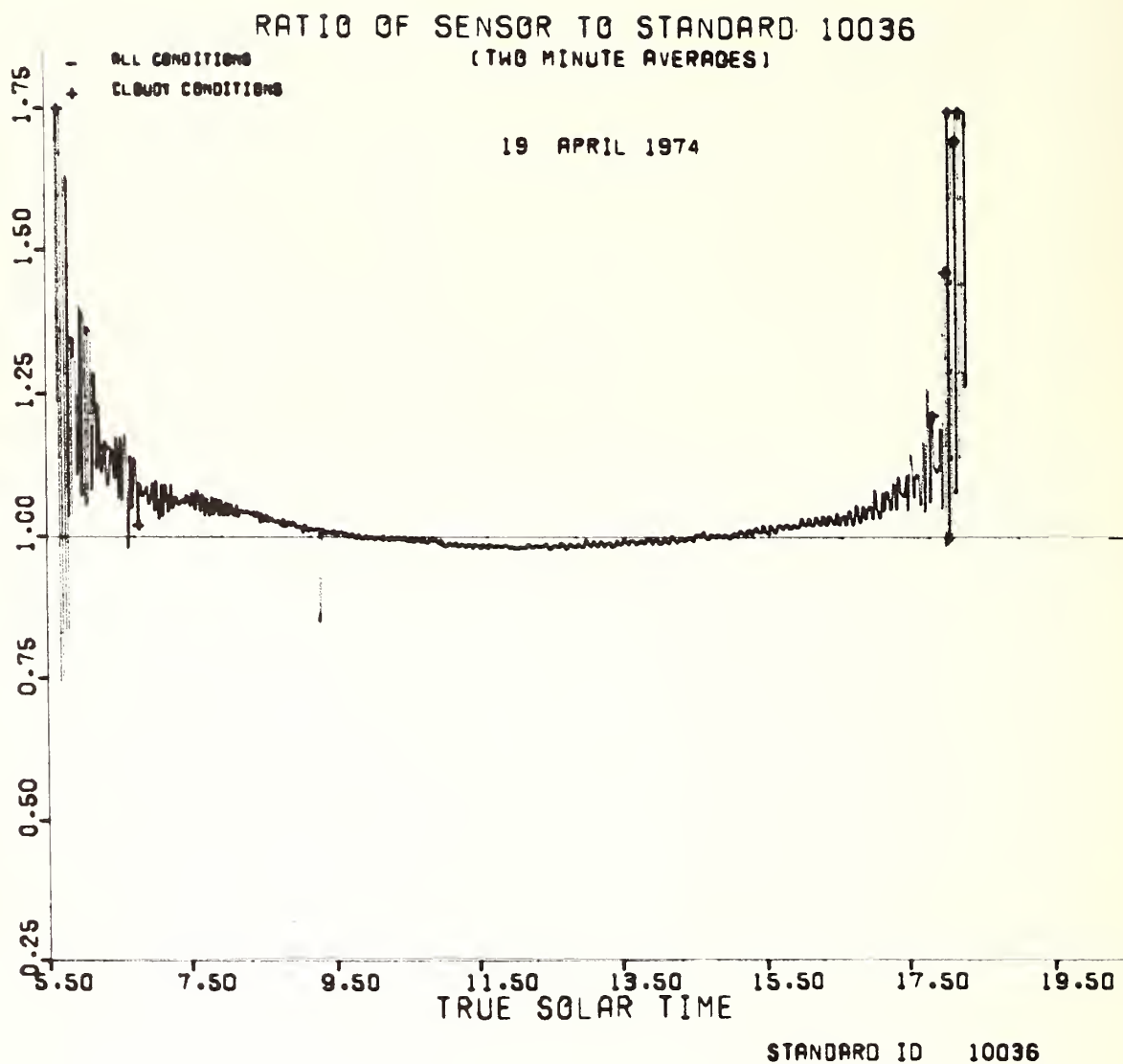


Figure B.2.--Response of an Eppley 8-48 pyranometer.

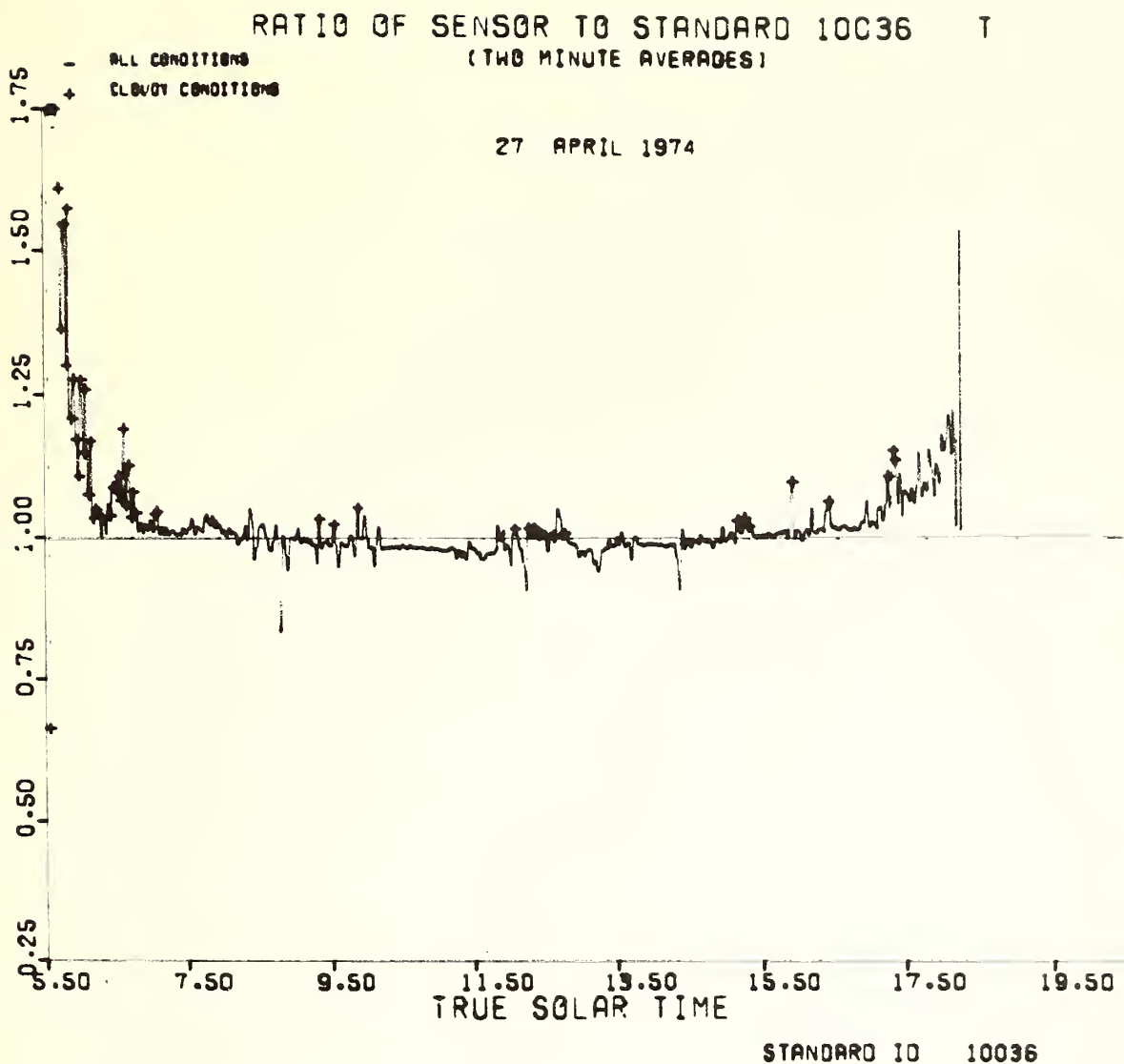


Figure B.3.--Response of a Yanishevsky pyranometer.

APPENDIX C

Translocation of Thermistor Probes and Bridges.

The dry-and wet- bulb temperature sensors on the Gilliss, and the sea-surface temperature sensors on the Researcher, Gilliss, and Dallas were not calibrated with the bridges that they were paired with for the pre-GATE calibrations. To establish the correct calibration for the matched thermistor and bridge pairs, it was necessary to subtract the calibration of the particular bridge that was used in calibrating the sensor and build in the calibration of the bridge that was used with the sensor in the field.

The following relationship was established relating the bath temperatures (T_{bath}) to the output voltage (V_{cal}) of the bridge used in the calibration:

$$T_{\text{bath}}(^{\circ}\text{C}) = b_{2B} \cdot V_{\text{cal}} + b_{1B}, \quad (\text{C.1})$$

where

b_{2B} = the slope,

b_{1B} = the intercept.

The separate bridge calibrations established the relationship between the voltage, V_{cal} , and the resistance, R , for each of the bridges. Thus, for any given bridge used in the water bath calibration,

$$R = a_{2B} \cdot V_{\text{cal}} + a_{1B}, \quad (\text{C.2})$$

where

a_{2B} = the slope, and

a_{1B} = the intercept.

For the bridge that was mated with a particular thermistor in the field, a similar resistance-to-voltage relationship was

$$R = a_{2F} \cdot V_{\text{field}} + a_{1F}, \quad (\text{C.3})$$

where

a_{2F} = the slope, and

a_{1F} = the intercept.

In reality, these relationships were slightly nonlinear. However, for the small resistance ranges associated with the nominal temperatures they represented and because the same two resistance values were used in all translocation operations, the error caused by approximating the nonlinear curve by a linear curve turned out to be negligible.

Solving eq. (C.2) for V_{cal} ,

$$V_{cal} = \frac{R - a_{1B}}{a_{2B}} ,$$

replacing R with eq. (C.3),

$$\begin{aligned} V_{cal} &= \frac{(a_{2F} \cdot V_{field} + a_{1F}) - a_{1B}}{a_{2B}} \\ &= \frac{a_{2F}}{a_{2B}} \cdot V_{field} + \frac{(a_{1F} - a_{1B})}{a_{2B}} , \end{aligned}$$

and substituting in eq. (C.1), yields

$$T_{bath} (^{\circ}C) = b_{2B} \cdot \frac{a_{2F}}{a_{2B}} \cdot V_{field} + b_{2B} \cdot \frac{(a_{1F} - a_{1B})}{a_{2B}} + b_{1B} ,$$

or

$$T_{bath} (^{\circ}C) = C_2 \cdot V_{field} + C_1 , \tag{C.4}$$

where

$$C_2 = \frac{b_{2B} \cdot a_{2F}}{a_{2B}} ,$$

and

$$C_1 = \frac{b_{2B}}{a_{2B}} (a_{1F} - a_{1B}) + b_{1B} .$$

Equation (C.4) was then used to derive voltage-to-temperature relationships for all thermistors that were mated during the GATE field operations, but were not mated during the calibrations.

APPENDIX D

Sensor and SAM Transfer Equations
Used in Data Processing

Table D.1.--SAM transfer equations

Variable	Channel No.	Counts to volts	
		Slope $\times 10^{-4}$	Intercept $\times 10^{-3}$
<u>Researcher</u> Bow SAM			
Sea-surface temperature	5	3.0523	-2.0094
Dry-bulb temperature	7	3.0597	-2.5752
Wet-bulb temperature #1	8	3.0545	-2.3418
Wet-bulb temperature #2	9	3.0562	-2.3686
Boom wind direction	12	3.0565	-3.6933
Boom wind speed	13	3.0583	-3.1092
<u>Researcher</u> Central SAM			
Mast wind speed	7	2.9468	-0.8104
Pressure (Rosemount)	8	2.9467	0.3438
<u>Gilliss</u> Bow SAM			
Sea-surface temperature	5	3.0600	-12.4694
Dry-bulb temperature	7	3.0522	- 0.9919
Wet-bulb temperature #1	8	3.0596	-12.1620
Wet-bulb temperature #2	9	3.0529	0.6869
Wind direction	12	3.0550	- 5.8808
Wind speed	13	3.0570	- 8.4060
<u>Gilliss</u> Mast SAM			
Mast wind speed	7	2.9639	- 6.7676
Pressure (Rosemount)	8	2.9626	- 6.0980
<u>Dallas</u> Bow SAM			
Sea-surface temperature	10	3.0539	-1.9087
Dry-bulb temperature	7	3.0536	-1.9594
Wet-bulb temperature #1	8	3.0538	-1.6542
Wet-bulb temperature #2	9	3.0555	-3.5139
Boom wind direction	12	3.0527	-0.1526
Boom wind speed	13	3.0533	-1.3994

Table D.1.--SAM transfer equations (continued)

Variable	Channel No.	Counts to volts	
		Slope x10 ⁻⁴	Intercept x10 ⁻³
<u>Dallas Mast SAM</u>			
Mast wind speed	12	2.9442	5.2259
Pressure (Rosemount)	13	2.9441	5.5692
<u>Oceanographer Bow SAM</u>			
Sea-surface temperature	5	3.0566	-2.6949
Dry-bulb temperature	7	3.0560	-2.5212
Wet-bulb temperature #1	8	3.0592	-6.2459
Wet-bulb temperature #2	9	3.0580	-5.8612
Boom wind direction	12	3.0560	-1.9864
Boom wind speed	13	3.0540	-1.3234
<u>Oceanographer Mast SAM</u>			
Mast wind speed	7	2.9675	-9.8422
Pressure (Rosemount)	8	2.9712	-10.1268

Table D.2.--Sensor transfer equations for the Researcher

Variable	Sensor serial No.	Volts to scientific units .		Units
		Slope	Intercept	
<u>Bow Boom Sensors</u>				
Sea-surface temperature	126	6.021	14.99	°C
Dry-bulb temperature	51	5.988	15.09	°C
Wet-bulb temperature #1	55	5.996	15.12	°C
Wet-bulb temperature #2	56	6.006	15.09	°C
Boom wind direction	201	-68.175	177.21	deg.
Boom wind speed	151	9.782	-0.05	m/s
Ship heading ¹	114	0.04036	0.21	deg.
Ship speed ¹	115	0.00157	-0.02	m/s
<u>Mast Sensors</u>				
Mast wind direction*	226	-0.02125	+181.77	deg.
Mast wind speed	176	9.721	0.01	m/s
Pressure (Rosemount)	136	5.8637	1001.02*	mb

¹These sensors were calibrated through the SAM, hence they convert recording counts to scientific units.

*Does not include +1.44 mb correction for sensor height above sea level.
This correction was applied, however, to the pressure in the archived data.

Table D.3.--Sensor transfer equations for the Gilliss

Variable	Sensor serial No.	Volts to scientific units		Units
		Slope	Intercept	
<u>Bow Boom Sensors</u>				
Sea-surface temperature	127	5.981	15.01	°C
Dry-bulb temperature	53	5.994	15.03	°C
Wet-bulb temperature #1	59	6.013	15.02	°C
Wet-bulb temperature #2	60	5.998	14.82	°C
Boom wind direction	203	-69.301	172.58	deg.
Boom wind speed	153	9.379	0.06	m/s
Ship heading ¹	214	-0.02645	+194.50	deg.
Ship speed ¹	96	-0.00041	-1.41	m/s
<u>Mast Sensors</u>				
Mast wind direction ^{2,1}	228	-0.0261	169.2	deg.
" " " ^{3,1}	228	-0.0214	169.2	deg.
" " " ^{4,1}	228	-0.0209	173.2	deg.
Mast wind speed	178	9.356	-0.04	m/s
Pressure (Rosemount)	201	5.636	1002.15*	mb

¹These sensors were calibrated through the SAM; hence the conversion is from recording counts to scientific units.

²Transfer equation for IC 1.

³Transfer equation for Phases I and II.

⁴Transfer equation for IC 3 and Phase III.

*Does not include +0.94-mb correction for sensor height above sea level. This correction was applied, however, to the pressure in the archived data.

Table D.4.--Sensor transfer equations for the Dallas

Variable	Sensor serial No.	Volts to scientific 'units		Units
		Slope	Intercepts	
<u>Bow Boom Sensors</u>				
Sea-surface temperature ¹	134 (7)	6.063	15.00	°C
" " " ²	134 (4)	6.054	14.91	°C
" " " ³	Unknown	5.962	15.15	°C
Dry-bulb temperature	54	5.995	15.06	°C
Wet-bulb temperature #1	61	5.958	15.08	°C
Wet-bulb temperature #2	62	5.988	15.00	°C
Boom wind direction	204	-71.188	179.00	deg.
Boom wind speed ⁴	154	9.902	-0.01	m/s
" " " ⁵	182	9.319	0.03	m/s
Ship heading ⁶	314	0.02313	-0.85	deg.
Ship speed ^{6,7}	315	0.00135	-3.34	m/s
" " ^{6,8}	315	0.00134	-8.71	m/s
<u>Mast Sensors</u>				
Mast wind direction ⁶	229	0.02230	-169.3	deg.
Mast wind speed	179	9.917	-0.07	m/s
Pressure (Rosemount)	205	5.7592	1000.96*	mb

¹Sensor 134 was used on bridge 7 from June 17, 0900 GMT, through September 9, 1930 GMT (Julian days 168-252).

²Sensor 134 was used on bridge 4 from September 9, 2130 GMT, through September 10, 0830 GMT (Julian days 252-253).

³A sensor of unknown serial number was installed with bridge 7 and used from September 10 (Julian day 253), 1400 GMT, through the end of GATE.

⁴Wind speed sensor 154 was used during ICI and from August 31 (Julian day 243) 1950 GMT through the end of GATE.

⁵Wind speed sensor 182 was used from June 27 through August 31, 1941 GMT (Julian days 178-243).

⁶These sensors were calibrated through the SAM; hence conversion is from recording counts to scientific units.

⁷This transfer equation applies from June 17, 0900 GMT, through July 28, 0000 GMT (Julian days 168-209).

⁸This transfer equation applies from July 29 (Julian day 210) through the end of GATE.

* Does not include a 1.43-mb correction for sensor height above sea level. This correction was applied, however, to the pressure in the archived data.

Table D.5.--Sensor transfer equations for the Oceanographer

Variable	Sensor serial No.	Volts to scientific units		Units
		Slope	Intercepts	
<u>Bow Boom Sensors</u>				
Sea-surface temperature	129	6.005	14.94	°C
Dry-bulb temperature	52	5.985	15.02	°C
Wet-bulb temperature #1	57	5.978	15.05	°C
Wet-bulb temperature #2 ¹	58	5.984	15.14	°C
Boom wind direction	202	-69.733	178.30	deg.
Boom wind speed	152	9.874	-0.07	m/s
Ship heading ²	414	0.0264	3.30	deg.
Ship speed ²	415	0.00152	-0.06	m/s
<u>Mast Sensors</u>				
Mast wind direction ²	227	0.02126	177.00	deg.
Mast wind speed	177	10.241	-0.06	m/s
Pressure (Rosemount)	137	5.705	1001.22*	mb

¹On August 8, 1974, at 1900 GMT (during Phase II), the Oceanographer converted wet-bulb #2 to dry-bulb #2.

²These sensors were calibrated through the SAM; hence conversion is from recording counts to scientific units.

*Does not include a 1.41-mb correction for sensor height above sea level. This correction was applied, however, to the pressure in the archived data.

Table D.6.--Kollsman pressure sensor transfer equations

Ship	Serial No.	Third order term	Second order term	First order term	Intercept
<u>Researcher</u>	101	-0.46126875 x 10 ⁻⁶	+0.27593486 x 10 ⁻³	-0.14563650	32.485489 [*]
<u>Gilliss</u>	104	-0.48655658 x 10 ⁻⁶	+0.27792824 x 10 ⁻³	-0.14452538	31.530260 ^{**}
<u>Dallas</u>	454	-0.55192828 x 10 ⁻⁶	+0.274278609 x 10 ⁻³	-0.141299257	29.9511838†
<u>Oceanographer</u>	102	-0.43167229 x 10 ⁻⁶	+0.27152394 x 10 ⁻³	-0.14459957	32.937520††

^{*} Includes correction to sea level of 0.82 mb.

^{**} Includes correction to sea level of 0.68 mb.

† Includes correction to sea level of 0.73 mb.

†† Includes correction to sea level of 1.02 mb.

(Continued from inside front cover)

- EDS 16 NGSDC 1 - Data Description and Quality Assessment of Ionospheric Electron Density Profiles for ARPA Modeling Project. Raymond O. Conkright, in press, 1976.
- EDS 17 GATE Convection Subprogram Data Center: Analysis of Ship Surface Meteorological Data Obtained During GATE Intercomparison Periods. Fredric A. Godshall, Ward R. Seguin, and Paul Sabol, October 1976. (PB-263-000)
- EDS 18 GATE Convection Subprogram Data Center: Shipboard Precipitation Data. Ward R. Seguin and Paul Sabol, November 1976. (PB-263-820)
- EDS 19 Separation of Mixed Data Sets into Homogenous Sets. Harold Crutcher and Raymond L. Joiner, February 1977.
- EDS 20 GATE Convection Subprogram Data Center--Analysis of Rawinsonde Intercomparison Data. Robert Reeves, Scott Williams, Eugene Rasmusson, Donald Acheson, Thomas Carpenter, and James Rasmussen, November 1976.
- EDS 21 GATE Convection Subprogram Data Center: Comparison of Ship-Surface, Rawinsonde and Tethered Sonde Wind Measurements. Chester F. Ropelewski and Robert W. Reeves, April 1977.

NOAA SCIENTIFIC AND TECHNICAL PUBLICATIONS

NOAA, the *National Oceanic and Atmospheric Administration*, was established as part of the Department of Commerce on October 3, 1970. The mission responsibilities of NOAA are to monitor and predict the state of the solid Earth, the oceans and their living resources, the atmosphere, and the space environment of the Earth, and to assess the socioeconomic impact of natural and technological changes in the environment.

The six Major Line Components of NOAA regularly produce various types of scientific and technical information in the following kinds of publications:

PROFESSIONAL PAPERS — Important definitive research results, major techniques, and special investigations.

TECHNICAL REPORTS—Journal quality with extensive details, mathematical developments, or data listings.

TECHNICAL MEMORANDUMS — Reports of preliminary, partial, or negative research or technology results, interim instructions, and the like.

CONTRACT AND GRANT REPORTS—Reports prepared by contractors or grantees under NOAA sponsorship.

TECHNICAL SERVICE PUBLICATIONS—These are publications containing data, observations, instructions, etc. A partial listing: Data serials; Prediction and outlook periodicals; Technical manuals, training papers, planning reports, and information serials; and Miscellaneous technical publications.

ATLAS—Analysed data generally presented in the form of maps showing distribution of rainfall, chemical and physical conditions of oceans and atmosphere, distribution of fishes and marine mammals, ionospheric conditions, etc.



Information on availability of NOAA publications can be obtained from:

**ENVIRONMENTAL SCIENCE INFORMATION CENTER
ENVIRONMENTAL DATA SERVICE
NATIONAL OCEANIC AND ATMOSPHERIC ADMINISTRATION
U.S. DEPARTMENT OF COMMERCE
3300 Whitehaven Street, N.W.
Washington, D.C. 20235**